The regenerative capacity of bone tissue and autograft dust exposed to heat shock induced by high speed surgical cutting

Veasna Sum-Coffey, B.Sc. (2015), M.Sc. (2016)

NUI Galway
OÉ Gaillimh

A thesis submitted to the National University of Ireland Galway as fulfilment of the requirements for the degree of Doctor of Philosophy

September 2020

Biomedical Engineering

School of Engineering

National University of Ireland Galway

Supervisor of Research: Prof. Laoise M. McNamara
Collaborative partner: Stryker Innovation Centre, Cork

Abstract

High speed surgical cutting tools induce heat (>47°C) for short durations on bone tissue, leading to a thermally-induced cell death in bone cells. Post-operative bone healing at the cut surface and bone dust are important for ensuring the success of surgery and preventing long recovery time for patients. Autograft bone dust prepared using surgical burs can be re-introduced into patients to enhance bone healing. Recent in vitro and in vivo studies have provided evidence that thermal elevations can in fact trigger osteogenic responses by bone cells, enhancing mineralisation and new bone formation. However, whether bone dust and the cut surface exhibit an osteogenic response to heat shock induced by cutting conditions is unknown. Moreover, the influence of cutting conditions on the osteogenic potential of bone dust is not understood. In particular, the influence of the tissue source, the design of the cutting tool and the use of irrigation have not been investigated. Thus, the global aim of this PhD Thesis is to assess the ex-vivo osteogenic potential of autograft bone dust and the cut surface resected under different cutting conditions, and associated temperature elevations, using surgical burs for cutting and heat induction.

The duration of bone surface exposure to elevated temperatures during surgical bone cutting and the extent of heat dissipation and its effect on the bone healing capacity are not well understood. The first study of this PhD thesis sought to address this gap by conducting experimental studies to determine (1) temperature generation and dissipation during surgical bone cutting with no irrigation and (2) the ex-vivo regenerative potential of bone dust and the cut surface. During surgical cutting of bovine bone using burs (Multi-Flute, 2Flute) the relative surface temperatures (using a thermal camera) and dissipated temperatures (measured by embedded thermocouples) were quantified. Ex-vivo culture of bone dust and the cut surface samples were conducted up to 20 days post-cutting. Histological staining and biochemical

assays (Alamar Blue, ALP, Alizarin red staining) quantified osteonecrosis and osteogenesis. The results of this study revealed that superficial heat generation induced by high speed surgical burs for short durations triggered an osteogenic response in bone dust, which was associated with apoptotic cell death. The cutting temperature was significantly higher with the Multi-Flute compared to the 2Flute bur, but the % heated tissue volume was lower and faster cooling was observed. Interestingly, the ex-vivo osteogenic capacity of both the bone dust and the cut surface were enhanced when using the Multi-Flute bur, even though increased apoptotic thermal damage was observed.

To reduce the risk of excess tissue necrosis during surgical cutting, irrigation is commonly used to minimise temperature elevation. Yet, the influence of irrigation approaches, namely using a surgical assistant to apply irrigation (*manual*) or using an automated irrigation (*continuous*) device, have not been investigated and as such there is no consensus regarding a favourable approach to minimise tissue necrosis or osteogenesis. The objective of the second study was to determine how irrigation techniques influence cellular responses to surgical bone cutting. Specifically, this study sought to (1) compare superficial temperature generation and dissipation during high speed surgical bone cutting with either manual or continuous irrigation and (2) determine the influence of irrigation technique on the ex-vivo regenerative potential of bone dust and the cut surface. The results of this study revealed that dissipated temperatures remained below 30°C throughout the cutting for both types of irrigation. Interestingly, the cut surface was preserved when continuous irrigation was used during cutting. In contrast, when using manual irrigation increased apoptotic thermal damage was observed and the ex-vivo osteogenic capacity of bone dust was enhanced. This study can inform surgical irrigation approaches to preserve the osteogenic potential of bone dust and the cut surface.

The most common implantation site for such autografts is in the spine, where bone dust is subjected to in vivo biophysical conditions, including compression and torsional forces.

However, previous studies of autograft bone dust have been conducted under static conditions and so the mineralisation potential of bone dust in a mechanical environment representative of in vivo conditions is unknown. The objective of the third study was to assess and compare ex-vivo osteogenesis by bone dust using a custom-made compression bioreactor to recreate in vivo mechanical stimulation. The effect of irrigation was assessed under both static and mechanical loading conditions. Interestingly, in this study a 3mm bur was used and the irrigation method (manual or continuous irrigation) did not influence the mineralisation potential of bone dust under either static or mechanically stimulated conditions. Here it is reported for the first time that the osteogenic capacity (in terms of viability and mineralisation responses) was significantly higher for mechanically stimulated bone dust when compared to those cultured under static conditions. These results suggest that the osteogenic potential of bone dust may be enhanced by the mechanical loading conditions that exist in vivo.

Together, these studies provide (1) an insight into the osteogenic response of bone tissue resected with different design burs and different irrigation approaches during cutting, and (2) uncovers how the mechanical environment that arises in vivo might influence the osteogenic capacity of autograft bone dust. The information elucidated from this body of work can inform future surgical instrument design to improve post-operative bone tissue regeneration.

Publications

Journal Articles

The following publications have arisen from the work presented in this thesis:

- Veasna Sum-Coffey, Conor E. McCarthy, Peter Curtin, Laoise M. McNamara "Temperature elevations during high speed cutting occur for short durations and enhance ex-vivo osteogenesis, which is associated with thermal damage" submitted to *Nature Scientific Reports* on April 2020.
- Veasna Sum-Coffey, Alexander Szymanski, Patrick Cushen, Jaco Jacobs, Laoise M. McNamara "The ex-vivo osteogenic capacity of surgically cut bone surfaces is enhanced using continuous irrigation by a device, whereas bone dust is preserved for osteogenesis with a manual intermittent irrigation approach*"* In preparation for submission to *The Spine Journal* on October 2020
- Veasna Sum-Coffey, Alexander Szymanski, Patrick Cushen, Jaco Jacobs, Laoise M. McNamara "Early and long-term mineralisation in porcine autograft bone dust surgically cut with a high speed bur using an ex-vivo bioreactor" In preparation for submission to *Annals of Biomedical Engineering* on October 2020

Conference Presentations

Peer Reviewed International Conferences

- Poster presentation at the Annual meeting of Orthopaedic Research Society (ORS), Phoenix, Arizona, U.S.A. February 2020
- Poster presentation at the World congress of Biomechanics, Dublin, Ireland. July 2018

Peer Reviewed National Conferences

- Podium presentation at 26th Annual conference of the section of Bioengineering of the Royal Academy of Medicine in Ireland (BINI), Carlow. January 2020
- Podium presentation at 25thAnnual conference of the section of Bioengineering of the Royal Academy of Medicine in Ireland (BINI), Limerick, and January 2019

- Podium presentation at 24th Annual conference of the section of Bioengineering of the Royal Academy of Medicine in Ireland (BINI), Kildare. January 2018
- Poster presentation at NUIG/UL Research day, Galway. April 2017
- Poster and Podium presentation at 23rd Annual conference of the section of Bioengineering of the Royal Academy of Medicine in Ireland (BINI), Antrim. January 2017

Acknowledgements

I would like to thank everyone who has helped me throughout my PhD. First and foremost, I would like to give a big thank you to Professor Laoise McNamara for her dedication, guidance and mentorship. She is a huge inspiration to me and I would not have been able to conduct this work without her encouragement and support. Thank you very much, Laoise!

I would like to say thank you to my industry partner, Stryker Innovation Centre, Carrigtwohill, Cork, Ireland. I would like to especially thank the Stryker employees, Conor McCarthy, Alex Szymanksi, Patrick Cushen, Jaco Jacobs, Kevin Packard, and Peter Curtin for your help in experimental design for each study, and your invaluable skills and knowledge on surgical instruments. Thank you Conor, for your help in designing the temperature analysis part of the experiments and for training me in using the surgical burs. Thank you, Alex, Paddy, and Jaco for making the trip to NUIG to help carry out the cutting for the irrigation and bioreactor studies, and for bringing me into the Bone Vac project. I have gained invaluable skills working alongside you all. Thank you, Alex and Paddy for taking me with you to the Deformity course, where I had my first experience with a cadaver!

Thank you to Anneke Verbruggen for proof reading this Thesis! You are a star!

And last but not least, I would like to thank my whole family. First and foremost, my husband, Kevin Coffey, who had to put up with me for the last 4 years and supported me for the last 9 years, ensuring that my academic studies came first. I would not have done this without you, Love of my life. And especially a big thank you to my 4 kids, Andrew, Ciara, Jason, and Conor, who had to take on extra chores the last 6 months, so I could write this Thesis. Thank you, mom, for supporting me and believing I can do anything!

Acronyms

FLIR	Forward-looking Infrared Radiometer
MSC	Mesenchymal Stem Cells
CSD	Critical size defect
ALP	Alkaline Phosphatase
OCN	Osteocalcin
OPN	osteopontin
RUNX2	runt-related transcription factor 2
BSP	Bone Sialoprotein
DMP-1	Dentin matrix acidic phosphoprotein 1
ECM	Extracellular matrix
HA	Hydroxy apatite
DKK1	Dickkopf-related protein-1
sFRP1	Secreted frizzled-related protein-1
RANKL	Receptor activator of nuclear factor kappa-B ligand
RANK	Receptor activator of nuclear factor kappa-B
MCSF	Macrophage colony-stimulating factor
OPG	Osteoprotegerin
PTH	Parathyroid
BMP-2	Bone Morphogenetic protein 2
TGF-β	Transforming growth factor beta
TNF	Tumour necrosis factor
COX2	Cyclooxegenase
VEGF	Vascular endothelial growth factor
PCR	Polymerase Chain Reaction
H&E	Haematoxylin and Eosin

Table of Contents

Table of Figures

Chapter 1 : Introduction and Objectives

1.1 Bone, mechanobiology and osteogenesis

The skeletal system is important for protecting our vital organs, such as the heart, lungs, and brain. It is a hard material that is constantly modelling its shape to adapt to the forces that are continually exerted at different locations of the skeleton throughout life. Bone is a highly adaptable material, and mechanical stress can induce an osteogenic response (Chao and Inoue 2003; Davies et al. 2006), whereas the absence of loading can lead to a net increase in bone resorption (Spengler et al. 1983; Vico et al. 1987). Different bone cell types play specific roles in bone regeneration, and these cells include mesenchymal stem cells (MSCs), osteocyte, osteoblast and osteoclast cells. MSCs are important for bone regeneration, because they differentiate into osteoprogenitor cells that are committed to become osteoblasts (McNamara 2011). The intimate partnership between osteoblasts and osteoclasts is key for bone modelling and remodelling, which will be discussed further in Chapter 2. Osteocytes are mature osteoblast cells, and they permeate the bone by embedding themselves in the extracellular matrix. Along with osteoblasts, they are the main mechanosensitive cells (Cowin 1983; Kleinnulend et al. 1995; C. 1990). Mechanical stimulation, such as compression, fluid flow shear stress induces cellular responses for bone modelling and remodelling, which will be discussed further in Chapter 2.

Bone formation during embryo development and adolescence occurs by one of two processes, endochondral ossification or intramembranous ossification. During endochondral ossification, which is the bone forming process in long bones, cartilage is formed first before mineral is laid down onto the cartilage template. The other type of bone formation process is intramembranous ossification, which does not involve the formation of a cartilage template,

instead, stem cells aggregate into a cluster creating a nodule that is surrounded by a membrane, within which MSCs differentiate into osteoprogenitor cells for bone formation. MSCs express osteogenic genes when they are differentiating into bone cells. Expression of these genes are markers for osteogenesis, and they include alkaline phosphatase (ALP), Collagen type I, osteocalcin (OCN), osteopontin (OPN), and runt-related transcription factor 2 (RUNX2), and cyclooxygenase 2 (COX2). Bone tissue damage due to aging, injury or disease can active bone remodelling and initiate repair to restore bone function.

Fracture healing is a complicated process involving osteoprogenitors, osteoblasts, and chondrocytes to repair the site of damage (McKibbin 1978; Einhorn 1998). The first step in this process is the recruitment of blood and inflammatory cells, forming a hematoma at the site of damage. Granulation tissue consisting of blood vessels with immune cells is then formed, where macrophages engulf damaged and unwanted tissues and debris at the site of injury. MSCs and osteoprogenitor cells are recruited to the site to begin the bone formation process, where osteoblasts produce woven bone, forming a callus around the fracture site. Osteoprogenitors differentiate into either osteoblasts or fibroblasts, which further differentiate into chondrocytes to form a hyaline cartilage and a fracture callus (Tsiridis, Upadhyay, and Giannoudis 2007). In time, osteoblasts secrete mineral onto the extracellular matrix and then terminally mature into osteocytes to embed themselves in the bone matrix and become the structural component of the new bone.

1.2 Surgical cutting tools for orthopaedic surgery

The market size value for orthopaedic products was estimated at $52.8 billion in 2017 and is projected to grow to $66.2 billion with a Compound Annual Growth Rate (CAGR) of 3.8%, according to GlobalData. Devices in these markets include spinal cage, surgical burs, bone mill, pedicles and screws, bone allografts, hip implants, and oscillating saws. The market size

of cutting tool devices was $944.99 billion in 2019, and it is estimated to be $1.5 trillion by 2027, according to Verified Market Research.

Bone resection using surgical cutting tools is required to gain access to specific skeletal sites or harvest autograft tissue for various procedures, such as tympanomastoidectomy (Roth AA 2017), spinal fusion (Perez-Cruet M 2013; Epstein 2017) or acetabular revision (Schreurs et al. 2004). High speed cutting tools used in surgical intervention for bone resection include orthopaedic drills, where holes are created for insertion of screws and pedicles (Cheng et al. 2015). Surgical burs are also a high speed cutting tool, and they are used in decortication of vertebrae and laminectomy during lumbar spinal fusion surgery (Epstein 2017; Yilmaz et al. 2015; MenMuir and Fielding 2017). Bone resection with surgical burs create bone dust autograft material that can be re-introduced into patients to enhance bone fusion (Epstein 2017; Kim et al. 2016). Bone dust are much smaller (<66,000 μm^2) in size compared to bone chips (>112,000 μm^2) (Ye et al. 2013; Eder et al. 2011; Roth AA 2017), which are resected with rongeurs or bone cutters but do not generate heat during cutting.

Surgical cutting induces both thermal and mechanical stress on bone cells, and this affects post-operative bone regeneration. In particular, these cutting tools can induce thermal damage, whereby cells undergo apoptosis and necrosis. Temperature elevations generated from high speed cutting exceed 47°C (Karaca, Aksakal, and Kom 2011; Dolan, Vaughan, Niebur, Casey, et al. 2014; Matthes et al. 2018; Livingston et al. 2015; Hosono et al. 2009), due to frictional heat at the interface of the bone and cutting tool, and induce cells to undergo apoptosis. Thermally-induced cell apoptosis can be detrimental if excessive tissue necrosis occurs, increasing patient recovery time (Ochsner, Baumgart, and Kohler 1998). However, the ensuring temperature elevations during cutting with surgical burs and their influence on the regenerative capacity of bone dust and the cut surface are not fully understood.

1.3 Biological implications of temperature

High speed cutting tools have been shown to generate temperature elevations above 47°C (Eriksson 1984; Karaca, Aksakal, and Kom 2011; Hosono et al. 2009), which induces thermal tissue damage (Dolan et al. 2016; Eriksson, Albrektsson, and Magnusson 1984). The extreme response to thermal damage is cell apoptosis and tissue necrosis. Necrosis is an immediate response to severe injury, where cell swelling and loss of cell membrane integrity occurs (Noble 2003c; Ziegler and Groscurth 2004), leading to tissue void of cells. Cell apoptosis is a systematic process initiated by external factors (extrinsic pathway) or internally (intrinsic pathway) to induce disassembly of cell structure and content into membrane-bound vesicles, which are then transported out of the cell to be phagocytosed by immune cells (Ziegler and Groscurth 2004; Noble 2003c). However, a slight increase in temperature for short durations can enhance the bone healing process, where thermally induced cell apoptosis led to an increase in COX2, RANKL, and M-csf in rat tibia exposed to 47°C and 60°C thermal elevations for 1 minute (Dolan et al. 2015). Another study reported a production of heat shock proteins, and growth factors for angiogenesis, osteoblastogenesis, and bone matrix protein in MC3T3 cells (Chung and Rylander 2012). Heat shock proteins play a crucial role in thermally damaged bone tissue, because they act as intracellular chaperones that facilitate folding of proteins into the correct conformation and they stably transport unfolded protein across the membranes within the cell (Walter and Buchner 2002; Borges and Ramos 2005). The heat shock protein implicated in bone, HSP70, is known to inhibit apoptosis by preventing the recruitment of pro-caspase-9 to the Apaf-1 apoptosome (Beere et al. 2000). Moreover, HSP70 promotes the induction of osteogenesis, where increase in ALP activity and mineralisation was observed in human MSCs (hMSCs) (Chen et al. 2015).

1.4 Flute design parameter affects temperature elevation during cutting

Cutting parameters such as drill speed, feed rate and cutting flute design affect temperature elevation (Karaca, Aksakal, and Kom 2011; Matthews and Hirsch 1972a; Saha, Pal, and Albright 1982; Davidson and James 2003; Choi et al. 2010). These parameters have been extensively studied (Davidson and James 2003; Dolan, Vaughan, Niebur, Casey, et al. 2014; Saha, Pal, and Albright 1982; Matthews and Hirsch 1972a), in order to optimise design of orthopaedic drills and limit osteonecrosis. In comparison to orthopaedic drills that cut at one location, surgical burs are considered as a moving heat source (Hou and Komanduri 2000; Shin and Yoon 2006), because they are not limited to one location on the bone during cutting. Constant movement of bur across the bone surface allows cooling to occur at the cut site. Moreover, design of cutting flutes on surgical burs affects heat generation, whereby clogging of flutes create higher frictional heat (Albright, Johnson, and Saha 1978; Jacob and Berry 1976; Pal and Saha 1981). The two main flute designs in surgical burs are the 2Flute and Multi-Flute, as seen in Figure 1.1, and bone resected with these designs produce bone dust of different sizes, with the Multi-Flute creating smaller bone dust sizes (Roth AA 2017). The Multi-Flute design has more cutting flutes than the 2Flute design. Therefore the induction of higher temperature elevation is expected with the Mult-Flute bur compared to 2Flute burs. However, the temperature magnitude of Multi-Flute and 2Flute burs have not been previously reported. Also shown in Figure 1.1A is a rongeur, a tool used to scrape out bone autograft material during cranial surgeries, in order to gain access to tissue beneath the skull. This device does not induce temperature elevation. The devices in Figure 1.1B-D below are high speed cutting tools, surgical saws and burs, where saws are used to resect bone such as long bones, while the surgical burs are used during spine surgery to resect lamina and obtain autograft material that can be used for spinal fusion.

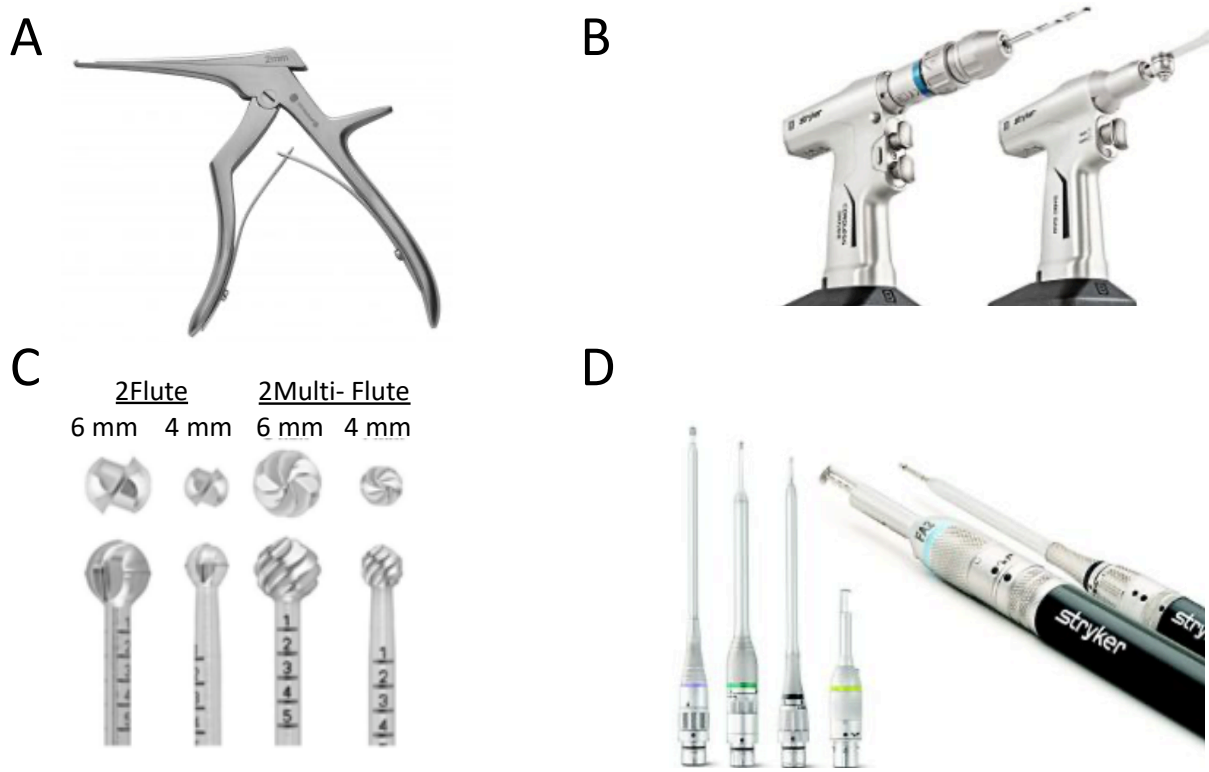

Figure 1.1: Orthopaedic devices used for bone resection in surgery, A) a rongeur image taken from the website of DTR Medical (Medical), B) drill and oscillating saw images taken from (Stryker) website, C) design of surgical burs, image taken from (Roth AA 2017) and D) Drill attachment for burs image taken from (Stryker).

Bone has low thermal conductivity and so heat generated during drilling does not dissipate quickly (Feldmann et al. 2018; Davidson and James 2000). It is not known whether the increase in surface temperature induced by cutting with surgical burs on the bone surface will also significantly increase heat dissipation within the bone, or if there is a significant difference in heat generation between cutting flute designs. Therefore, there is a need to quantify heat generation both at the cut surface and inside the bone, and also investigate temperature elevations during high speed cutting with surgical burs of different flute designs. The first research hypothesis of this Thesis addresses this problem, which is "***A Multi-Flute surgical cutting tool bur generates higher temperature at the superficial surface than a 2Flute bur design***".

1.5 Thermally induced apoptosis enhances regenerative response in bone cells

As a result of high speed surgical cutting, cells lose their tissue integrity and lamellar structure (Eder et al. 2011; Kuttenberger, Polska, and Schaefer 2013) and are subjected to extreme temperature elevations (>60°C) during cutting without the presence of irrigation (Hosono et al. 2009; Livingston et al. 2015; Xu et al. 2014). Thermal stress conditions (> 44°C for 10 minutes duration) have been shown to induce recruitment of heat shock proteins (HSP40, HSP70) and upregulation of osteogenic genes in MC3T3 osteoblast-like cells (Chung and Rylander 2012). The mechanism that governs the osteogenic response in cells subjected to thermal damage involves the cell apoptosis pathway, whereby cells undergoing necrosis and apoptosis initialise a remodelling signalling repair response (Dolan et al. 2015).

Thermally induced remodelling pathway begins with thermal damage by an external heat induction such as high speed cutting. Figure 1.2 is a schematic that summarises the cell signalling cascade of a cell undergoing apoptosis, and the bone remodelling cascade induced by cell apoptosis and necrosis. Under thermal stress conditions, the cell's mitochondria express cytochrome C, which binds to Apaf-1 to activate Caspase 9 (Du et al. 2000; Garrido et al. 2006; Chinnaiyan 1999; Hill et al. 2004). The activation of Caspase-9 leads to cleavage of pro-caspase-3 into activated Caspase-3, which commits the cell for apoptosis (Crowley and Waterhouse 2016). Osteocytes undergoing apoptosis send signals (COX2 and OPG) to initiate a bone remodelling cascade, whereby osteoclastogenesis is initiated to produce the bone resorbing cells, osteoclasts (Dolan et al. 2015). They are recruited to the site of damage and begin resorbing bone, along with other macrophages to phagocytose cellular debris. Moreover, nearby osteocytes receive signals from their dying neighbours to begin osteoblastogenesis, by increasing expression of COX2 and RANKL, which leads to the differentiation of MSC into bone forming cells, which upregulate ALP activity and calcium (Dolan et al. 2015). When

osteoclast has resorbed tissue in the damaged area, osteoblast cells follow closely behind to begin forming bone matrix. They mature into osteocytes and embed themselves in the bone matrix, to become part of it. Here, they reside and act as sensory cells to regulate bone remodelling, which will be discussed in detail in Section 2.4.2.

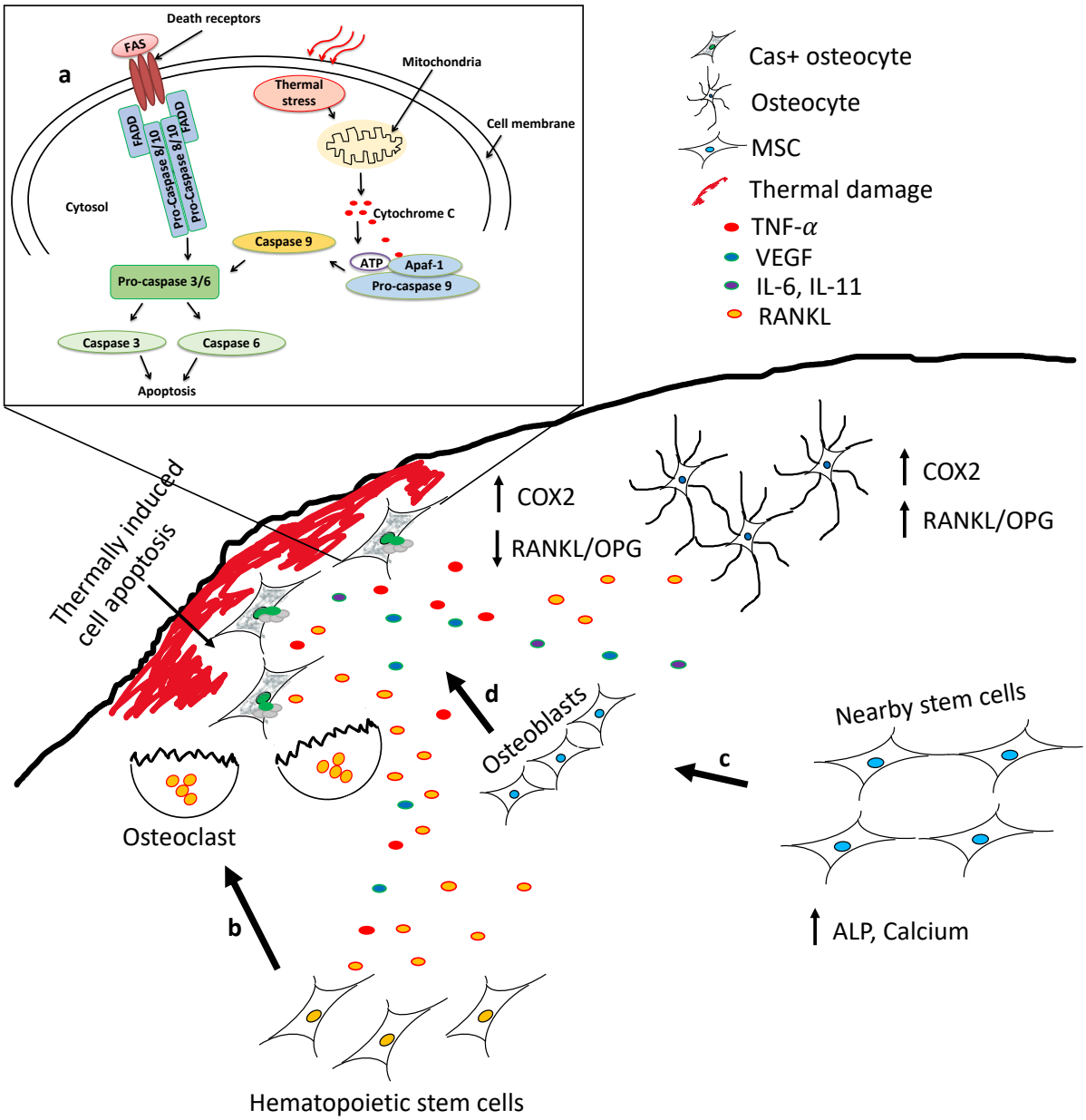

Figure 1.2: Schematic of a) cell signalling in thermally induced cell apoptotic osteocytes, which initiates a healing response, where an increase in COX2 and decrease in RANKL/OPG is expressed in heat treated osteocytes leading to b) differentiation of hematopoietic stem cells (HSC) into osteoclast precursors. c) Differentiation of MSCs into osteoblasts, which follows behind osteoclasts to lay down new bone in the necrotic zone. Image created from literature review.

However, the cellular response to thermal damage is dependent on the cell phenotype, magnitude of temperature elevation, and duration of heat shock (Dolan et al. 2012). Previous in vitro and in vivo studies have investigated the effect of low to moderate temperature elevations (<60°C) for long (>1 hour) (Norgaard, Kassem, and Rattan 2006) and short (<1 minute) durations (Dolan et al. 2015; Dolan et al. 2016; Dolan et al. 2012; Eriksson and Albrektsson 1983; Eriksson, Albrektsson, and Magnusson 1984; Eriksson, Albrektsson, and Albrektsson 1984; Eriksson and Albrektsson 1984). However, cutting temperature and duration is not consistent between cutting tools, or even between cutting procedures used from surgeon to surgeon. Moreover, previous studies have artificially induced temperatures using in vitro approaches (water bath), to represent the temperature elevations arising in orthopaedic cutting and investigate in vitro cell viability and mineralisation responses. Temperature measured in vivo with surgical burs and orthopaedic drills show fluctuations, whereby bone tissue is subjected to a rise and fall of heat generation (Matthes et al. 2018; Xu et al. 2014; Sener et al. 2009). In vitro and in vivo studies have shown that heat generated above 47°C, when artificially inducing heat, can enhance an osteogenic response in bone cells (Dolan et al. 2012; Dolan et al. 2015) and rat tibia (Dolan et al. 2016), even though cell apoptosis occurred as a response to thermal damage. High speed cutting tools such as drills and burs were reported to create temperatures above 47°C, but the cellular response was not further assessed (Matthes et al. 2018; Hosono et al. 2009; Livingston et al. 2015; Karaca, Aksakal, and Kom 2011; Saha, Pal, and Albright 1982; Eriksson, Albrektsson, and Albrektsson 1984). To fully understand the osteogenic capacity of surgically cut bone, a cutting tool needs to be used to generate heat and then viability and osteogenic responses be investigated as a response to this cutting and associated temperature elevations. The second hypothesis of this thesis is "***Bone surfaces and autograft dust exposed to temperature elevations induced by high speed cutting undergo cell apoptosis, which enhances the osteogenic response ex-vivo***".

1.6 The role of using irrigation during orthopaedic cutting

In order to limit thermally induced osteonecrosis, temperature elevations can be minimised using an irrigation method during surgical cutting. The two main irrigation methods used in surgery are manual irrigation, whereby a surgical assistant applies irrigation solution onto the cutting tool while the surgeon is conducting the surgical cutting, and the second method is continuous irrigation, which involves using an automated irrigation device that is attached to the cutting tool. Irrigation parameters, such as flow rate and temperature of irrigation solution, affect heat generation during surgical cutting (Sener et al. 2009; Isler et al. 2011; Hosono et al. 2009; Xu et al. 2014). For example, surgical cutting with a high speed diamond-tipped bur with automated continuous irrigation (540 ml/hr) led to a decrease in temperature elevation (52°C), measured by a Forward-Looking Infrared Radiometer (FLIR) camera on porcine lamina, when compared to temperatures reported (174°C) at a lower flow rate (180 ml/hr) with the same bur (Hosono et al. 2009). Furthermore, temperature elevations measured using a FLIR thermal camera during bony decompression surgery (59 patient study), revealed significantly higher temperature when manual irrigation (148.17 ± 42.62°C) was used, when compared to continuous irrigation (119.46 ± 28.19°C) (Matthes et al. 2018). The major factor causing a higher temperature elevation during manual irrigation, compared to continuous, is the fluctuation of temperature elevation, because the assistant has to follow the movement of the instrument tip, which is not always predictable and can be associated with short durations during which dry cutting occurs (Matthes et al. 2018). However, the cellular response to bone cutting in the presence of irrigation, representative of methods used in surgery, is not fully understood and it is still unclear which irrigation approach is more suitable to enhance post-operative bone regeneration. Since cutting in the presence of manual irrigation induces higher heat than continuous irrigation, and a degree of thermal damage can enhance osteogenesis, this method might be more suitable for post-operative bone regeneration, but this has never been

investigated. Therefore, the third hypothesis is "***Surgical cutting with manual irrigation induces higher temperatures, when compared to cutting with continuous irrigation, but the ex-vivo osteogenic potential of autograft bone dust is enhanced***".

1.7 The influence of implantation site on the osteogenic potential of autograft bone dust

Autograft bone dust is commonly re-introduced into patients to enhance bone regeneration, to take advantage of the osteogenic capacity of native cells and growth factors within the bone dust to encourage both osteo-induction and osteo-conduction (Kuttenberger, Polska, and Schaefer 2013). Studies have shown that mechanical stimulation can increase bone matrix formation (Guo et al. 2012), osteogenesis of bone marrow cells (Matziolia et al. 2011) and bone formation in trabecular explants (Birmingham et al. 2015). Therefore, autograft bone dust implanted into different sites may have different osteogenic responses arising from the different mechanical loading at these locations. For example, bone dust implanted between two vertebrae will undergo compression and torsional forces, whereas bone dust implanted as a filler in cranial surgical procedures do not experience loading forces, and so osteogenic response will differ. Previous studies of the osteogenic potential of bone dust (Ye et al. 2013; Eder et al. 2011; Gao et al. 2018; Gupta et al. 2009; Roth AA 2017) were all conducted in static conditions, whereas autograft bone dust is intended for implantation, where a mechanically stimulated environment exists. However, the regenerative capacity of bone dust under mechanical stimulation is not known. Therefore, the final hypothesis of the Thesis is "***The mineralisation potential of autograft bone dust is enhanced by mechanical stimulation representative of in vivo conditions***".

1.8 Objectives and Hypotheses

The global objective of this PhD thesis is to investigate the effect of surgical cutting with high speed surgical burs, which induce mechanical and thermal stress, on the osteogenic potential of bone dust and the cut surface. Therefore, the first specific objective is to determine the temperature elevations during surgical cutting with a high speed bur without irrigation. The second specific objective is to determine the effect of heat generation during surgical cutting without irrigation on the cellular response of ex-vivo bone dust and the cut site, which were resected with 2Flute and Multi-Flute bur designs. The third specific objective is to investigate the cellular viability and mineralisation response in ex-vivo bone dust and the cut site resected in the presence of manual and automated irrigation methods used in surgery. The final specific objective is to conduct an ex-vivo bioreactor experiment, in order to investigate the osteogenic potential of autograft bone dust in a mechanical environment representative of in vivo conditions. Four hypotheses have been identified to address each of these objectives, which will underpin the research of Chapters 3-5 of this Thesis, respectively.

Hypothesis 1: A Multi-Flute surgical cutting tool bur generates higher temperature at the superficial surface than a 2Flute bur design

Hypothesis 2: Bone surfaces and autograft dust exposed to temperature elevations induced by high speed cutting undergo cell apoptosis, which enhances the osteogenic response ex-vivo

Hypothesis 3: Surgical cutting with manual irrigation induces higher temperatures, when compared to cutting with continuous irrigation, but the ex-vivo osteogenic potential of autograft bone dust is enhanced

Hypothesis 4: The mineralisation potential of autograft bone dust is enhanced by mechanical stimulation representative of in vivo conditions.

By testing each of these hypotheses, the research objectives, as outlined above, can be answered and the proposed research will deliver significant advances in understanding the effect of temperature induced by surgical cutting with a high speed bur on post-operative osteogenic potential of bone.

1.9 Thesis structure

This Thesis comprises the work completed for the duration of the candidate's Ph.D. studies. Chapter 2 provides a thorough review of relevant literature, detailing the specific roles of each bone cell on bone morphology and function, and the bone cell's response to thermal and mechanical stress conditions. The processes of bone formation, bone remodelling, and fracture healing, as well as the influence of high speed cutting tools on bone regeneration, are described in detail. In Chapter 3, the experimental studies conducted to measure *surface* and *dissipated* temperatures during high speed cutting with surgical burs are described, which tests Hypothesis 1 of the Thesis. The influence of heat generation induced by surgical cutting with a high speed bur on bone regeneration during recovery days is also investigated in Chapter 3, testing Hypothesis 2. In Chapter 4, the viability and regenerative capacity of bone resected in the presence of manual and continuous irrigation methods are investigated, testing Hypothesis 3 of the Thesis. Chapter 5 investigates the mineralisation response of autograft bone dust in a mechanical environment compared to a static environment, using a compression bioreactor to mechanically stimulate bone dust, testing Hypothesis 4.

Chapter 2 : Literature Review

2.1. Introduction to Bone Biology

The musculoskeletal organs form a very important system in the human body. It helps to protect our vital organs, such as the brain, heart, and lungs. The two main components of the system are bone and muscle, and they work together to move the human body through mechanical forces generated by muscle contraction and relaxation. Bone is a very versatile composite material that can adapt to mechanical cues and biochemical cues in its microenvironment, which are described below in detail (Chao and Inoue 2003). Bone tissue has a high stiffness and strength and is organised into a hierarchical architecture, as discussed in detail below.

2.1.1. Bone Composition

Bone is a hard material, where 35% comprises organic phase and 65% is made up of a stiff mineral phase, which consists of hydroxyapatite crystals containing calcium and phosphorus (Fratzl et al. 2004). The high mineral content of the tissue serves as a reservoir for calcium, and changes in this mineral density can occur according to mechanical load. The organic phase consists of bone cells, water, lipids, and other non-collagenous protein such as osteopontin, osteocalcin, osteonectin, and bone sialoprotein, which enable bone mineralisation (Thurner et al. 2009; Roach 1994). Of this organic phase, 90% is collagen, which provides the structural integrity and matrix of bone. Bone is mainly composed of collagen Type I, although, Types III, IV, and V also exist in trace amounts (Miller 1984; Miller, Vanderko.Jk, and Sokoloff 1969). The intricate physical interaction between the structural organisation and mechanical integrity of these phases determine the structure and mechanical behaviour of bone tissue (McNamara 2011).

2.1.2. Hierarchical Structure of Bone

Bone function is dependent on the intricate and complex hierarchical organisation of bone. This architecture consists of component phases at levels of structural organization and can be classified from the organ level to the macro-scale, micro-scale, and nano-scale structure (see Figure 2.1). The adult skeleton comprises of approximately 80% of cortical bone and the remaining 20% is known as trabecular bone, which is also known as spongy bone or cancellous. Cortical bone is a hard and dense connective tissue with a low porosity of 5-10% (McNamara 2011). It is found in the shafts of long bones and also acts as a shell around the ends of bones such as the vertebra, scapula and pelvis. This dense property of cortical bone facilitates high-load bearing, absorbs mechanical forces from the musculature to facilitate movement of body parts. Structural units in mature bone are known as lamellae and osteons. Immature bone, also known as woven bone, is irregularly organized with random osteocyte cells and collagen fibre bundles. As bone remodelling occurs, this woven bone is replaced by lamellar bone, which are collagen fibrils organised into parallel layers. In each lamella, the collagen fibrils are oriented in the same direction. In bone tissue containing blood vessels, lamellae are organised in concentric rings around a Haversian canal containing a central vessel, called an osteon (McNamara 2011).

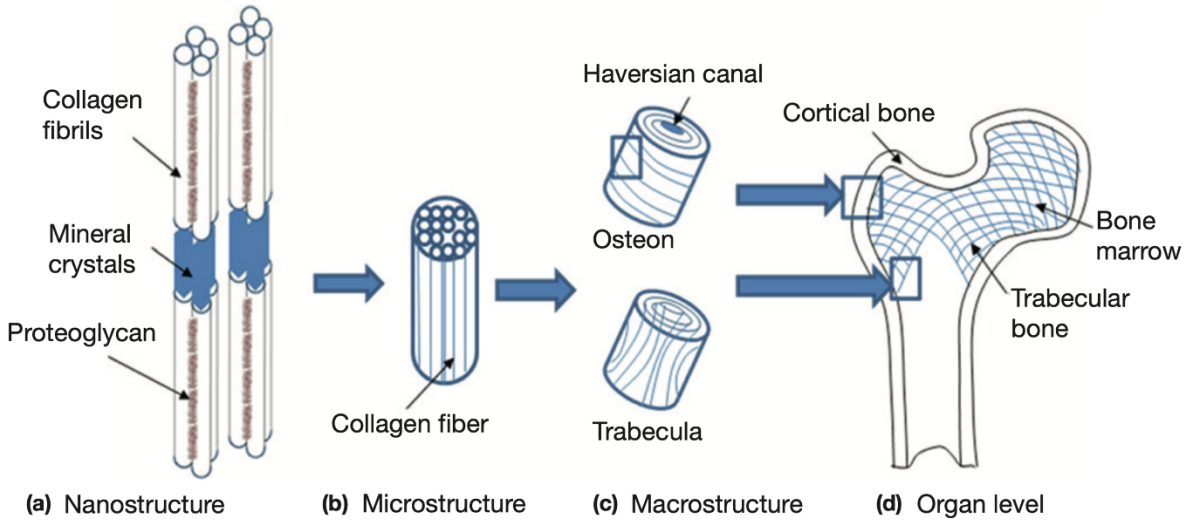

Figure 2.1: Hierarchical structure of bone showing the structure at the a) nanoscale, b) microscale, c) macroscale and d) organ level (McNamara 2011).

2.2. Bone formation

In early life, bone formation occurs during embryonic development by two distinct methods, endochondral or intramembranous ossification. As humans mature and grow, bone formation continues to alter the geometry of bone, providing larger bones that are adaptable to mechanical loading (modelling), and to replace aged or damaged bone (remodelling), discussed further in Section 2.3.1 and Section 2.3.2, respectively. During bone formation, an organic matrix of osteoid/cartilage template is laid down first by osteoblasts, then mineralisation crystals are gradually formed over time to produce the bone composite material and becomes mechanically more stable.

2.2.1. Endochondral ossification

Endochondral ossification is the process by which long bones are formed in early foetal development. There are two crucial aspects of the process that occur for bone to be formed. The first is the formation of the cartilage template and the second is the vascularisation of the cartilage template. When these two processes have taken place, bone mineral is produced and laid down onto the vascularised cartilage template (Ortega, Behonick, and Werb 2004). Mesenchymal stem cells (MSCs) differentiate into chondroblast cells to form a membrane template known as the perichondrium (Figure 2.2). The chondroblasts proliferate and the template grows in length and thickness, after which the cells secrete extracellular matrix (ECM) comprising mainly of collagen and proteoglycans. Eventually, the chondroblasts differentiate into chondrocytes and begin to secrete alkaline phosphatase, a nucleator enzyme for deposition of minerals onto the template. Chondrocytes also secrete growth factors to initiate vascularisation. An outer membrane, known as the periosteum, is formed at the outermost layer of bone. The periosteum is an important source for undifferentiated osteoprogenitor cells, where the outer layer is a source for fibroblasts while the inner layer is a source for

osteoprogenitor cells that develop into osteoblast cells (Gerber and Ferrara 2000). Ligaments, tendons and muscles attach to the periosteum. Primary ossification occurs in the centre of the perichondrium, where chondrocytes undergo apoptosis during the mineralisation process, giving rise to a cavity that is invaded by blood vessels from the perichondrium. These blood vessels are a source of hemopoietic cells, which form the bone marrow. Endothelial cells on the lining of the blood vessels produce growth factors that aid in recruitment, proliferation and differentiation of osteoblasts (Sumpio, Riley, and Dardik 2002). Osteoclasts are also recruited to form the medullar cavity in bone marrow. At birth, a secondary ossification centre in the epiphyses of long bone is produced, and this is known as the growth plate (Figure 2.3).

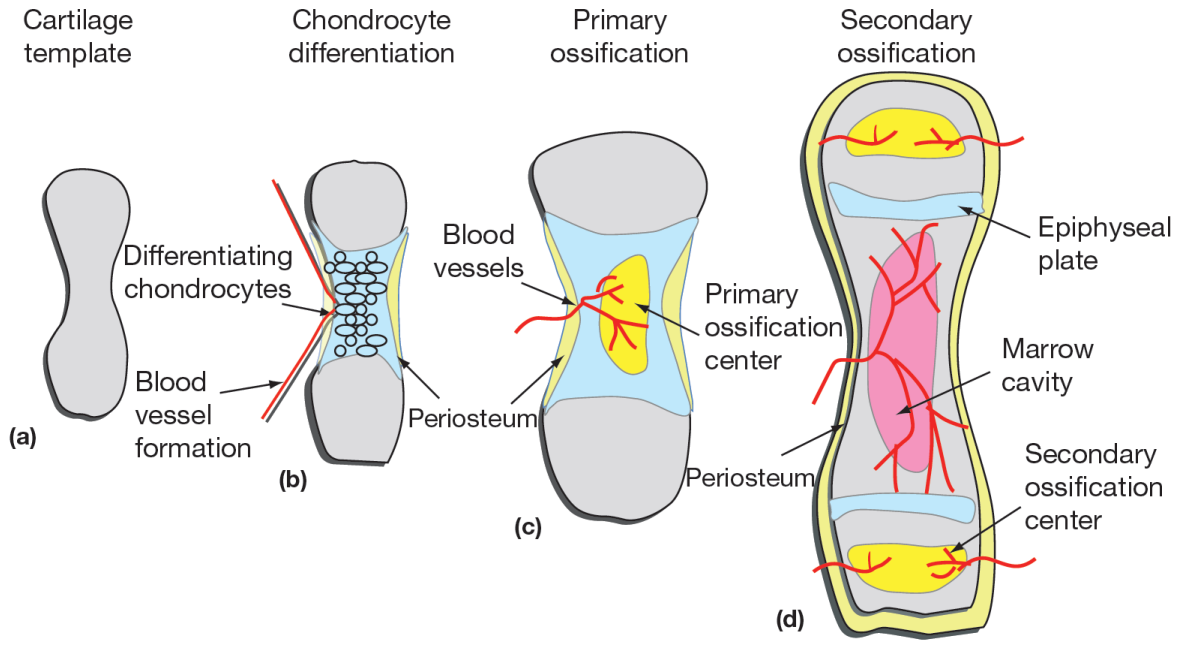

Figure 2.2: Process of endochondral ossification showing a) the cartilage template, b) chondrocyte differentiation c) primary ossification at the centre and d) secondary ossification at the two ends of long bone (McNamara 2011).

The growth of bones is ongoing throughout childhood and is regulated by the growth plate, which continuously produces cartilage to be replaced by bone mineral over time. This lengthens the bone and is the reason for growth during childhood and adolescence. In adults,

this lengthening stops and the growth plate fuses to form bone, creating the epiphyseal line. Endochondral ossification is important in development and growth of long bones, but it also regulates fracture repair, which will be discussed further in Section 2.3.3.

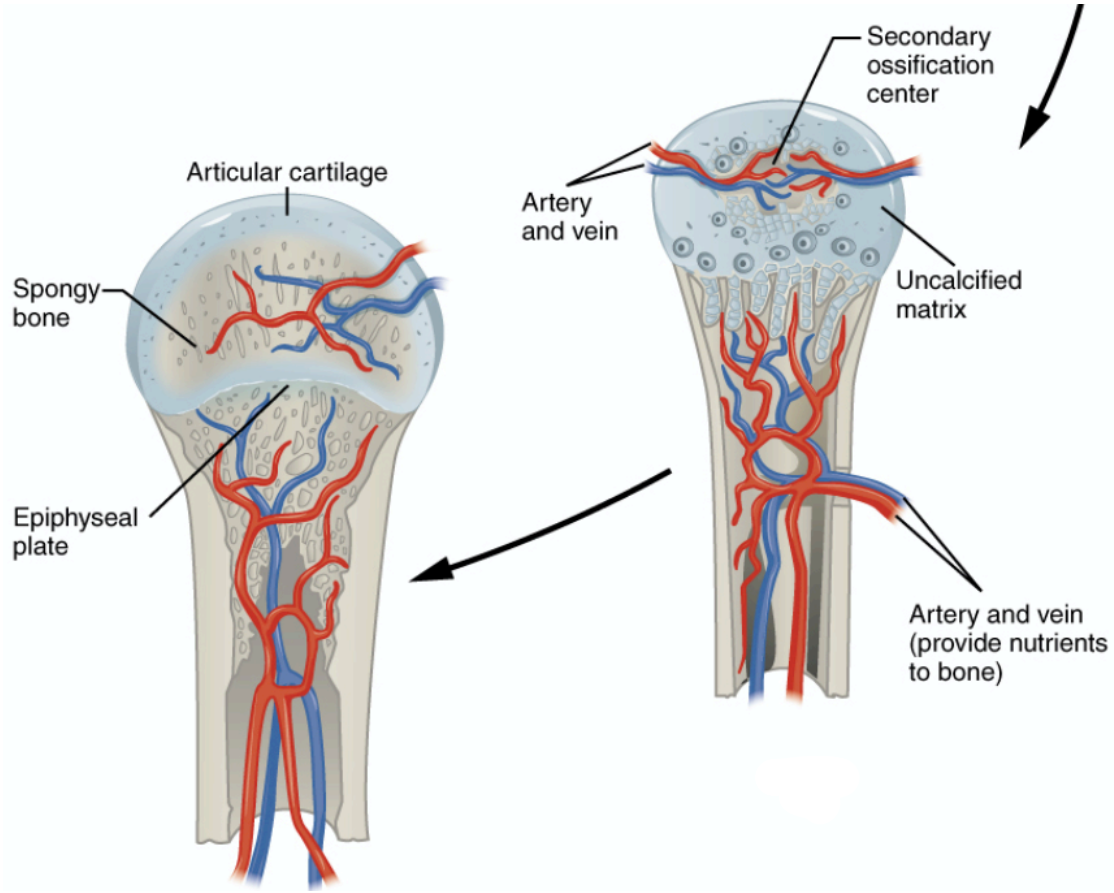

Figure 2.3: Growth plate showing secondary ossification. The epiphyseal plate elongates during childhood and adolescence, which is when human grow in size (Betts et al. 2013).

2.2.2. Intramembranous ossification

Bone formation also occurs by a process called intramembranous ossification during embryonic development (Figure 2.4). This process regulates the formation of non-long bones, such as bones of the skull, clavicle, and ribs. Unlike endochondral ossification, the formation of a cartilage template does not proceed bone formation in intramembranous ossification. Instead stem cells divide, condense and then aggregate together to form a nodule surrounded

by a membrane. Next, differentiation of MSCs inside the membrane occurs towards osteoprogenitors and osteoblasts. The osteoblasts line the membrane nodule and begin to secrete ECM comprising of type I collagen fibrils within the centre of the nodule. Some osteoblasts begin to embed themselves into the bone matrix and differentiate into osteocytes by forming cytoplasmic processes, which creates an interconnecting network with other osteocytes. Osteoblast cells in the outer surface of this new bone matrix form a periosteum, and bone growth continues to create the trabeculae. Over time, the trabeculae fuse to form a woven bone, which is remodelled to become a lamellar structure, with concentric lamellae surrounding Haversian systems, known as an osteon (Chung et al. 2004; Kanczler and Oreffo 2008; Cowin 2001).

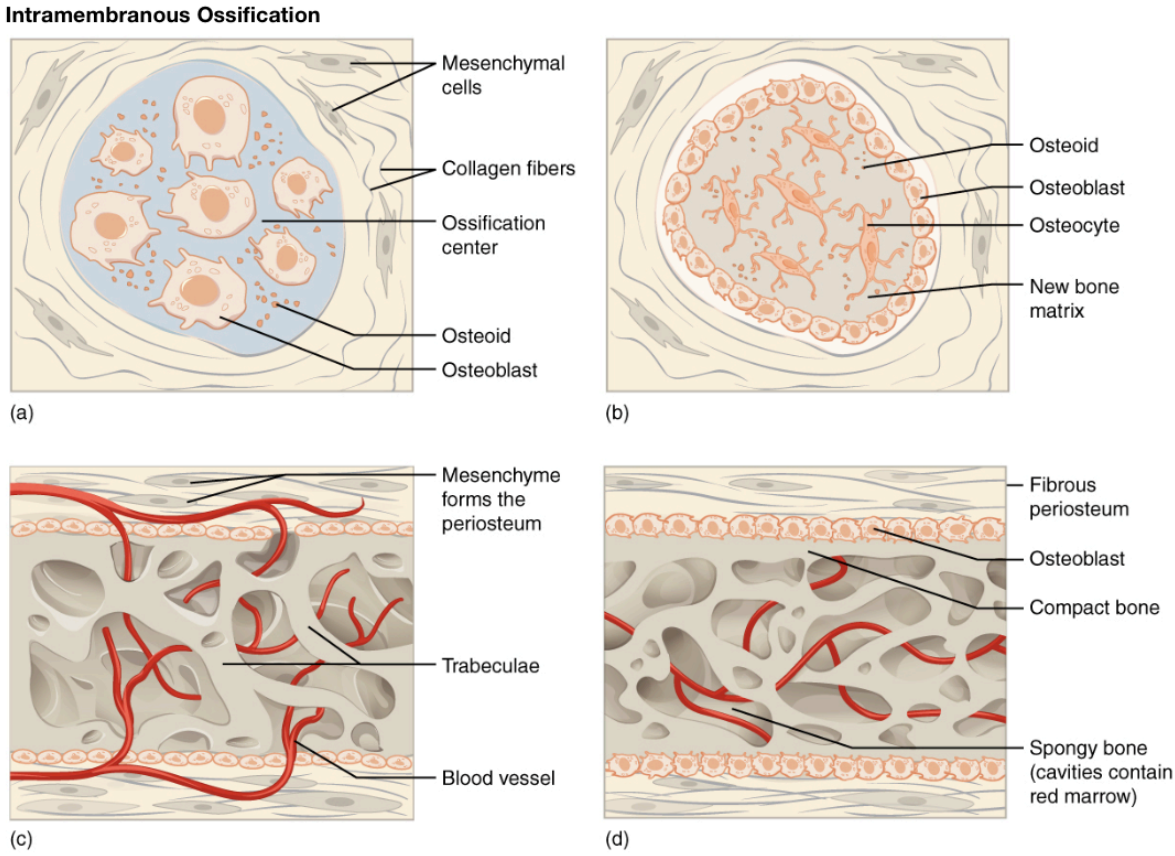

Figure 2.4: Diagram of intramembranous ossification showing aggregation of MSCs, which induces the formation of a membrane comprising bone lining cells. Cells inside the membrane start to differentiate and create a matrix, ultimately forming trabecular bone (Betts et al. 2013).

2.3. Bone as a Natural Material

Bone is an adaptive material under constant modelling and remodelling, which is a response to forces exerted onto the bone in everyday physical activity (Carter 1984; Forwood and Turner 1995; Jee, Li, and Schaffler 1991; Mosley and Lanyon 1998; Woo et al. 1981; Oconnor, Lanyon, and Macfie 1982). Bone modelling and remodelling is a physiological process that continuously alters and renews the shape of bone by making micro changes in bone mass and microstructural architecture. Bone modelling is a process where bone shape is modified, while bone remodelling is a process of bone repair and renewal. These two processes are orchestrated by the actions of osteoblast and osteoclast cells, which are regulated by osteocytes (Bonewald and Johnson 2008; Nakashima et al. 2011; Xiong et al. 2011; Xiong et al. 2015). Microcracks occur in bone, and this is regenerated through a process known as fracture healing, which also renews bone in macro fractures (McKibbin 1978; Einhorn 1998). The bone physiological adaptive process allows bone to survive and adapt under diverse loading conditions (McNamara 2011). This adaptive property of bone is facilitated by residing specialised cells on the bone surfaces, bone marrow and blood vessels. These special cells constantly remove bone from damaged sites and replace it with newly formed bone mineral (Frost 1990). Each of these cells will be discussed further in Section 2.4.

2.3.1. Bone modelling

Bone modelling is a process by which bone forms its shape during development throughout childhood and adolescence, and continues throughout adulthood in response to mechanical loading in everyday life. Osteoclasts (bone resorption cells) resorb bone, and osteoblasts (bone forming cells) form new bone, working together to shape bone during the modelling process. This process is different from bone remodelling because of an overall alteration in bone morphology (Frost 1990).

2.3.2. Bone Remodelling

Bone remodelling is a process controlled primarily by cells (Parfitt 1987, 1994), whereby osteoclasts move along the bone surface to resorb any unwanted or damaged bone tissue while osteoblasts follow closely behind to fill in the resorption cavity with new bone. This coordination and harmonised partnership is known as the Basic Multi-cellular Unit (BMU), and it occurs in six successive phases: resting, activation, resorption, reversal, formation and mineralisation (Frost 1973; Cowin 1989), discussed further in Section 2.4. Bone mass and strength is preserved because this cellular activity is continuously active during bone physiology.

2.3.3. Fracture Healing

Bone fracture healing occurs when traumatic injuries or certain diseases lead to bone fractures, where repair is needed to restore the bone to its normal physiological shape. Fracture healing is a process to repair the site of damage and it is carried out through a synchronised activity of osteoprogenitor, chondroblast and osteoblast cells (McKibbin 1978; Einhorn 1998). Figure 2.5 is an illustration of the fracture healing process, where damage and bleeding has occurred leading to recruitment of inflammatory cells, forming a hematoma. These cells begin to form a granulation tissue consisting of blood vessels with the invasion of immune cells, which engulf damaged and unwanted tissues and debris. This inflammatory phase usually lasts 3 – 7 days. The next stage is the reparative phase, which lasts for approximately one month, and is initiated by the differentiation of osteoprogenitor cells into osteoblasts or fibroblasts. Osteoblast cells are responsible for producing woven bone, which forms the periosteal and marrow callus to fill in the fracture space. Fibroblasts differentiate into chondrocytes and form the hyaline cartilage to create a fracture callus (Tsiridis, Upadhyay, and Giannoudis 2007). Woven bone inside the callus has a low mechanical stiffness compared to the surrounding native bone. The cross-sectional area of the callus is therefore larger in order to compensate for the lower mechanical

stiffness. This woven bone is eventually remodelled to become lamellar bone with vascularisation, and the cartilage undergoes endochondral ossification. Over time, the callus will remain present under bone modelling and bone remodelling phases to shape the healed fracture site into its original geometry, strength and stiffness, which is dependent of the mechanical forces applied to the bone (McNamara 2011; Tsiridis, Upadhyay, and Giannoudis 2007; McKibbin 1978).

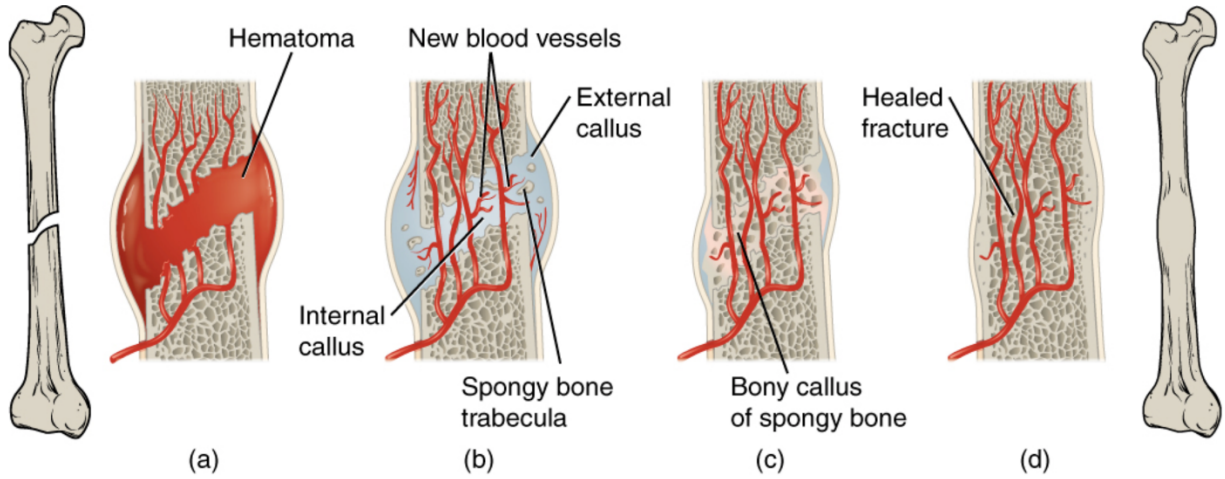

Figure 2.5: Schematic of the fracture healing process. A hematoma is formed, leading to recruitment of immune and blood cells, followed by formation of woven bone by osteoblast cells occurs and a callus is formed. Over time this callus is reshaped by bone remodelling (Betts et al. 2013).

2.4. Bone Cells

Bone cells make up the organic phase of bone, and there are different types of bone cells that have different roles in bone remodelling. Mesenchymal stem cells (MSCs) play an important role by differentiating into osteoprogenitor cells, which are precursors for osteoblast cells. Osteoblasts are responsible for bone formation (Aubin 2001; Cowin 2001), while osteoclasts resorb bone mineral (Watanabe, Yanagisawa, and Sasaki 1995). The fine balance between these two cells is a process called bone remodelling and they make up the Basic Multi-cellular unit (BMU), as seen in Figure 2.6. Osteoblasts mature into osteocytes to form the structure of

bone matrix. The coordination of each of these cell types in bone formation, resorption, and remodelling dictates the unique behaviour of bone as a material (McNamara 2011), as is described below.

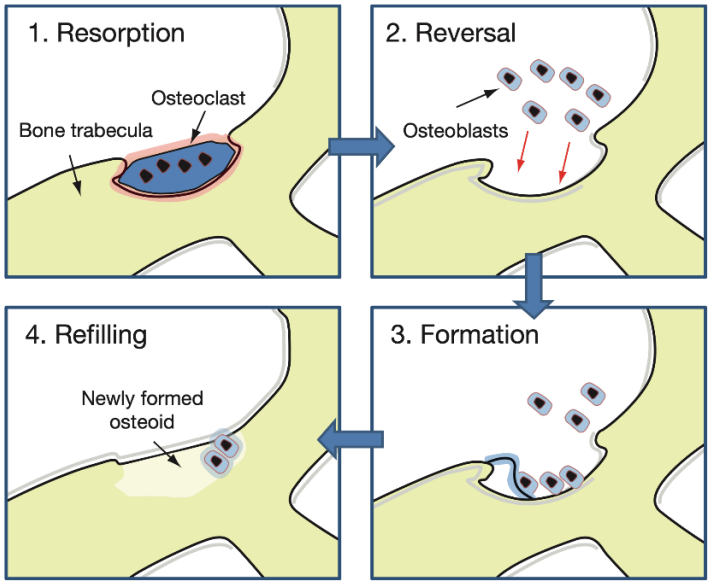

Figure 2.6: Basic Multi-cellular unit cell system, where osteoclast cells resorb bone and osteoblast cells fill in the area of resorption by laying down new bone (McNamara 2011).

2.4.1. Mesenchymal Stem Cells and Osteoprogenitors

Mesenchymal stem cells (MSCs) are nonspecialised cells that capable of differentiating into multiple pathways for tissue regeneration, and these pathways include osteogenesis, chondrogenesis, adipogenesis, and myogenesis. These cells play an important role during embryo development, and later in life they reside in the bone marrow, periosteum and endosteum, from where they may be recruited to initiate tissue regeneration. During bone remodelling, growth factors, cytokines, and mechanical stimuli induce MSCs to differentiate into osteoprogenitor cells that can thereafter commit to the chondrogenic or osteogenic pathway to form cartilage or bone cells, respectively (McNamara 2011).

Bone marrow cells are important for bone healing, because MSCs and osteoprogenitors reside here, along with hematopoietic cells, adipocytes and immune cells, such as T cells and

macrophages. Bone healing is initiated when biochemical cues are sent to MSCs to induce differentiation into osteoprogenitors, leading to osteogenesis (Subbiah et al. 2015). MSCs are also influenced by mechanical cues, which are observed in a bone niche environment. When osteoprogenitors receive biochemical and mechanical cues, they differentiate into osteoblast cells (Okazaki et al. 2002), which are responsible for the production of bone by laying down bone matrix and minerals. Their main function is to produce new bone when micro-damage occurs or in the replacement of aged bone and repair fractures. They form new bone by secreting osteoid, which is an organic extracellular matrix composed of collagen type I (Aubin 2001). Osteoid is formed by the presence of alkaline phosphatase (ALP), a glycoprotein enzyme found in the plasma membrane of osteoblasts in the early stages of mineralisation that removes inhibitor proteins for mineral deposition (Clarke 2008). ALP also provide an attachment site for mineral nucleation along the collagen fibrils, and it is vital for increasing local phosphate concentration (Cowin 2001). Known as an early marker for bone regeneration, production of ALP leads to an upregulation of osteocalcin (OCN), osteopontin (OPN) and bone sialoprotein (BSP) expression, which is deposited onto the bone matrix to be mineralised (Aubin 2001). During the process of new bone formation, osteoblasts become embedded in the bone matrix by surrounding themselves with minerals, and then mature into osteocytes, forming the matrix structure of bone. Osteoblasts that do not become osteocytes become bone lining cells, and they reside on the bone surface as quiescent osteoblasts (Mulcahy 2012; McNamara 2011). It is believed that bone lining cells act as a functional membrane on the bone surface, and they regulate exchange of fluids and ions to initiate bone resorption and remodelling, as well as playing an important role in the marrow stromal system (Miller et al. 1989).

2.4.2. Osteocytes

Osteocytes are the most abundant bone cell type, making up 90% of all cells in mature bone (Kato et al. 1997; Bonewald 2011). Representing the terminal differentiation of the osteogenic lineage, they are embedded within the bone matrix, where they are immobilised to play a structural role (Frost 1960a), as shown in Figure 2.7. When osteoblast cells terminally differentiate into osteocytes, their anabolic activity changes as well as losing much of their organelles. Here, osteoblast morphology changes from a cuboidal shape into a cell body with many dendritic processes that extend in an unorganised pattern towards nearby cells, the vascular space, and the bone surface (Bonewald 2011). Osteocytes produce bone matrix non-collagenous proteins such as osteocalcin (OCN), osteopontin (OPN), and dentin matrix 1 (DMP1), and they also produce hyaluronic acid (HA) and proteoglycans (Noonan et al. 1996; Noble 2008; Thompson et al. 2011).

Osteocytes are believed to play a role as mechanosensors, where they sense their mechanical environment and communicate with their neighbours through a complex network of communication using their processes (Cowin, Weinbaum, and Zeng 1995; Bonewald 2002). These mechanosensors are important for monitoring bone remodelling throughout life, providing signals to nearby cells to initiate bone resorption and formation. The intricate balance of these two functions is monitored by osteocytes to adapt to altered mechanical demands or repair tissue caused by bone injury and fractures (McKibbin 1978; Einhorn 1998). Osteocytes express inhibitors of the Wnt pathway such as DKK1, sFRP1 and sclerostin, a negative regulator for bone formation (Bonewald 2011; Dallas, Prideaux, and Bonewald 2013; Prideaux, Findlay, and Atkins 2016). The Wnt pathway is known to regulate the differentiation of osteoblast cells from their early precursors (Bonewald and Johnson 2008). Receptor Activator Nuclear factor-kB Ligand (RANKL) from osteocytes is responsible for bone remodelling

(Xiong et al. 2011; Xiong et al. 2015; Nakashima et al. 2011). This ligand binds to the RANK receptor on osteoclast precursors to induce osteoclastogenesis, as discussed below.

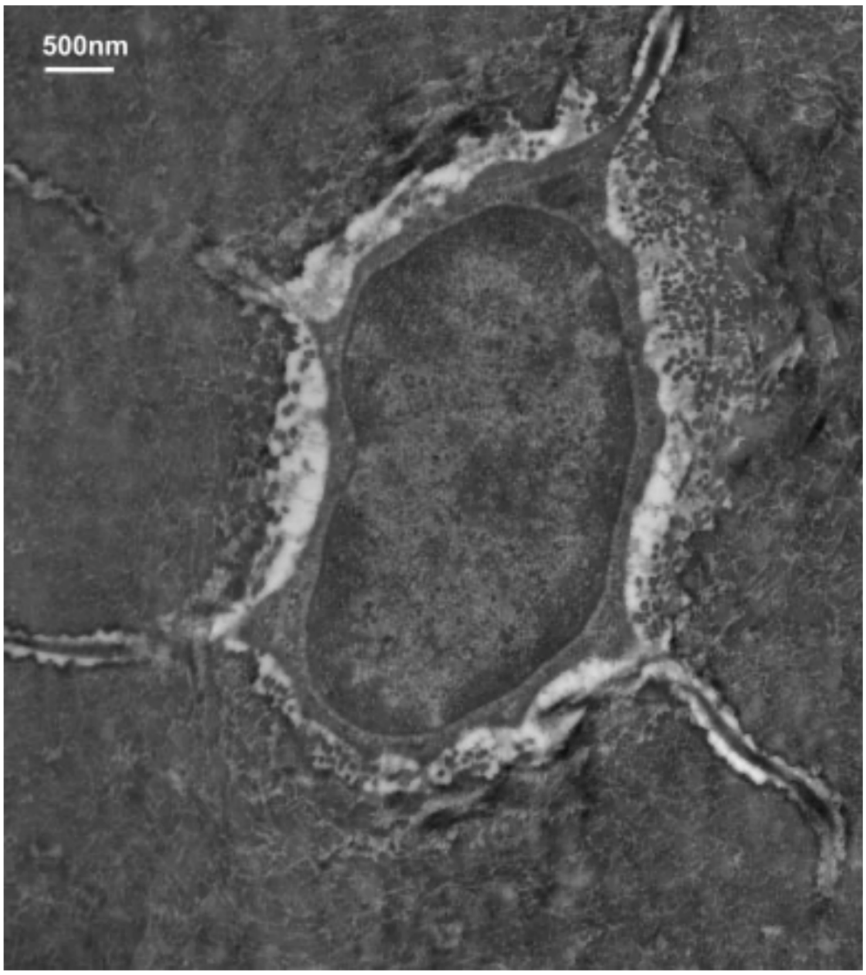

Figure 2.7: TEM image of osteocyte in a lacunar-canalicular system using acrolein fixation method (McNamara et al. 2009).

2.4.3. Osteoclasts

Osteoclasts are multinucleated cells, derived from precursor stem cells of the macrophage lineage, known as bone marrow stromal cells of monocytes, and they reside in the hematopoietic bone marrow (You et al. 2001). They are commonly found in the small depressions called Howship's lacunae during the resorption process (Watanabe, Yanagisawa, and Sasaki 1995; Udagawa et al. 1990). Their role is to resorb bone by digesting damaged and

aged bone during the physiological process of modelling and remodelling. Resorption takes place when bone lining cells begin to degrade osteoid and secrete growth factors for recruitment of pro-osteoclast cells and monocytes, which fuse together to form active, mature osteoclasts with multiple nuclei and a ruffled cell membrane border for attachment onto the bone surface. This ruffled border is essential for maximizing the release of hydrogen ions, which acidify and dissolve calcium and phosphate minerals in the bone matrix. The digested components of the matrix are then packaged into small vesicles and released into the extracellular fluid as waste products. Osteoclastogenesis begins with the secretion of pro-osteoclastogenic factors, which include the Receptor Activator Nuclear factor-kB Ligand (RANKL), the macrophage colony-stimulating factor (MCSF), and osteoprotegerin (OPG). RANKL is a surface ligand on osteoblast and bone lining cells, and it binds to the RANK receptor on the surface of osteoclast precursor cells to induce the differentiation of mature multinucleated osteoclast cells. OPG is produced by osteoblasts as a soluble decoy receptor for RANKL to prevent osteoclast formation and bone resorption (McNamara 2011; Boyce and Xing 2008). The recruitment and differentiation of osteoclast cells is controlled by hormonal and growth factors (Cowin 2001) and these include oestrogen, vitamin D, and parathyroid hormone (PTH), bone morphogenetic protein 2 (BMP-2), transforming growth factor β (TGF-β), and calcitonin. These factors inhibit osteoclast differentiation and maturation (Cowin 2001; Filvaroff and Derynck 1998; Boyle, Simonet, and Lacey 2003).

2.5. Cell Apoptosis and Necrosis

There are two forms of cell death, necrosis and apoptosis, categorised according to the nature of their cellular death (Figure 2.8). Cell death by necrosis is a premature death and it is caused by an external factor, such as tissue exposure to poison, trauma, and infections. On the other hand, cell apoptosis is a programmed cell death, that commonly arises in cells that have reached

the end of their lifespan and are signalled to commit suicide, but also occurs under thermal stress conditions wherein temperatures elevation exceeds 47°C (Dolan et al. 2012; Dolan et al. 2015; Dolan et al. 2016).

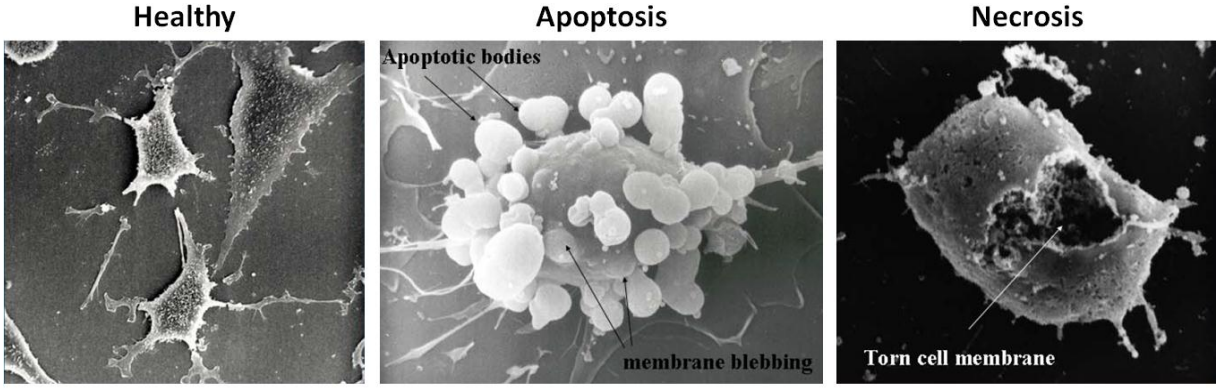

Figure 2.8: Image of healthy, apoptotic, and necrotic cells showing morphological differences between each type of cell death (Noble 2003c).

There are morphological differences between cells that are necrotic and apoptotic. Cells undergoing necrosis are characterised by passive cell swelling, deterioration of cell organelles and loss of internal homeostasis, whereby the cell membrane is lysed, as shown in Figure 2.8 (Bonfoco et al. 1995; Wylie, Kerr, and Currie 1980; Noble 2003c). Figure 2.8 also shows apoptotic cells, which are characterised by cell shrinkage, retention of organelles, condensation and margination of the chromatin, changes in their nuclear membrane, protein fragmentation and cleavage of DNA (Noble 2003c; Wylie, Kerr, and Currie 1980; Hengartner 2000). Once these cellular contents have been disassembled, they are packaged into vesicles as apoptotic bodies with or without nuclear fragments. Specific membrane surface markers signal their removal by phagocytotic cells, such as macrophages, parenchymal cells and neoplastic cells, which degrade the cellular components (Hengartner 2000; Kogianni, Mann, and Noble 2008; Savill and Fadok 2000).

Cell apoptosis is initiated either through an intrinsic or extrinsic pathway. The intrinsic pathway is a non-receptor mediated stimulus and involves intracellular cues, such as DNA

damage, to signal cell death. These intracellular cues create a knock on effect to supress death inhibitors, and thereby trigger apoptosis. Stimuli induce changes in the inner mitochondrial membrane to release two groups of normally sequestered pro-apoptotic proteins from the intermembrane space into the cytosol (Saelens et al. 2004). Cytochrome c and serine proteases HtrA2/Omi work to bind and activate Apaf-1 as well as procaspase 9 to form an apoptosome (Du et al. 2000; Garrido et al. 2006; Chinnaiyan 1999; Hill et al. 2004). The second group, AIF, endonuclease G and CAD are released from the mitochondria after the cell has committed to death. Their role is to cause DNA fragmentation and condensation of peripheral nuclear chromatin (Joza et al. 2001). The extrinsic pathway is initiated by external biochemical cues, such as ligands (TNF-α/TNFR1, Apo3L/DR3, Apo2L/DR4, Apo2L/DR5) binding to the death receptors that are members of the tumour necrosis factor (TNF) receptor gene super family (Chicheportiche et al. 1997; Ashkenazi and Dixit 1998; Peter and Krammer 1998; Suliman et al. 2001; Rubio-Moscardo et al. 2005; Locksley, Killeen, and Lenardo 2001). Members of this family have a cytoplasmic domain called the death domain which, when bound, transmits a death signal from the cell surface to the intracellular signalling pathways (Ashkenazi and Dixit 1998). Clustering of membrane-bound receptors and binding of trimeric homologous ligands leads to recruitment of cytoplasmic adapter proteins FADD and RIP (Wajant 2002; Hsu, Xiong, and Goeddel 1995), which is associated with procaspase-8 via dimerization of the death effector domain, resulting in auto-catalytic activation of procaspase-8 (Kischkel et al. 1995). The activation of either Caspase-8 or Caspase-9 leads to cleavage of Caspase-3, which is a marker for active apoptosis (Crowley and Waterhouse 2016).

Thermal stress conditions initiate bone healing by inducing cells to express heat shock proteins and growth factors such as osteopontin (OPN) and osteocalcin (OCN) for bone remodelling (Chung and Rylander 2012). In this study MC3T3 cells were exposed to a slight elevation in temperature (44°C) for short durations of 10 minutes, and it was reported that

mRNA expression of OPN and OCN were higher at 8 hours and 24 hours after heat treatment, compared to control cells which were not exposed to heat treatment (Chung and Rylander 2012). Another study assessed the remodelling signalling cascade in osteocyte-like (MLOY4) cells exposed to moderate temperature elevations (47°C) for 1 minute durations (Dolan et al. 2015). In this study, cell apoptosis and necrosis were observed in the MLOY4 cells exposed to heat treatment at 47°C, and when these cells were co-cultured with control MLOY4 cells (37°C), higher expression of COX2, ALP and calcium were also observed (Dolan et al. 2015). Furthermore, an in vivo study conducted by the same author demonstrated thermally induced cell apoptosis in bone (rat tibia) exposed to a thermal probe at 47°C and 60°C for 1 minute duration, and cells in the vicinity of thermal damage had expressed an upregulation of osteogenic genes, COX2 and RANKL (Dolan et al. 2016). These studies confirm that thermally induced cell apoptosis can initiate a bone healing response in bone cells. In comparison to a controlled cell signalling response in cell apoptosis, the cellular membrane of necrotic cells are lysed whereby cellular content is released, and these contents contain pro-inflammatory signals which induce inflammation and a healing response (Majno, Lagattuta, and Thompson 1960).

2.6. Surgical Cutting

Cutting tools include the high speed bone mill (Figure 2.9A), which cuts by milling a large piece of autograft such as one from the iliac crest into morselised autograft bone for implantation into small spaces, and the ultrasonic device (Figure 2.9B), which cuts by creating tiny vibrations on the tissue. Most cutting tools induce heat, especially high speed orthopaedic drills, oscillating saws, and round surgical burs, which are known to induce temperatures of more than 47°C on bone. The extent of tissue and cellular damage as a response to this temperature has been explored using orthopaedic drills. Different parameters affecting heat generation has been investigated in an effort to decrease temperature elevation and limit

osteonecrosis. The cellular response to thermal damage has also been explored by artificially inducing temperature, where heat treatment (>37°C) for short (< 10 minute) and long (>1 hour) durations were investigated (Dolan et al. 2015; Dolan et al. 2016; Eriksson and Albrektsson 1983; Eriksson, Albrektsson, and Magnusson 1984; Eriksson and Albrektsson 1984; Norgaard, Kassem, and Rattan 2006).

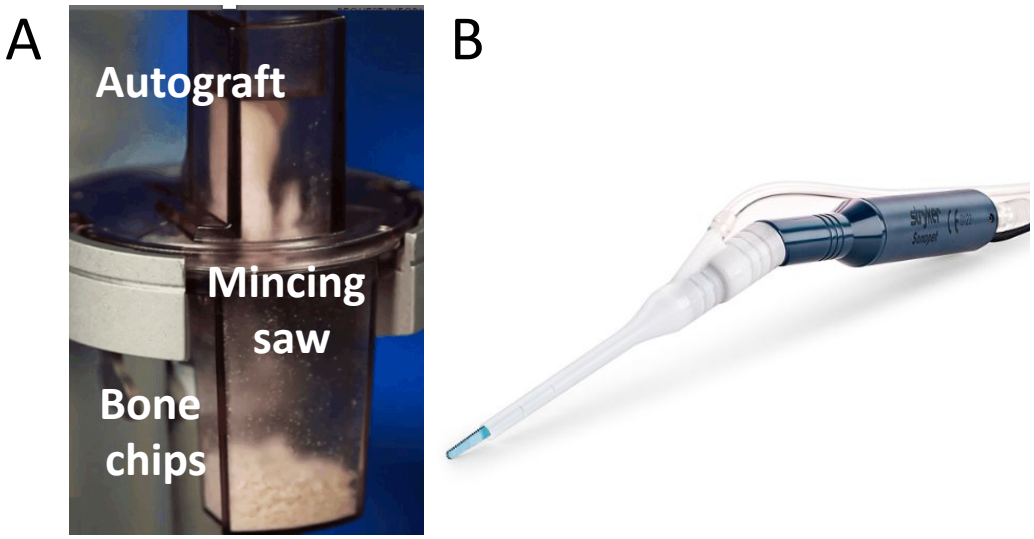

Figure 2.9: Cutting instruments A) bone mill process large bone into small autograft B) SONOPET ultrasonic cutting device that simultaneously cuts and removes waste tissue during surgery (Stryker).

2.6.1. Heat Generation Caused by High Speed Cutting Tools

Post-operative bone healing after bone resection is associated with the mechanical forces and temperature elevations generated by surgical cutting tools (Dolan et al. 2012; Karaca, Aksakal, and Kom 2011). High speed surgical instruments generate heat and create mechanical loading onto the bone during cutting. Temperature elevations have been reported for orthopaedic drills (Sener et al. 2009; Karaca, Aksakal, and Kom 2011; Saha, Pal, and Albright 1982; Davidson and James 2003; Matthews and Hirsch 1972b; Augustin G 2008; Matthes M 2018), where parameters such as spindle speed, feed rate, depth of drilling, cutting flute designs, and forces have been extensively studied (Karaca, Aksakal, and Kom 2011; Davidson and James 2003; Saha, Pal, and Albright 1982; Matthews and Hirsch 1972a). Temperature elevations are

influenced by cortical thickness depending on mineralisation distribution and porosity of the bone (Toews et al. 1999). For example, a surgical drill used on a canine femur with a cortical thickness of 3.5 mm created lower temperature (56 ± 1.5°C) compared to a human femur (89 ± 4.9°C), which has a cortical thickness of 6.5 mm (Eriksson, Albrektsson, and Albrektsson 1984). Moreover, cortical bone experiences higher temperature elevations than trabecular bone, because bone mineral density is higher in cortical bone (Karaca, Aksakal, and Kom 2011). Heat generation above 47°C causes osteonecrosis, and temperatures above this threshold have been quantified to occur during cutting with orthopaedic twist drills (Karaca, Aksakal, and Kom 2011) and surgical saws (Dolan, Vaughan, Niebur, Casey, et al. 2014).

One study investigated the effect of feed rate and drill speed on osteonecrosis and temperature elevations (Karaca, Aksakal, and Kom 2011). They reported a high drill force (100N) led to lower temperature generation (57°C), compared to a force of 40N generating a temperature of 83°C on bovine tibia which was measured by a T-type thermocouple 0.5 mm away. They also reported lower temperature (<57°C) for lower bone densities (<2.051 g/cm^3) when the force applied was 40N and 70N, where osteonecrosis was observed 150 μm away from the cut site when these lower temperatures were generated. Another study used experimental and computational methods to explore the influence of blade design and feed rate on temperature elevations (Dolan, Vaughan, Niebur, Casey, et al. 2014). It was reported that operating at a lower feed rate (50 mm/min vs. 150 mm/min) led to lower temperature generation (<53.78 ± 2.54°C measured by a thermal camera) (Dolan, Vaughan, Niebur, Casey, et al. 2014). A blade design with a unique centre region removed induced lower temperature elevations, when compared to a conventional solid blade (Dolan, Vaughan, Niebur, Casey, et al. 2014). This unique design also resulted in higher force of 20.14 ± 5.13N and 9.90 ± 1.22N, compared to 9.99 ± 0.51N and 4.85 ± 0.21N for feed rates, 150 mm/min and 50 mm/min

respectively. This corroborated other studies also reporting higher force leading to decreased temperature generation (Karaca, Aksakal, and Kom 2011; Matthews and Hirsch 1972a).

Another high speed surgical cutting tool is a surgical round bur, which is used in spinal laminectomy and vertebrae resection during spinal fusion surgery. The design of the bur (diameter size, 2Flute, Multi-Flute) affects the viability of cells in the bone dust resected with these burs (Roth AA 2017). Temperature is also affected because of the contact surface between the cutting flutes and the bone tissue, which creates frictional heat during cutting (Davidson and James 2003). High frictional heat is dependent on the feed rate, which also increases with dull cutting flutes (Davidson and James 2003).

2.6.2. Cellular Response to Thermal Damage

It is well established that temperature above 47°C is detrimental to cells in vitro and in vivo (Eriksson, Albrektsson, and Magnusson 1984; Eriksson, Albrektsson, and Albrektsson 1984; Eriksson and Albrektsson 1984; Dolan et al. 2015; Dolan et al. 2016). However, a slight increase in temperature for short (30 seconds, 1 minute) and long (>1 hour) durations has been shown to enhance osteogenic response in bone cells, when compared to physiological temperature (37°C) (Chung and Rylander 2012; Norgaard, Kassem, and Rattan 2006; Dolan et al. 2012; Dolan et al. 2015; Dolan et al. 2016). In a study carried out by (Dolan et al. 2015) MLO-Y4 cells subjected to 47°C were necrotic and apoptotic compared to control cells (37°C) which had a healthy cell morphology. They reported an upregulation of COX2 (osteoblast differentiation marker) in co-culture of 37°C MLO-Y4 cells with heat treated MLO-Y4 cells (47°C for 1 minute) compared to control group (37°C MLO-Y4 with 37°C MLO-Y4 cells). Moreover, higher osteogenic expression (ALP activity and calcium deposition) were observed in co-culture of heat treated MLO-Y4 cells with BALB/c MSCs with no heat treatment, compared to control co-culture, which received no heat treatment. Cells underwent cell death

as a response to temperature elevation during heat treatment, but this response initiated an osteogenic response in MLO-Y4 cells and BALB/c MSCs (Dolan et al. 2015). In an in vivo study by the same author, the surface of tibiae of Sprague-Dawley rats were heat treated with 47°C and 60°C for 1 minute duration with a thermo probe, which resulted in thermally induced apoptotic cells in the area where the thermo probe was used (Dolan et al. 2016). They also reported an upregulation in gene expression for bone healing (RANKL, OPG, COX2) in osteocyte-enriched segment of rat tibia after heat treatment to 47°C and 60°C for 1 minute. These studies suggest that a slight increase in temperature for short duration could have a beneficial effect on the regenerative capacity of bone resected with high speed cutting tools which induce heat generation.

Thermally induced cellular apoptosis and necrosis are a response to thermal damage when cells are exposed to temperatures above 47°C (Dolan et al. 2012; Dolan et al. 2015; Dolan et al. 2016). The effect of heat on bone regeneration has been investigated using a bone growth chamber, which was implanted in rabbits (tibial metaphysis) to assess tissue growth after four weeks of recovery from heat exposure to 44°C, 47°C, and 50°C for 1 minute durations (Eriksson and Albrektsson 1984). In this in vivo study heat was induced by an electric heater attached to the top of a thermal glass chamber implanted into the rabbit tibia, where a thermocouple was embedded in the bone in the narrow canal side of the chamber. They reported a disturbance of regenerative capacity at a temperature of 47°C, whereby only blood clots were seen in bone subjected to 50°C, whereas bone ingrowth was observed in both the 47°C and 44°C groups. In another study by the same author, rabbit femurs exposed to heat trauma (60°C for 1 minute) led to a permanent cessation of blood flow and bone tissue necrosis (empty lacunae), which showed no sign of repair following 100 days recovery (Eriksson, Albrektsson, and Magnusson 1984). They reported a 10 μm wide zone of empty osteocyte lacunae in their histological stains. Moreover, high speed cutting tools are known to generate

high temperatures (> 60°C), and some have been recorded to elicit temperatures higher than 100°C using a thermal camera or thermocouple (Karaca, Aksakal, and Kom 2011; Dolan, Vaughan, Niebur, Casey, et al. 2014; Eriksson and Albrektsson 1984; Eriksson, Albrektsson, and Magnusson 1984; Xu et al. 2014; Matthes et al. 2018; Livingston et al. 2015; Hosono et al. 2009).

2.6.3. Tissue and Thermal Damage Induced by Cutting with a High Speed Bur

Cutting with high speed drills will induce tissue and thermal damage, where heat generated during cutting affect cell viability and osteogenic potential (Roth AA 2017; Ye et al. 2013; Eder et al. 2011; Kuttenberger, Polska, and Schaefer 2013; Karaca, Aksakal, and Kom 2011; Livingston et al. 2015; Sener et al. 2009). No study has been conducted on thermal damage induced by cutting with surgical burs. Bone dust autograft is used for spinal fusion surgeries, and it has been shown to contain viable cells that have osteogenic, osteo-inductive, and osteoconductive properties (Patel et al. 2009; Gao et al. 2018; Kuttenberger, Polska, and Schaefer 2013; Eder et al. 2011; Roth AA 2017). Previous studies only investigated viability and osteogenic potential of bone resected with surgical burs. They reported bone chips have more bone mineral and intact tissue structure for regeneration, compared to bone dust (Ye et al. 2013; Eder et al. 2011). Bone chips are harvested with rongeurs or Kerrisons, which resemble scissors. One study using bone dust from patients undergoing lumbar spinal surgery reported higher viability and mineralisation in laminectomy bone chips, because their lamellar structure is more intact (Eder et al. 2011). Another study reported higher resorption in human bone dust groups compared to human iliac bone chips, when ectopically implanted in rats (Ye et al. 2013). They also reported lower viability (MTT assay), less ALP activity, and higher TRAP staining in cells from bone dust groups, where tissue staining showed decrease in osteoblast cells compared to staining of bone chips groups (Eder et al. 2011). However, a

comparison between bone dust and bone chips is not a full assessment of the regenerative capacity of bone dust, because both were resected in different cutting temperature conditions.

Bone dust are resected with a high speed cutting bur, which induces temperatures above 47°C (Hosono et al. 2009; Shin and Yoon 2006), and it has been shown to have osteogenic potential (Kuttenberger, Polska, and Schaefer 2013; Roth AA 2017). One study compared bone dust resected with burs of different designs (6mm 2Flute, 6mm Multi-Flute, 4mm 2Flute, or 4mm Multi-Flute). Mineralisation, assessed by Alizarin red staining, was not significant between all the bur groups, but a high concentration of positive osteoid could be observed around the edges of the bone dust (Roth AA 2017). Gene expression of osteoblast markers (ALP, COL1a, osteonectin) and osteocalcin were observed in all bone dust groups, as assessed by polymerase chain reaction (PCR). Bone dust size was quantified using haematoxylin and eosin (H&E) staining images, and they reported that the 6 mm 2Flute generated large bone dust ($112{,}632 \pm 14{,}216\ \mu m^2$) and had a higher cell concentration (cells/µg bone) after two weeks in culture, when compared to bone dust prepared using a 6 mm Multi-Flute ($66{,}637 \pm 8{,}387\ \mu m^2$) (Roth AA 2017). This was relevant because previous studies have shown that more bone structure remained intact where bone dust sizes were larger. However, thermal damage in the form of cell apoptosis and necrosis was not assessed in this study, and it is not known whether irrigation was used, which is another variable influencing heat generation and thermal damage during surgical cutting.

It is difficult to separately assess osteogenic response of surgically cut bone induced by thermal and mechanical stress, because bone is simultaneously exposed to both stress factors during high speed cutting. Separate in vivo experiments using either thermal stimulation or mechanical stimulation need to be conducted side by side. Recently, a previous study has assessed the thermally induced osteogenic response in a rat tibia, whereby there was an increase in gene expression of COX2 (Dolan et al. 2016), which is an enzyme that promotes

osteoblastogenic differentiation by producing prostaglandins during bone repair (Zhang et al. 2002). This study was conducted using thermal stimulation only under no mechanical stress, and so it was determined that thermal stress had led to cell apoptosis and an increase in osteogenic genes such as COX2, RANKL, and OPG (Dolan et al. 2016). No study has been conducted to assess the effects of mechanical stimulation representative of cutting on bone, and this assessment would add further knowledge on whether thermal or mechanical stress alone or simultaneously plays a crucial role on the osteogenic response in surgically cut bone.

2.6.4. High speed cutting in the presence of irrigation

In order to minimise temperature elevation, high speed drills and sagittal saws are irrigated during cutting, and thus limiting thermally induced osteonecrosis. Studies have shown that irrigation during orthopaedic surgery significantly decrease temperature elevations compared to cutting with no irrigation, even below body temperature of 37°C (Livingston et al. 2015; Hosono et al. 2009; Sener et al. 2009). However, the effects of irrigation on the bone dust and the cut site during spinal surgery have not been investigated. Previous studies have only reported temperature data and not cell viability or mineralisation potential (Livingston et al. 2015; Sener et al. 2009). One study measured the magnitude of temperature generated by cutting with surgical burs on sheep vertebrae using a thermal camera and thermocouple, comparing temperature elevation between dry cutting and cutting with continuous irrigation (Livingston et al. 2015). Temperature generated during cutting in the presence of irrigation was significantly lower than heat generated during dry cutting, where the thermal camera recorded significantly higher temperatures (71.1±14.7°C dry, 43.3±6.25°C irrigation) than the thermocouple (25±0.9°C dry, 22±1.9°C irrigation). Another study assessed temperature generated by cutting with an orthopaedic drill on 37°C bovine mandibles, using a thermocouple to measure temperature elevations and continuous irrigation at 10°C and 25°C (Sener et al. 2009). Cutting in the presence of irrigation, both 10°C and 25°C, significantly decreased

temperature elevation (<37°C) compared to cutting without irrigation (>37°C). They reported temperatures below physiological temperature, maintained using a water bath, but they did not further assess the cellular response as it would be influenced by irrigation temperature. Thus, there still remains a lack of knowledge in the regenerative response of bone subjected to cutting with irrigation.

2.6.5. Autogenous bone grafting

A large defect space where the fracture healing process cannot spontaneously take place is called a critical size defect (CSD). The gold standard treatment is to use an autogenous bone graft, which is resected from another location on the skeleton (usually from the iliac crest). This is the gold standard material because it contains the native growth factors and cells needed for bone repair. The size of the graft is dependent on the CSD. However, obtaining autograft creates donor site morbidity, which is painful for a patient. Autograft bone dust obtained from resection with surgical burs can be used as space filler in spinal fusion surgery such as lumbar interbody fusion, where a spinal cage is inserted into the intervertebral disc space with or without bone dust autograft material with the intention of bone fusion in the vertebra. This autograft material is collected during laminectomy surgery and can be re-introduced into patients to enhance bone healing at the resected site, which was discussed earlier in Section 2.6.3.

Autograft bone chips (>4 x 10^5 μm^3), which are harvested with a rongeur cutting tool, are not exposed to temperature elevations, because there is no frictional heat induction. On the other hand, bone dusts (<4 x 10^5 μm^3) are harvested by bone resection with a high speed cutting bur, and their sizes are much smaller than bone chips, as seen in Figure 2.10. Cells in bone dust are exposed to temperature elevations above 47°C during high speed cutting, which induces thermal damage (Hosono et al. 2009). In comparison to bone chips, tissue integrity is not intact in bone dust, whereby osteocytes lose their lamellar structure, as seen in Figure 2.10 (Eder et

al. 2011). Bone dust are resected using surgical burs, which are designed to harvest autograft tissue to use as a filler. The design of the burs dictate the sizes of the bone dust, whereby a 2Flute design create bigger size dust (112,632 ± 14,216 μm^2) than a Multi-Flute design (66,637 ± 8,387 μm^2) (Roth AA 2017). In this study, cell viability (Cell count) from bone dust resected with a 2Flute design bur was higher compared to cells from bone dust created by a Multi-Flute design (Roth AA 2017).

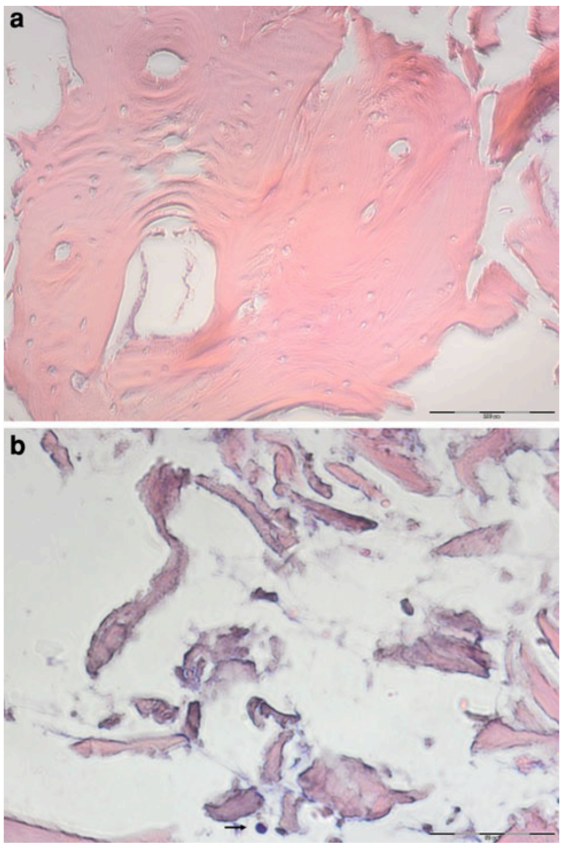

Figure 2.10: Image of (a) bone chips and (b) bone dust that was stained with H&E, showing the different sizes. Image was taken from (Eder et al. 2011).

As discussed in Section 2.4, bone cells such as MSCs, osteoprogenitors osteoclasts, and osteoblasts, reside in a mechanical environment, where they are exposed to various mechanical factors such as compression loading, perfusion, fluid flow shear stress, and tensional strains. These factors also influence cells in bone dust, because they are stimulated by the mechanical

factors, which has been shown in previous studies that assessed osteogenic potential of mechanically stimulated bone cells (Davies 2006; Sittichokechaiwut et al. 2010). During high speed cutting with surgical round burs, chattering occurs when resection of bone takes place. This chattering is caused when the cutting flute scrapes the bone, whereby each cutting flute induces a chattering compression motion onto the bone. The Multi-Flute design bur induces more frequency of chattering than the 2Flute design, because there are more cutting flutes. No study has been conducted to understand the influence of chattering on the osteogenic potential of bone dust resected with burs of a 2Flute and Multi-Flute design.

2.7. Thermal Imaging and Thermocouple

Two temperature measurement techniques were used in Chapters 3 and 4 of this Thesis; thermal imaging and a K-type thermocouple. These two instruments are used simultaneously to measure *surface* and *dissipated* temperatures induced by surgical cutting with a high speed cutting tool. The background theory in relation to these are provided here.

Thermal imaging is used to detect invisible infrared energy. A thermal camera captures infrared images, in the form of electromagnetic waves, and converts this into a visual image through digital and analog video outputs (Fig. 2.10). The components of a thermal camera are a lens, thermal sensor, processing electronics, and a mechanical housing. The lens focuses the infrared energy onto the sensor, which can have different resolutions of 80 x 60 to 1280 x 1024 pixels (FLIR).

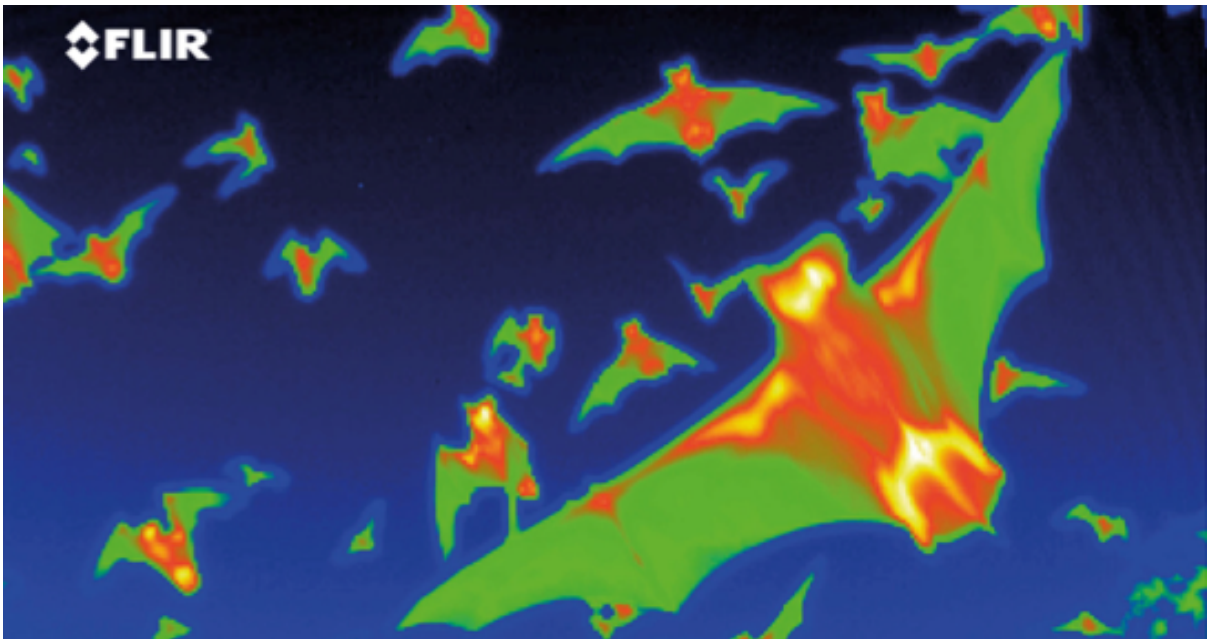

Figure 2.11: Images taken by a FLIR thermal camera where heat is detected by thermal radiation energy (FLIR).

Objects with temperatures above absolute zero will emit thermal radiation, and as temperature increases more thermal radiation is created. Emission of heat is caused by changes in the electron configurations of constituent atoms or molecules, where energy of the radiation is transported by electromagnetic waves. The Stefan-Boltzmann law describes the radiated power emitted from a black body in terms of temperature (Moran et al. 2003), and the equation is

$$E_b = \sigma \, T_s^4 \tag{2.1}$$

Where:

E_b = emissivity power,

T_s = absolute temperature (K) of the surface,

σ = *Stefan-Boltzmann constant* (σ = 5.67 X 10^{-8}W/m^2·K^4).

A blackbody is an ideal radiator, where a *real surface* is less than that of a blackbody at the same temperature and is given by

$$E_b = \varepsilon\sigma\ T_s^4 \tag{2.2}$$

Where:

E_b = emissivity power

ε = the emissivity, known as the *radiative property* of the surface

σ = the *Stefan-Boltzmann constant*

T_s = absolute temperature (K) of the surface

The radiation exchange rate quantifies the difference between internal energy that is released due to radiation emission and the energy that is gained from radiation absorption, and this is calculated by:

$$q'' = \varepsilon\sigma(T_s^4 - T_{sur}^4) \tag{2.3}$$

Where:

q" = the radiation incident on a unit area of the surface *(*W/m^2),

ε = emissivity,

σ = the *Stefan-Boltzmann constant*

A thermal camera is a good instrument to measure heat generation on the surface bone, but it does not measure temperature elevation inside the bone.

A thermocouple can be used to measure temperature inside an object by embedding the thermocouple inside the object at specific locations (Fig. 2.11). There are different types of thermocouples (J, K, T, etc.) depending on the metals that are used in the wiring. Figure 2.12 is a schematic of a thermocouple, which is joined together by two dissimilar metals. For

example, a K-type thermocouple is joined by an aluminum wire and a chromium wire. This junction joined by the two metal wires is called the measurement junction, and the junctions where the metals are not joined is called the reference junction. The temperature at the reference junction must be known in order to measure absolute temperature at the measurement junction, which is embedded in the object of interest (Corporation ; Duff and Towey 2010).

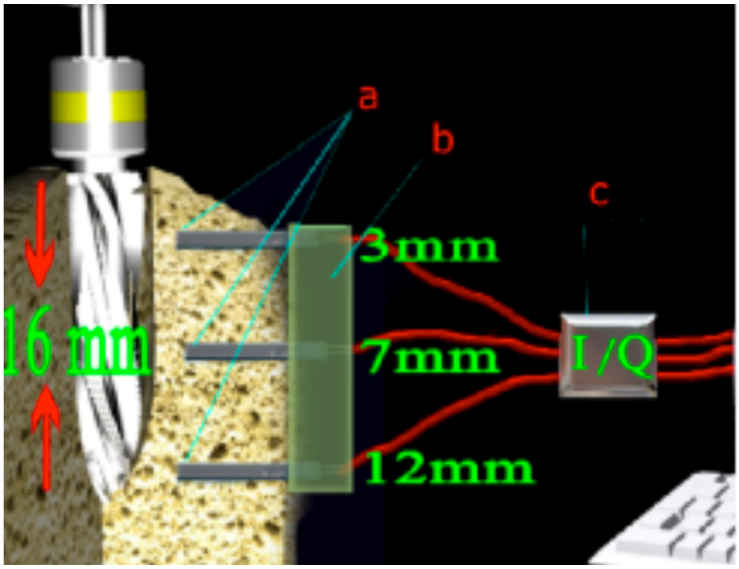

Figure 2.12: Thermocouple embedded in bovine mandible at different locations to measure temperature elevations at different drill depths. Image taken from (Sener et al. 2009).

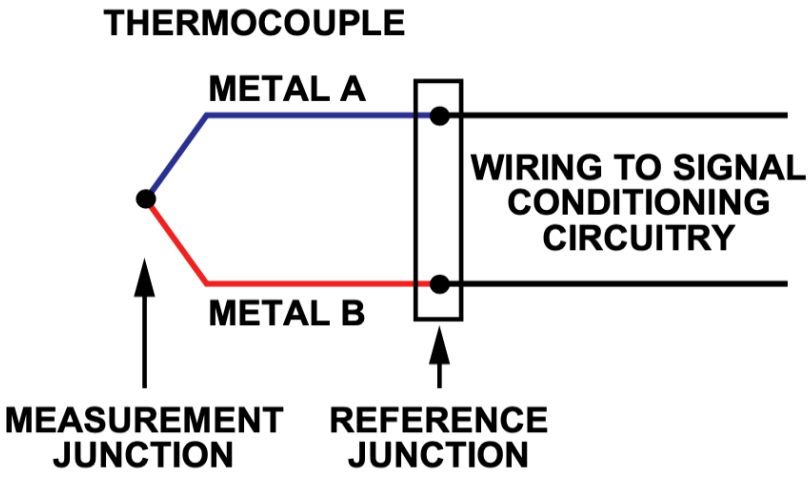

Figure 2.13: Schematic of thermocouple, which is joined together by two metal wirings that are dissimilar. Accuracy of the absolute temperature recorded at the measurement junction is dependent on the voltage generated at the reference junction. Image taken from (Duff and Towey 2010).

The accuracy of measuring absolute temperature is dependent on measuring the temperature at the reference junction. To do this, a reference-junction compensation technique is used, whereby another temperature sensitive device (thermistor, diode or resistance temperature-detectors) is used. The voltage reading at the measurement junction is compensated by this reference reading (Duff and Towey 2010). This reference-junction compensation is based on the relationship:

$$\Delta V = V @ J_1 - V @ J_2 \tag{2.4}$$

where:

ΔV = thermocouple output voltage

$V @ J_1$ = voltage generated at measurement junction (thermocouple)

$V @ J_2$ = voltage generated at reference junction

There are limitations in using a thermocouple for measuring temperature in bone, because a hole needs to be drilled for embedding the couple inside the bone. Using a high speed drill to create a hole could also change the tissue properties in the hole area that is being measured. For example, if copious irrigation is not used during the drilling process, bone could burn and create excessive necrotic tissue. Also, the tissue properties of thawed bone changes if it is frozen to be used later in the experiment. These changes in tissue properties affect the heat dissipation that is being measured by the thermocouple. Another limitation is the space created between the thermocouple and bone tissue during embedment. This is often resolved using thermal paste, which has similar properties to bone.

2.8. Mechanobiology

Cells residing in bone tissue are in a mechanical environment in vivo, where forces such as torsional, compression and tensional forces are exerted on them. In bone, these forces induce tissue repair, regeneration and remodelling, which is modulated by a biophysical stimulation (Chao and Inoue 2003). These forces also induce mechanical stimulation at the cellular level, such as hydrostatic pressure, direct cell strain, electrical fields and fluid-flow shear stress (Rauh et al. 2011). Bone dust experience mechanical loading conditions when they are re-introduced into patients at a site of implantation where a mechanical environment exists but the role of biophysical stimulation on bone dust is not well understood.

2.8.1. In vitro bioreactors

Many bioreactors have been designed to replicate the in vivo mechanical environment of bone (Freeman et al. 2017; Campbell, Lee, and Bader 2006; Davies et al. 2006). For bone tissue engineering applications, they can be used to expand a population of cells on a scaffold construct and/or provide a controlled environment for tissue formation (Sladkova and de Peppo 2014). There are many types of bioreactors used to represent an in vivo microenvironment, and some of these are explained below. The dynamic properties of cell culture and cell-cell interactions are difficult to control in vitro, with organ cultures deemed a suitable solution. However organ cultures have a short lifespan, because the centre of the organ undergoes necrosis if there is insufficient nutrient flow through the organ (Gantenbein et al. 2015; Walter et al. 2014). Perfusion bioreactors are designed to solve this problem by creating a flow of media with nutrients through the organ or scaffold, ensuring every organ surface gets the required nutrients. Due to the flow of liquid across the cell surface, perfusion bioreactors create a fluid flow shear stress as a mechanical stimulus. Some examples are spinner flasks, rotating wall vessels and perfusion bioreactors (Gaspar, Gomide, and Monteiro 2012). The spinner flask

is a stirred tank bioreactor, where there is a rotating stir bar to keep the movement of media flowing constantly over the cells (Vunjak-Novakovic et al. 1998; Kim et al. 1998). The rotating wall bioreactor was developed by NASA to provide upward hydrodynamic drag force that would balance with downward gravitational force (Schwarz, Goodwin, and Wolf 1992).

A limitation to many tissue culture studies is the lack of controlled physical loading which is normally seen in vivo. This physical loading is important for bone remodelling, because it aids in extracellular matrix formation (Sittichokechaiwut et al. 2010). A study has shown that compressive loading upregulates ALP activity and bone transcription factor, RunX2/cbfa in MSCs (Liu et al. 2009). Moreover, MSCs experience secondary effects caused by scaffold compression (Sittichokechaiwut et al. 2010; Delaine-Smith and Reilly 2011). Dynamic compression bioreactors were designed to allow for direct compressive strain on bone constructs. An example of this bioreactor system was used by (Sittichokechaiwut et al. 2010), which consisted of a BioDynamic^{TM} chamber mounted on a ELF3200 mechanical testing machine (ElectroForce System Group, Bose, USA). This bioreactor was capable of applying a compressive strain of 5% at 1 Hz to polyurethane scaffolds (Sittichokechaiwut et al. 2010). They reported an upregulation of genes associated with bone matrix formation (ALP, COL1) and mineralisation in human bone marrow cells seeded on a polyurethane foam scaffold (Sittichokechaiwut et al. 2010). Just 2 hours of compressive loading (BioDynamic^{TM}) every 5 days was enough to induce osteogenic differentiation and increase calcium deposition by 50% (Sittichokechaiwut et al. 2010). Another example of a compression bioreactor is the Zetos system, as seen in Figure 2.13, which was able to mechanically stimulate by compression and perfusion simultaneously (Davies et al. 2006). Human trabecular cores were cultured in this bioreactor system, whereby dead cells were observed on the bone surface of all samples, with live cells observed inside the cores using a Live/Dead stain for viability assessment. They also reported that the centre of human bone cores contained calcified trabecular matrix, with

adipocytes and haemopoietic cells, assessed via Giemsa, Toluidine blue and Masson tissue staining (Davies et al. 2006).

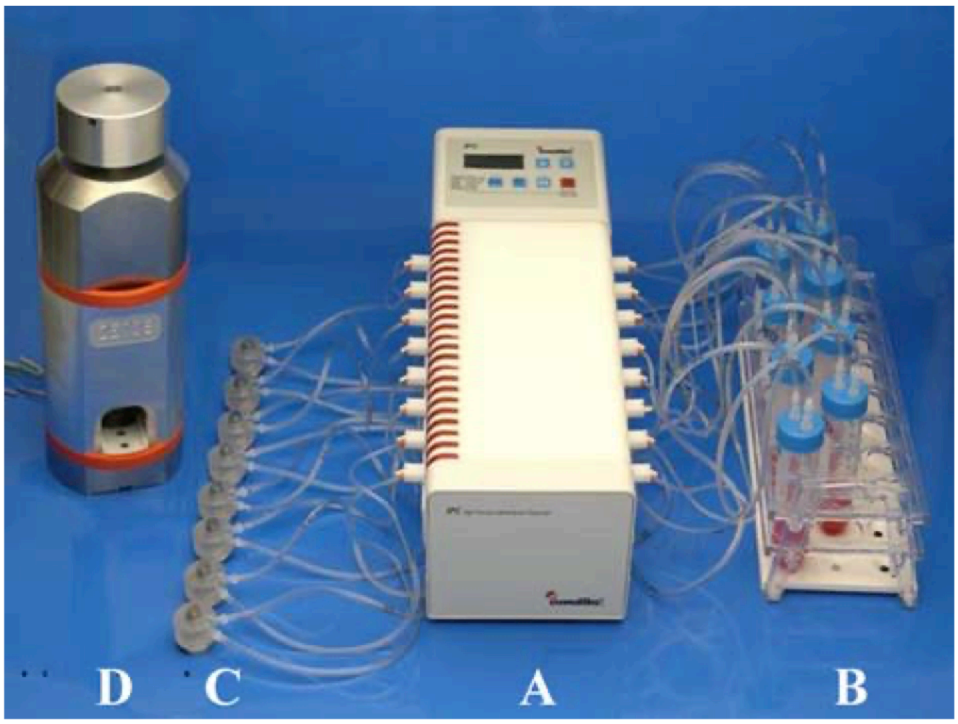

Figure 2.14: The Zetos system, which is a bioreactor with the ability to mechanically stimulate by compression and perfusion. Image taken from (Davies et al. 2006).

2.9. Summary

This Chapter has presented an overview of bone structure, composition, and the roles of specific bone cells in the function of bone modelling and remodelling. Bone is an adaptable material capable of regenerating in response to fracture damage. This adaptability is important in maintaining the structure of bone by responding to mechanical loading cues. Osteocytes residing in the area of damage orchestrate the healing response by bone forming osteoblast and bone resorbing osteoclast cells. The studies referenced in this Chapter discuss cell apoptosis and necrosis, specifically the response to thermal and mechanical damage induced by high speed surgical cutting tools such as orthopaedic drills. Moreover, the theoretical bases of the experimental techniques used in this thesis are presented in this Chapter. Many studies have

measured temperature elevations during high speed cutting in order to understand the different parameters affecting heat generation. In vitro and in vivo studies have investigated the influence of heat generation on bone cell's response to thermal damage, by artificially inducing temperature elevations above physiological temperature. However, no study has investigated the heat shock response of bone to heat generation induced by high speed cutting with surgical burs or the role of irrigation in influencing these biological processes.

To address the lack of knowledge of cellular response to surgical cutting with surgical burs, Chapter 3 of this Thesis investigates *surface* and *dissipate*d temperatures generated by surgical burs of two designs (2Flute, Multi-Flute), and then the regenerative capacity of ex-vivo bone as a response to cutting with these burs under no irrigation were also assessed, using temperature measurement tools and biochemical assays. Chapter 4 compares the osteogenic potential of ex-vivo bone surgically cut in the presence of different irrigation approaches used in surgery (manual vs continuous), using similar experimental methods to Chapter 3. In Chapter 5, the role of a mechanical environment on the osteogenic potential of autograft bone dust is investigated, using an in vitro compression bioreactor to mimic in vivo mechanical stimulation and conducting experimental studies to assess osteogenic response ex-vivo, which includes micro-CT analysis to quantify long-term mineralisation in bone dust autograft constructs.

Chapter 3 : Temperature elevations during high speed cutting occur for short durations and enhance ex-vivo osteogenesis, which is associated with thermal damage

3.1. Introduction

Bone resection using surgical cutting tools is required to gain access to specific skeletal sites or harvest autograft tissue for tympanomastoidectomy (Roth AA 2017), spinal fusion (Perez-Cruet M 2013) or acetabular revision (Schreurs et al. 2004). Post-operative bone healing at the resected surgical surface itself is affected by many factors, in particular elevated temperatures arising from high speed cutting. It has long been proposed that 47°C is the cell death threshold (Karaca, Aksakal, and Kom 2011; Dolan, Vaughan, Niebur, Casey, et al. 2014; Matthes et al. 2018; Livingston et al. 2015). Using a thermal camera for measurement, high speed cutting tools have been shown to generate temperatures higher than 80°C (Xu et al. 2014; Matthes et al. 2018; Livingston et al. 2015; Hosono et al. 2009). One study reported heat generation (88.4°C to 249.7°C) measured by a thermal FLIR camera in the spine of patients undergoing bony decompression surgery using a high speed diamond bur (for 2.4 - 12.7 minutes) with manual irrigation (Matthes et al. 2018). However, the duration of exposure to such extreme temperatures, the extent of the tissue volume exposed to these temperatures, and the cooling rate are not yet understood.

The effects of surgical cutting and irrigation on temperature generation has been assessed using histological staining to observe bone healing at the cut surface (Emmett R. Costich 1964; Saha, Pal, and Albright 1982; Augustin G 2008; Karaca, Aksakal, and Kom 2011; Isler et al. 2011; Xu et al. 2014). A previous study, using a twist drill to create holes in human cadaveric cortical bone, reported a link between drill cutting force (2 to 12 Kg of force)

and temperature elevations (50°C to 80°C), measured by a thermocouple 0.5 mm away (Matthews and Hirsch 1972b). A later study investigated temperature generation during orthopaedic drilling of bovine tibia using a thermocouple (embedded 0.5 mm from the cut area), and quantified the influence of drilling parameters (force, speed, feed rate) and bone mineral density on temperature elevations, which were related to osteocyte density (a measure of tissue necrosis) by histological staining (Karaca, Aksakal, and Kom 2011). It was reported that lower drill force (40 N) and higher bone density (>2 g/cm^2) resulted in high temperatures (60°C - 79°C), which also lead to lower osteocyte density at the drill site. Low to moderate temperature elevations (35°C - 52°C) were also measured using a thermocouple when lower drill speed (800 rpm) and higher feed rate (70 mm/min) was used for cutting, however, there were damages to tissue integrity (Karaca, Aksakal, and Kom 2011). However, staining for necrosis using H&E is limited because it offers no information on the cellular osteogenic response in resected bone during recovery days. The regenerative potential of the cells at the cut surface prepared by surgical burs has never been investigated in ex vivo bone.

High speed surgical burs are used to harvest autologous bone dust from locations such as the spine, and this bone dust is commonly re-introduced to enhance bone regeneration at a surgically resected site. Bone dust, also known as bone shavings and bone paté, is an autograft material commonly implanted in bone spaces to enhance the formation of new bone, and in the spine can encourage fusion of two or more vertebrae (Perez-Cruet M 2013; Matsumoto et al. 1998). The osteogenic potential of human bone dust has been investigated from tissue resected during spinal or orthodontic surgery (Eder et al. 2011; Ye et al. 2013; Roth AA 2017). Bone chips, collected by rongeur, and shavings, generated using a high speed drill under irrigation, from patients undergoing laminectomy were compared (Eder et al. 2011). It was reported that both chips and shavings had osteogenic potential, as assessed by Alizarin red staining on day 21, but that bone chips demonstrated higher viability (Eder et al. 2011). A later study compared

bone chips harvested from the iliac crest to bone dust (spine) created by different bur diameter sizes (3 mm, 4 mm, 5 mm), and it was reported that bone chips had significantly higher cell viability and mineralisation, assessed by Alizarin red staining on recovery day 21 (Ye et al. 2013). A more recent study comparing different design burs (2Flute, Multi-Flute) reported a higher cell count after 21 days of recovery following cutting with a 2Flute, compared to the Multi-Flute (Roth AA 2017). These studies did not characterise temperature elevation, but speculated that low viability in the bone dust groups was accredited to high temperature (>47°C) generated by the high speed bur. However, in order to fully understand the influence of heat generation on osteogenic potential of bone dust, the temperature created by surgical burs needs to be characterised.

In vitro studies have investigated the influence of moderate temperature elevations (44°C - 60°C), representative of cutting with an orthopaedic twist drill (Karaca, Aksakal, and Kom 2011), for short durations (30 seconds, 1 minute) on bone cell viability (Dolan et al. 2012; Dolan et al. 2015; Dolan et al. 2016; Chung and Rylander 2012; Eriksson and Albrektsson 1983; Eriksson and Albrektsson 1984; Eriksson, Albrektsson, and Magnusson 1984). It was reported that in vitro cellular responses, such as apoptosis, paracrine signalling for osteoclastogenesis and regeneration were higher in heat treated cells compared to control (37ºC) (Dolan et al. 2015; Dolan et al. 2016). Interestingly, it was reported that Balb/c MSCs and osteoblast-like cells exposed to severe heat-shock (60ºC for 30 seconds and 1 minute) underwent apoptosis but also stimulated an osteogenic mineralisation response by day 14 (Dolan et al. 2012). Moreover, in vivo rat tibia exposed to temperatures of 47ºC and 60ºC for 1 minute durations upregulated osteoblastogenic genes (receptor activator of nuclear factor kappa B ligand, osteoprotegrin, COX2, vascular endothelial growth factor) (Dolan et al. 2016). Interestingly, in the heat treated tibia, apoptotic cells were observed along the thermal damage boundary, and it was proposed that thermally induced osteocyte damage can initiate an

osteogenic healing response (Dolan et al. 2016). These studies investigated 30 second and 1 minute durations in an attempt to reflect the usage time of cutting tools, which is not always consistent between surgical procedures or even between surgeons. However, the precise durations of temperature elevation during high speed cutting have not been fully characterised. Cellular response to thermal damage has been only investigated using moderate and artificial (not using cutting tool) temperature (Dolan et al. 2012; Dolan et al. 2015; Dolan et al. 2016; Dolan, Vaughan, Niebur, Casey, et al. 2014; Dolan, Vaughan, Niebur, Tallon, et al. 2014; Chung and Rylander 2012; Eriksson and Albrektsson 1983; Eriksson 1984; Eriksson and Albrektsson 1984; Eriksson, Albrektsson, and Magnusson 1984). Therefore, an advanced understanding of the effect of severe temperature elevations, arising during surgical cutting, on tissue damage and cellular response in surgically cut bone is required. Moreover, heat generation during cutting with a surgical bur have not been fully characterised to understand the bur's influence on osteogenic potential in thermally damaged tissue (bone dust and cut surface).

In this Chapter, the hypotheses that (1) "A Multi-Flute surgical cutting tool bur generates higher temperature at the superficial surface than a 2Flute bur design" and (2) "Bone surfaces and autograft dust exposed to temperature elevations induced by high speed cutting undergo cell apoptosis, which enhances the osteogenic response ex-vivo" were tested. The first specific objective of the study was to measure the surface and dissipated temperature elevations in surgically cut bone using high speed surgical burs with a FLIR camera and a K-type thermocouple. The duration of exposure of the bone surface to elevated temperatures, the cooling rate, and the extent of tissue volume damage were quantified. No irrigation was used during cutting in order to achieve and investigate high temperatures, but these are higher than those expected when they are used with irrigation, which is recommended in order to minimise temperature elevation. The second objective of this study was to investigate the role of this

heat generation for dictating the cellular thermal damage after 24 hours of recovery and the osteogenic capacity of autologous bone dust and the cut surface during 20 days of recovery, using ex-vivo cell culture techniques and biochemical assays.

3.2. Materials and Methods

3.2.1. Bone harvesting

Bone samples for cell culture and biochemical assays were harvested from the metatarsal and cervical vertebra of recently sacrificed cattle (Local abattoir, Athenry). Bovine femur and scapula was used for temperature analysis (Local abattoir in Middleton, Cork). The extractable protein and hydroxyproline content of bovine bone is similar to human (Aerssens et al. 1998) and has been used for previous temperature measurement studies (Saha, Pal, and Albright 1982; Karaca, Aksakal, and Kom 2011; Sener et al. 2009; Gehrke et al. 2016). For ex-vivo culture studies bone was transported within 1 hour of sacrifice on ice. Within 1 hour of arrival to the lab, all excess soft tissues, except for the periosteal membrane, were removed. To ensure sterility, the bone was generously sprayed with 70% ethanol before immediately transferring the tissue into a laminar flow hood for cutting.

3.2.2. Surgical Cutting

Surgical cutting on femur, scapula, metatarsal and vertebra (all bovine) were conducted using either a 2Flute or Multi-Flute bur (Stryker Innovation Centre, Cork) attached to a high speed pi drill (Stryker Innovation Centre, Cork) at a rotation speed of 75000 rev/min using a clockwise hand motion (Figure 3.1a and b). Cutting with surgical burs were conducted according to manufacturer's manual, whereby the bur was angled at 45° to the bone. All bones were at room temperature when cutting took place. No irrigation technique was used, therefore, the bone dust generated had a powder form (Figure 3.1c). Bone dust was collected in a gamma irradiated plastic bag and transferred into a 50 mL falcon tube then washed three times with

calcium free phosphate buffered saline (PBS, Sigma). Afterwards, to handle the bone dust, 6 laboratory spoons of it were transferred into a T75 culture flask and incubated in 37°C, 5% CO_2.

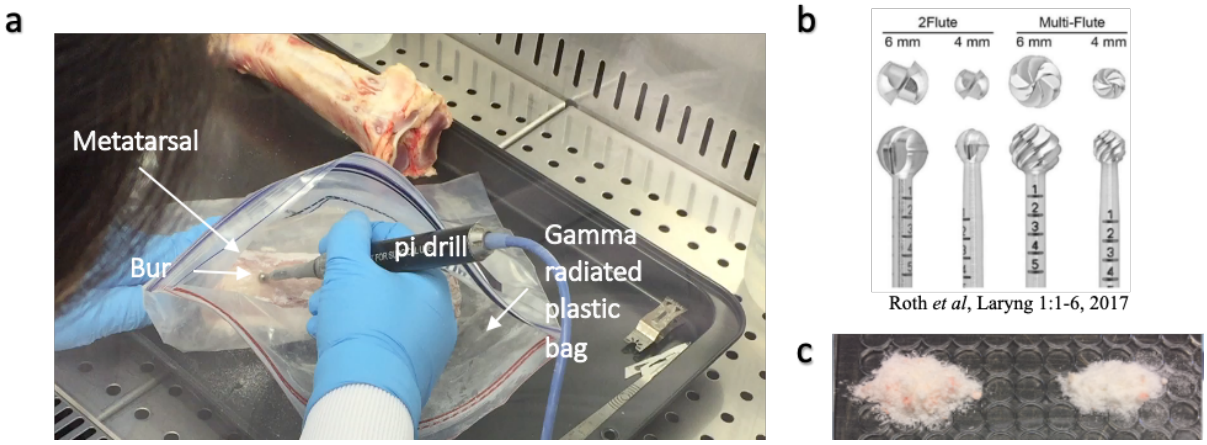

Figure 3.1: (a) Set up of surgical cutting with a high speed pi drill, using (b) 2Flute and Multi-Flute bur designs. (c) Bone dust resected with surgical burs have a powder form when no irrigation is used. The design of burs (2Flute, Multi-Flute) also determines the size of a single bone dust particle.

The cut surfaces were further processed to create bone cores (10 mm x 10 mm x 5 mm) for ex-vivo cell culture. Cores with no cut site were also prepared and used as a control. Both samples were immediately placed in cell culture media at 37°C, 5% CO_2 for the ex-vivo cell culture experiments, described in detail below.

3.2.3. Surface Temperature determined by FLIR camera

Temperatures generated on the surface of femur and scapula (Fig 3.2a) during cutting with surgical burs was determined using a Forward-looking Infrared Radiometer (FLIR, FLIR T440) thermal camera. The FLIR camera imaged at a frame rate of 7.5 frames/second, and the thermal emissivity of bone was determined as 0.95 (Feldmann 2016). The Ar1 setting was used to gather temperature on the cut surface. This setting provides temperature measurement in a wide field of view where a square (120 pixels x 120 pixels) dictates the area for the camera to measure surface temperature (Fig 3.2b). Temperature data was analysed to determine (1) the

relative *surface* temperature during surgical cutting. The bone temperature reading was taken in a location close to the intended cut surface prior to cutting, using the FLIR camera, and this reading was used to quantify the *relative* increase in temperature from the initial temperature of the bone before cutting. (2) The duration of relative temperature elevation above 80°C, and (3) the cooling rate was also analysed using the FLIR data. The Sp1 setting was also used to determine surface temperature at one location during 60 seconds of cutting (Fig 3.2b) to further investigate exposure time to high temperature increase at one specific location on the bone. Furthermore, heated cut surface and total cut surface was quantified using ImageJ and used to calculate percentage of heated cut surface area.

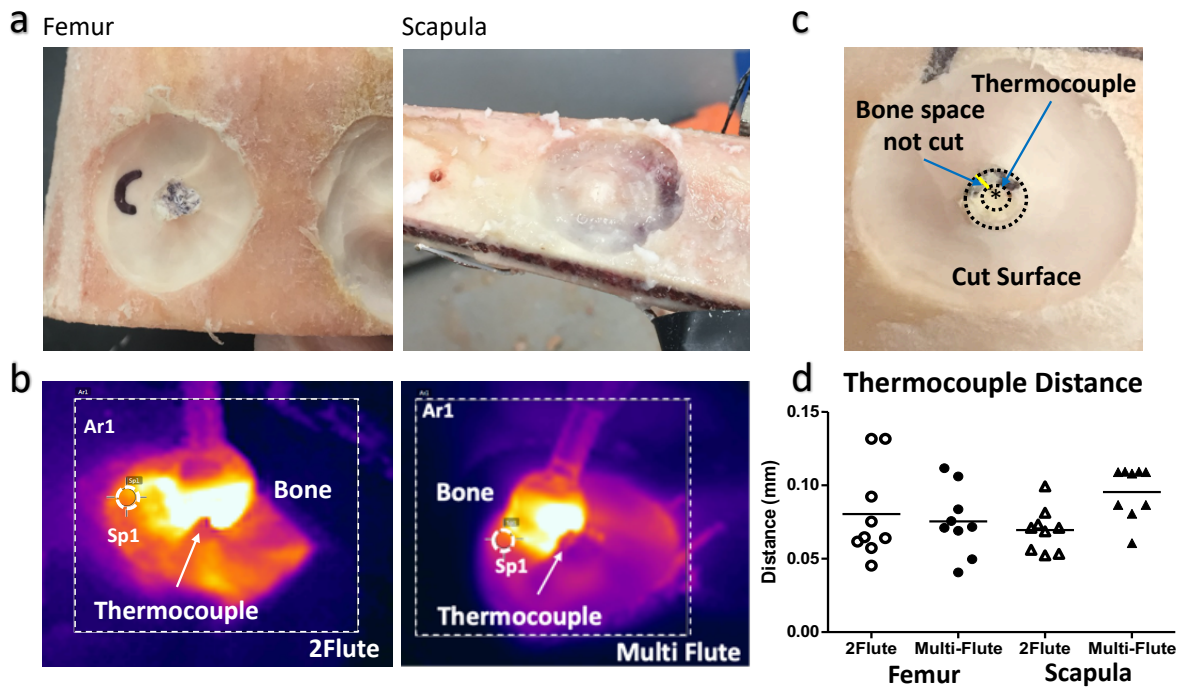

Figure 3.2: Picture showing the cut surface of (a, left) cortical and (a, right) cortico-cancellous bone. FLIR camera image of surgical cutting using a (b, left) 2Flute and (b, right) Multi-Flute bur. Dashed square indicates where temperature was measured for Ar1 setting, while dashed circle (Sp1) shows local temperature measurement for one specific location. The thermocouple location is indicated (white arrow). (c) The smallest bone space not cut (yellow line) between the thermocouple (* inner dashed circle) and the edge of the cut surface (outer dashed circle) is the (d) thermocouple distance.

3.2.4. Dissipated Temperature determined by Thermocouple

Dissipated temperature, which is heat dissipation within the bone to the thermocouple, was measured using a K-type thermocouple (Agilent) embedded in the bone, at the centre of the intended cutting area. Using a πdrill with a 1 mm router attachment (both Stryker), a hole was drilled into the bone before embedding the thermocouple, and thermal paste (Sigma) was used to fill in the spaces between the thermocouple and the bone. Cutting took place around this thermocouple, while the FLIR camera was pointed at the cut site. The space between the thermocouple and the cut surface (thermocouple distance) ranged between 40 µm and 131 µm (Fig 3.2c and d). Thermocouple data was extracted from the data logger and analysed to determine the absolute maximum temperature and relative temperature (normalised to the initial bone temperature). For all temperature analyses, cutting was repeated 3 times with 3 technical replicates for each condition, and the duration of cutting was 60 seconds. Data are expressed as mean ± standard deviation.

3.2.5. Thermal damage determination at the cut surface

Bone tissue necrosis and cell death arising within 24 hours of cutting were determined using histological staining techniques. A hematoxylin and eosin staining (H&E, Sigma) was used. Hematoxylin stains for DNA, indicating the presence of cells. On the other hand, eosin stains non-specifically for proteins, showing tissue in different shades of pink. Necrotic bone tissue was identified as lacunae that were empty of osteocytes.

To determine cell death, an antibody for cleaved caspase 3 (Cell Signalling) was used. Pro-caspase 3 is cleaved to activate the cell apoptosis pathway (extrinsic and intrinsic), where cell morphology changes, and blebbing occurs due to lysed cellular and nuclear membrane, releasing cellular content. On day 1 of recovery, cut surface samples were fixed with 4% paraformaldehyde (PFA) and then decalcified in 10% w/v ethylenediaminetetraacetic acid

(EDTA, Sigma) and processed in an automated tissue processor (Leica) overnight, embedded in paraffin wax and sectioned at 4 μm using a microtome (Leica). Sectioned samples were mounted on a glass slide and dewaxed overnight in an oven at 60°C before staining with either H&E or cleaved caspase 3.

Deparaffinised sections of the cut surface were stained with H&E ready to use solutions as described previously (Kuttenberger, Polska, and Schaefer 2013). Briefly, samples were dewaxed in xylene and rehydrated in graded ethanol. After staining with H&E, slides were mounted in distyrene plasticiser xylene (DPX mountant for histology, Sigma) for imaging. Imaging was carried out using an upright microscope BX 43 (Olympus) at 20x magnification.

Immunostaining was carried out according to a previous protocol (Dolan et al. 2016). Briefly, samples were blocked for 30 minutes with 1% bovine serum albumin (BSA, Sigma) to prevent non-specific binding, and then incubated overnight with cleaved caspase 3 antibody (Cell Signalling) at a concentration of 1:100. The following day, samples were washed with BSA and stained with Alexa Fluor 488 (ThermoFisher) at a dilution of 1:700 for 1 hour at room temperature in the dark. Samples were then counterstained with mounting media containing 4',6-diamidino-2-phenylindole (DAPI, Sigma), and imaged on a confocal laser scanning microscope (Olympus Fluoview 100 system) with 40x magnification.

3.2.6. Ex-vivo cell culture

Bone dust and the cut surface samples were cultured in T75 flasks with Dulbecco Modified Eagle Medium Glutamax (Biosciences) and Hyclone Nutrient Ham's/F12 (ThermoFisher) (DMEM/F12 1:1 ratio) media supplemented with 10% foetal bovine serum (FBS, Sigma), 2% antimycotic antibiotic streptomycin solution (Sigma) and osteogenic supplements; 50 μM ascorbic acid, 1% w/v Dexamethasone and 20 mM β-Glycerol phosphate (all from Sigma). Media was changed twice per week, or two days before collecting media for extracellular ALP

activity. Time points for metabolic activity and extracellular alkaline phosphatase (ALP) activity were at 5, 10, 15, and 20 days recovery. Calcium was quantified on days 10, 15, and 20 of recovery. All ex-vivo culture experiments were repeated 3 times with 3 replicates.

3.2.7. Metabolic Activity

Metabolic activity of the cells in bone dust and the cut surface was assessed using an Alamar Blue assay (Bioscience, DAL 1100) to measure metabolic activity of cells through glycolysis. Briefly, bone dust and the cut surface groups were washed three times with calcium free phosphate buffered saline (PBS, Sigma). Then samples were incubated in 10% Alamar Blue with media for 4 hours in 37°C, 5% CO_2. Afterwards, absorbance values were measured at 570 nm and 600 nm using a microplate reader (BioTek Synergy HT) and calculated for Alamar Blue reduction, which was normalised to weight and expressed as mean ± standard deviation.

3.2.8. Osteogenic Capacity

Osteogenic capacity was determined using an alkaline phosphatase (ALP) assay and alizarin red staining. ALP activity is an early marker for mineralisation and indicates differentiation down the osteoblast lineage. An ALP assay is commonly used to quantify ALP content, using a calorimetric test for *p*-nitrophenyl phosphate (*p*-NPP) as a phosphate substrate. Extracellular ALP activity for bone dust, the cut surface and controls were determined using a modified protocol described previously (Dolan et al. 2012). Briefly, spent media was taken from all groups on specific recovery days and stored in -20°C until use. A 40 µl sample of spent media was added to 40 µl of deionized water (ddH_2O) in a 96-well plate, to which 50 µl of 5 mM *p*-NPP (Sigmafast, Sigma) solution was added and incubated for 1 hour at room temperature. An absorbance value was measured at 405 nm using a microplate reader (BioTek Synergy HT). Using a standard curve of 0-80 nM of *p*-NPP content, ALP activity was calculated as units (U), then normalised to weight and reported as mean ± standard deviation in units per gram (U/g).

Mineralisation was quantified on specific recovery days as described in cell culture and using Alizarin Red S (AR, Sigma). AR binds to mineralised matrix, where 1 mole of alizarin red binds to 2 moles of calcium. Bounded AR creates an AR-calcium complex, which can be quantified by de-staining with cetylpyridinuim chloride (CpCl, Sigma). Quantification was carried out according to previous protocols (Dolan et al. 2012). Briefly, bone dust was washed five times with PBS, and then fixed with 4% PFA until use. After fixing bone dust, samples were washed 3 times with distilled water (ddH_2O), then incubated in 40 mM AR solution at room temperature for 50 minutes in an orbital shaker (350 rev/min). After incubation, bone dust groups were washed with ddH_2O until liquid was clear, which indicates that all unbound AR was removed. To quantify calcium, bound AR was de-stained by adding 10% w/v CpCl solution to each sample then incubated on an orbital shaker at 350 rev/min for 50 minutes at room temperature. Absorbance was measured in triplicates at 562 nm. Using a standard curve from 0-4 mM AR, calcium content was calculated, normalised to weight of bone dust, and reported as mean ± standard deviation in mM/g.

3.2.9. Live/Dead stain on the cut surface

Cell viability in the cut surface was analysed on day 44 of recovery, using a Live/Dead fluorescent staining. Live cells break down calcein AM (Sigma), which is then able to bind to the cellular membrane and is observed as green. Dead cells have a lysed membrane, therefore, ethidium homodimer-1 (Sigma) is able to penetrate through the cell's membrane and stain parts of the nucleus. Live/Dead assay was carried out according to a previous protocol with modifications (F.A. Saleh 2011). Briefly, the cut surface and control samples were washed 3 times in PBS for ten minute duration washes, and then incubated in 8 µM calcein AM and 8 µM ethidium homodimer solution for 4 hours at 37°C, 5% CO_2. After incubation, samples were washed 3 times with PBS and transferred to a glass bottom petri dish for imaging, using a confocal laser scanning microscope (Olympus Fluoview 1000 system).

3.2.10. Statistical Analysis

Statistical analysis for temperature measurement and analysis, Alamar Blue reduction, ALP activity, and calcium was carried out using GraphPad (version 5) software. Two-way ANOVA was used with Bonferroni's post-test to compare between 2Flute and Multi-Flute groups. The results are displayed as a mean ± standard deviation with significance at $p \leq 0.05$.

3.3. Results

3.3.1. Surface and Dissipated Temperature Analysis

Surgical cutting with a Multi-Flute bur on a femur and scapula bone resulted in a significantly ($p<0.01$) higher relative *surface* temperature, whereby the Multi-Flute generated a temperature increase of more than 120°C on the cut surface (Table 3.1, Fig 3.3a). Relative *surface* temperature ranged between 80°C to 120°C when using a 2Flute bur for cutting (Table 3.1, Fig 3.3a).

Table 3.1: Maximum Surface Temperature (Thermal Camera)

Thermal Camera n=9	Bone	2Flute	Multi-Flute	p-value*
Relative Temperature	Femur	94.37±10.56°C	129.56±16.23°C	0.01424
	Scapula	89.89±4.19°C	124.27±8.80°C	0.00163

*p-value shows significance of 2Flute versus Multi-Flute

Dissipated temperature recorded by the thermocouple were all below 40°C (Table 3.2). Using a 2Flute for cutting on a femur and scapula, maximum temperature was 30.51 ± 2.48°C and 32.96 ± 1.17°C, respectively. Cutting with a Multi-Flute on femur and scapula generated a maximum temperature of 34.63 ± 3.35°C and 35.85 ± 3.06°C, respectively (Table 3.2). The

increase in *dissipated* temperature had a higher trend for Multi-Flute groups compared to 2Flute when cutting took place on both bones (Fig 3.3b).

Table 3.2: Maximum Dissipated Temperature (Thermal Couple)

Thermal Couple n=9	Bone	2Flute	Multi-Flute	p-value*
Maximum Temperature	Femur	30.51±2.48°C	34.63±3.35°C	0.099
	Scapula	32.96±1.17°C	35.85±3.06°C	0.155
Relative Temperature	Femur	11.16±2.47°C	14.43±1.91°C	0.083
	Scapula	13.29±0.97°C	16.56±2.91°C	0.107

*p-value shows significance of 2Flute versus Multi-Flute

A closer analysis of relative *surface* temperature at a local (Sp1) level reveals a curve with multiple peaks (heat shock pulse) and fluctuations, during a period of 60 seconds of surgical cutting (Fig 3.3c-f). For both the scapula and femur bone groups, some peaks for the Multi-Flute showed a temperature increase of more than 120°C, indicated by the red baseline in Fig 3.3c-f. The peaks never went above 120°C during cutting with the 2Flute bur.

During cutting for 60 seconds, the duration time for *surface* temperature elevations above 80ºC was significantly higher ($p<0.05$) when a Multi-Flute was used compared to using a 2Flute (Fig 3.4a). The cooling rate (Fig 3.4b) was significantly faster ($p<0.05$) and the percentage of heated surface area (Fig 3.4c and d) was significantly lower ($p<0.001$) when using a Multi-Flute for cutting, in comparison to a 2Flute.

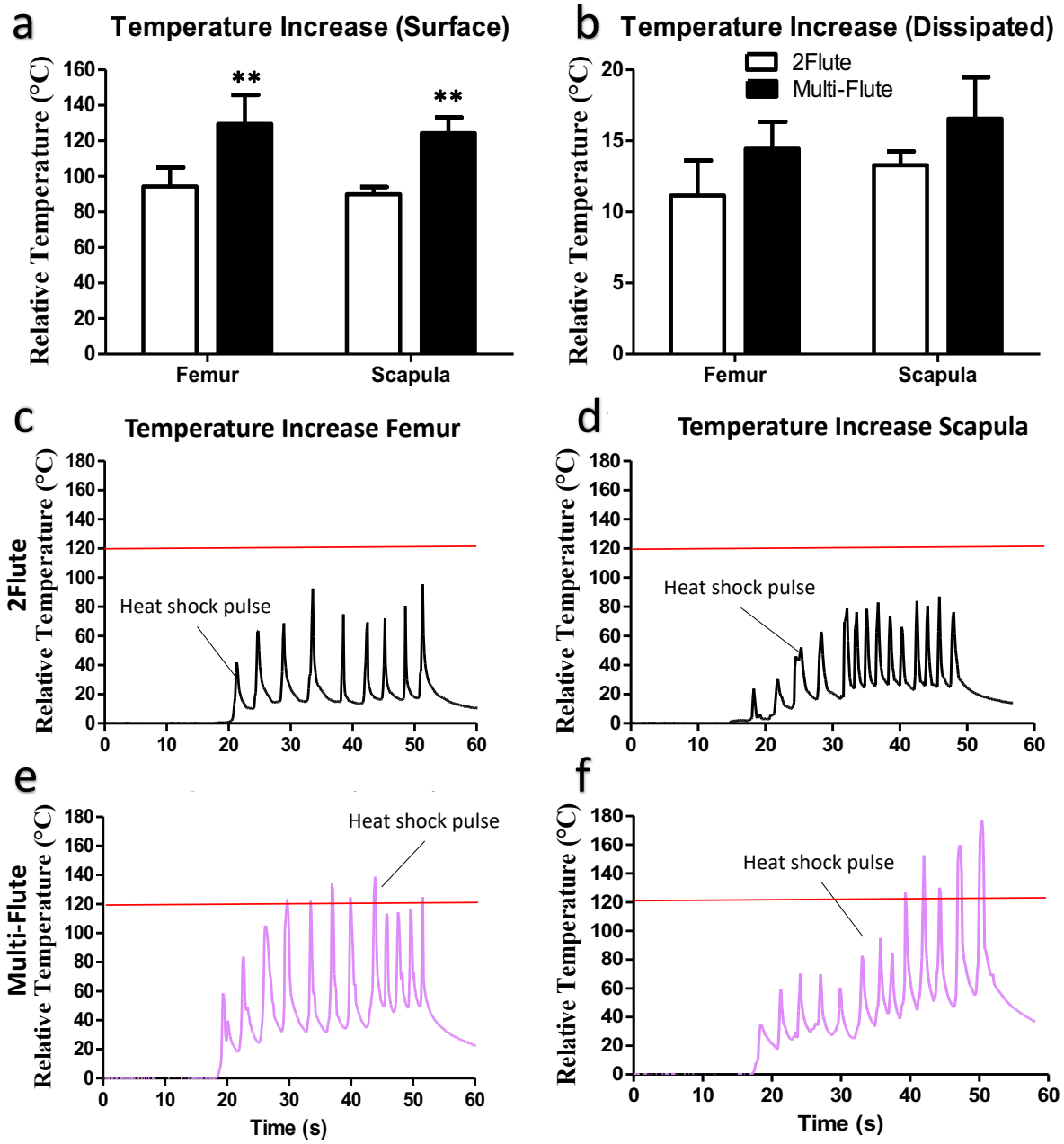

Figure 3.3: Relative (a) *surface* and (b) *dissipated* temperature was higher in Multi-Flute groups. (c-f) Temperature curve showing temperature fluctuations on one location on the bone. Red line is the baseline for relative temperature above 120°C. *p<0.05, **p<0.01, **p<0.001; Multi-Flute compared to 2Flute.

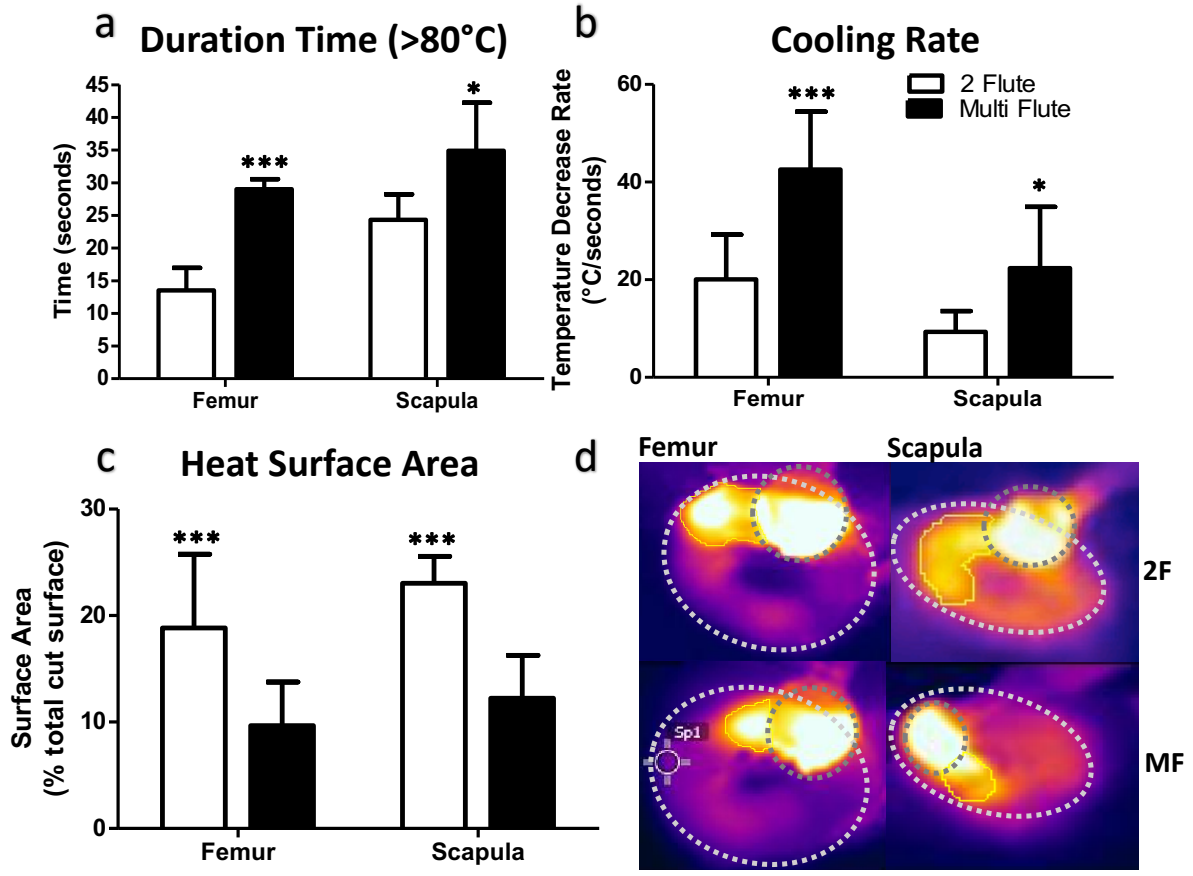

Figure 3.4: (a) The duration time of relative temperature elevations above 80°C. (b) Cooling was faster immediately after contact with cutting bur. (c) Extent of tissue volume damage showing percentage of heated surface to total cut surface. (d) FLIR images showing heated surface (yellow boundary line) and total cut surface (dashed grey circle). Bur is indicated by dashed blue circle.

3.3.2. Tissue Analysis and Thermal Damage in the cut surface

On day 1 of recovery, no significant difference in necrotic tissue was observed in both of the cut surface groups, 2Flute and the Multi-Flute, where empty lacunae were seen as far as 182.4 µm away from the cut surface (Fig. 3.5). Apoptotic positive cells were identified for both bur groups (Fig. 3.6), where more positive apoptotic cells could be observed in the Multi-Flute cut surface (34.3% apoptotic, Fig 3.6b) when compared to the 2Flute groups (15.7% apoptotic, Fig 3.6a). Apoptotic bodies (grey arrows) on the edge of the cut surface could also be seen in the Multi-Flute group (Fig 3.6b). Moreover, in both groups, caspase negative cells (white arrow)

were also seen in proximity to apoptotic cells, indicating cell survival from thermal damage (Fig 3.6 merge).

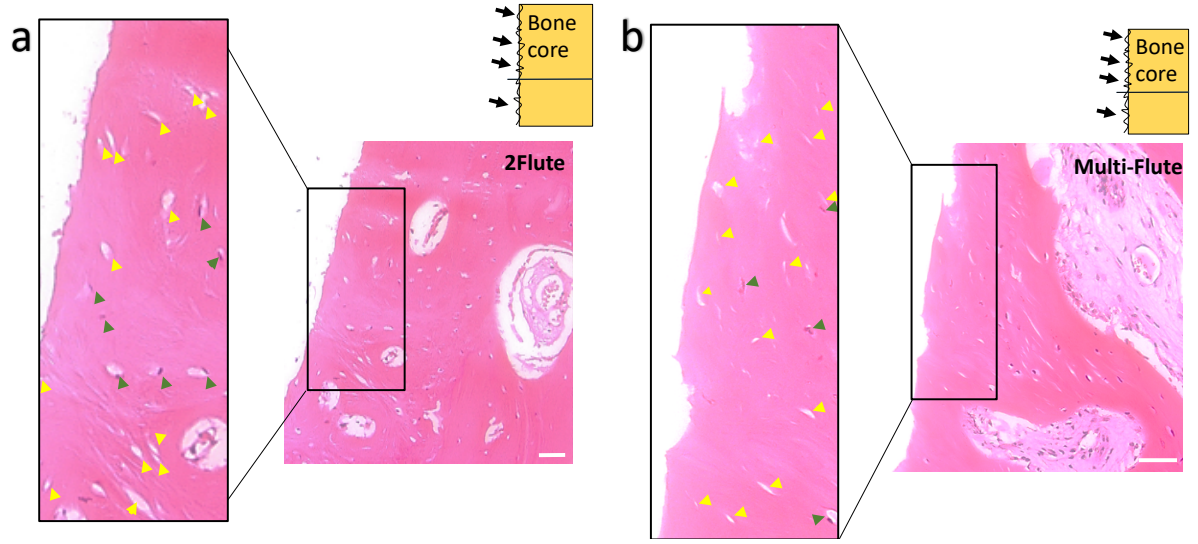

Figure 3.5: Hematoxylin and Eosin stain of bone cores with (a) 2Flute and (b) Multi-Flute cut surface (black arrow on diagram above). Zoomed in box shows that both cut sites had necrotic tissue with empty lacunae (yellow arrow) and filled lacunae (green arrow). Scale bar is 50 µm.

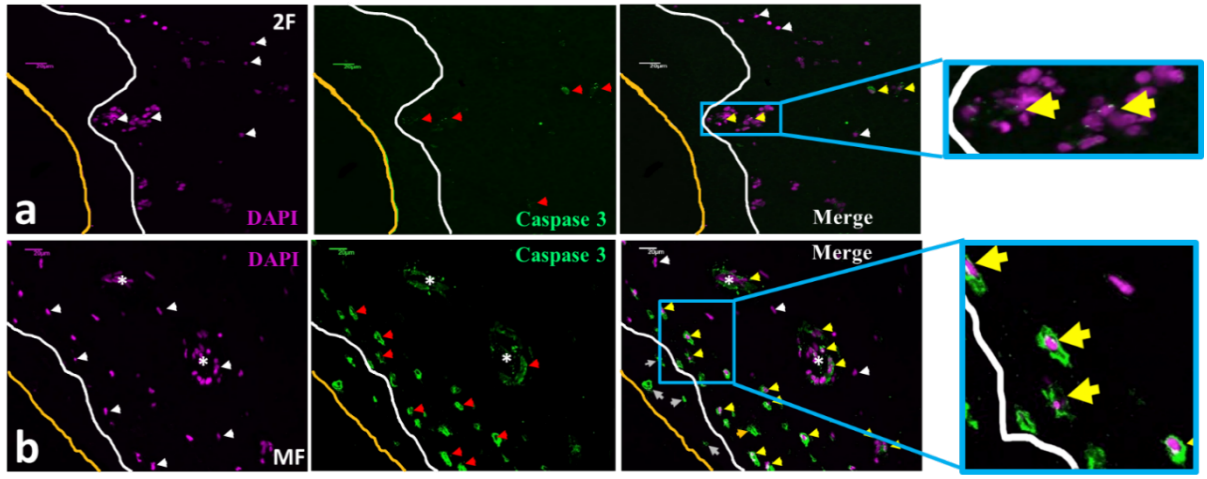

Figure 3.6: Apoptosis fluorescence staining. Orange line indicates the cut surface, while white line shows boundary of DAPI-negative region. Cells with DAPI (magenta) are indicated by white arrows. Cleaved-caspase 3 (green) is shown by red arrow. Apoptosis positive cells (yellow arrow) and apoptotic bodies (grey arrows) were observed in the cut surface of both (a) 2Flute and (b) Multi-Flute. More apoptotic positive cells in the cut surface of Multi-Flute, compared to the cut surface prepared by 2Flute.

3.3.3. Metabolic Activity and Osteogenic Capacity of Bone Dust

At recovery day 15 in both the metatarsal ($p<0.05$) and vertebra ($p<0.001$) groups, DNA content was significantly higher in bone dust resected with Mult-Flute compared to those resected with a 2Flute bur (Fig 3.7a and b). Metabolic activity from all bone dust groups decreased after day 5 of recovery (Fig 3.7c and d). Bone dust in Multi-Flute groups showed significantly ($p<0.001$) higher metabolic activity on day 5 and 15 for metatarsal, compared to 2Flute groups (Fig 3.7c). This significance was also seen on day 5 ($p<0.05$) and day 20 ($p<0.001$) for the vertebra groups (Fig 3.7d).

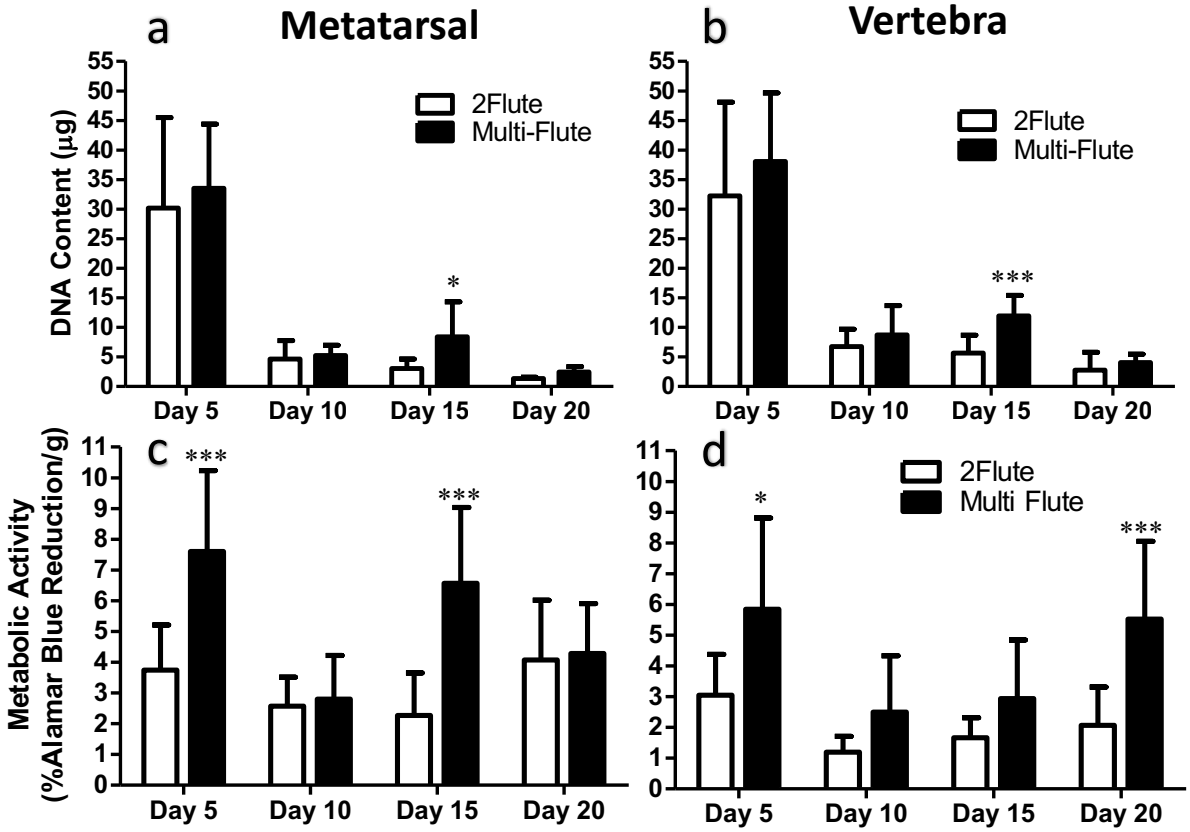

Figure 3.7: (a and b) DNA content and (c and d) Metabolic activity from metatarsal (left) and vertebra (right) bone dust groups. At various time points, DNA content and Alamar Blue reduction were higher in Multi-Flute groups. *p<0.05, **p<0.01, ***p<0.001; significance of 2Flute compared to Multi-Flute.

Extracellular ALP activity decreased after 5 days of recovery and increased again after day 10 for all bone dust groups (Fig 3.8a and b). In the metatarsal groups on recovery days 5

(p<0.01) and 15 (p<0.01), ALP activity was significantly higher in the Multi-Flute groups when compared to the 2Flute group (Fig 3.8a). Furthermore, on days 5 (p<0.05) and 20 (p<0.05) for vertebra, bone dust created by Multi-Flute showed significantly higher extracellular ALP activity in comparison to 2Flute groups (Fig 3.8b).

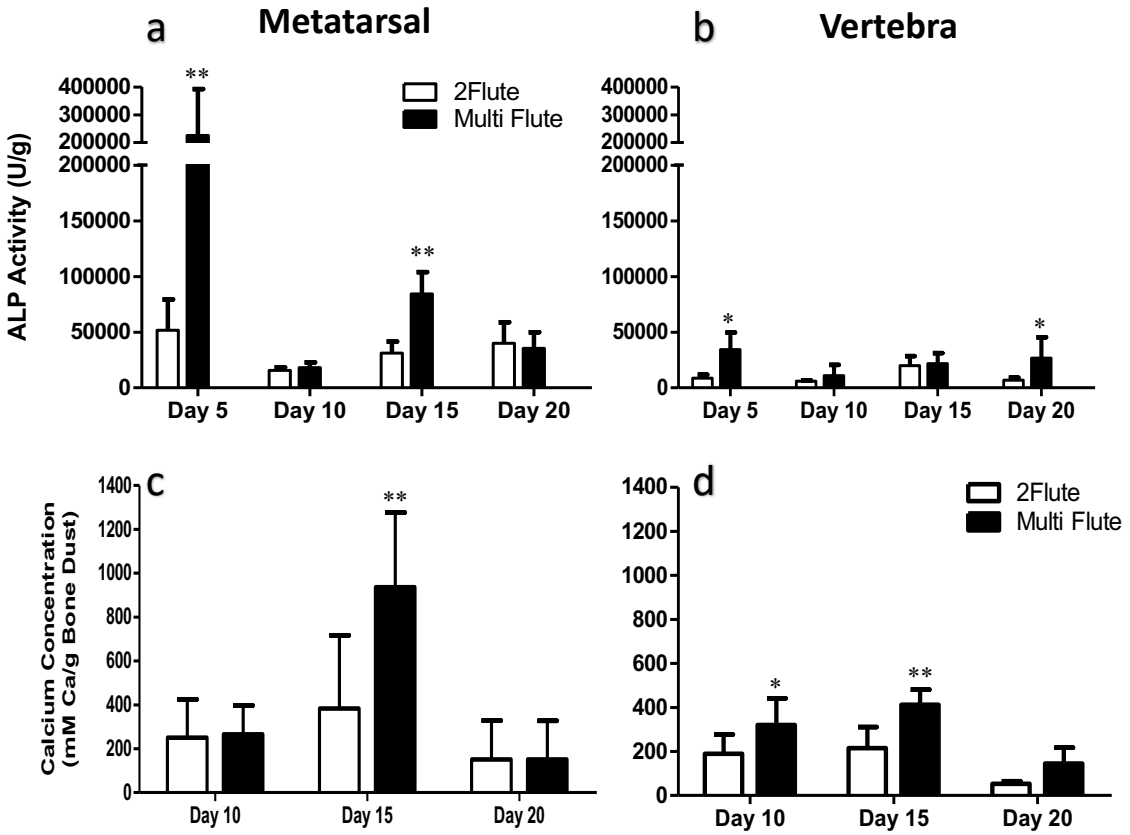

Figure 3.8: (a and b) Extracellular ALP activity and (c and d) calcium content were also higher in Multi-Flute groups. *p<0.05, **p<0.01, ***p<0.001; significance of 2Flute compared to Multi-Flute.

On recovery day 15 for all groups, calcium content was significantly (p<0.01) higher in the bone dust group created by Multi-Flute cutting (Fig 3.8c and d). On recovery day 10 in the vertebra group, the Multi-Flute group had a significantly (p<0.05) higher calcium content than the 2Flute group (Fig 3.8d).

3.3.4. Viability and Osteogenic Capacity of the cut surface

For all the cut surface groups, metabolic activity increased after 10 days of recovery. In the metatarsal group, there was no significant difference between the 2Flute and Multi-Flute

groups (Fig 3.9a). Metabolic activity was significantly higher when a Multi-Flute was used for cutting on vertebra bone, compared to 2Flute groups, on days 10 ($p<0.01$), 15 ($p<0.001$), and 20 ($p<0.001$) (Fig 3.9b).

In the metatarsal cut surface group, extracellular ALP activity remained the same for all recovery days (Fig 3.9c). On days 5 and 10, control groups from the metatarsal bone had significantly ($p<0.001$) higher ALP than the 2Flute and Multi-Flute groups (Fig 3.9c). In the vertebra cut surface groups, extracellular ALP activity was significantly higher on day 20 ($p<0.05$) for Multi-Flute group, in comparison to the 2Flute (Fig 3.9d).

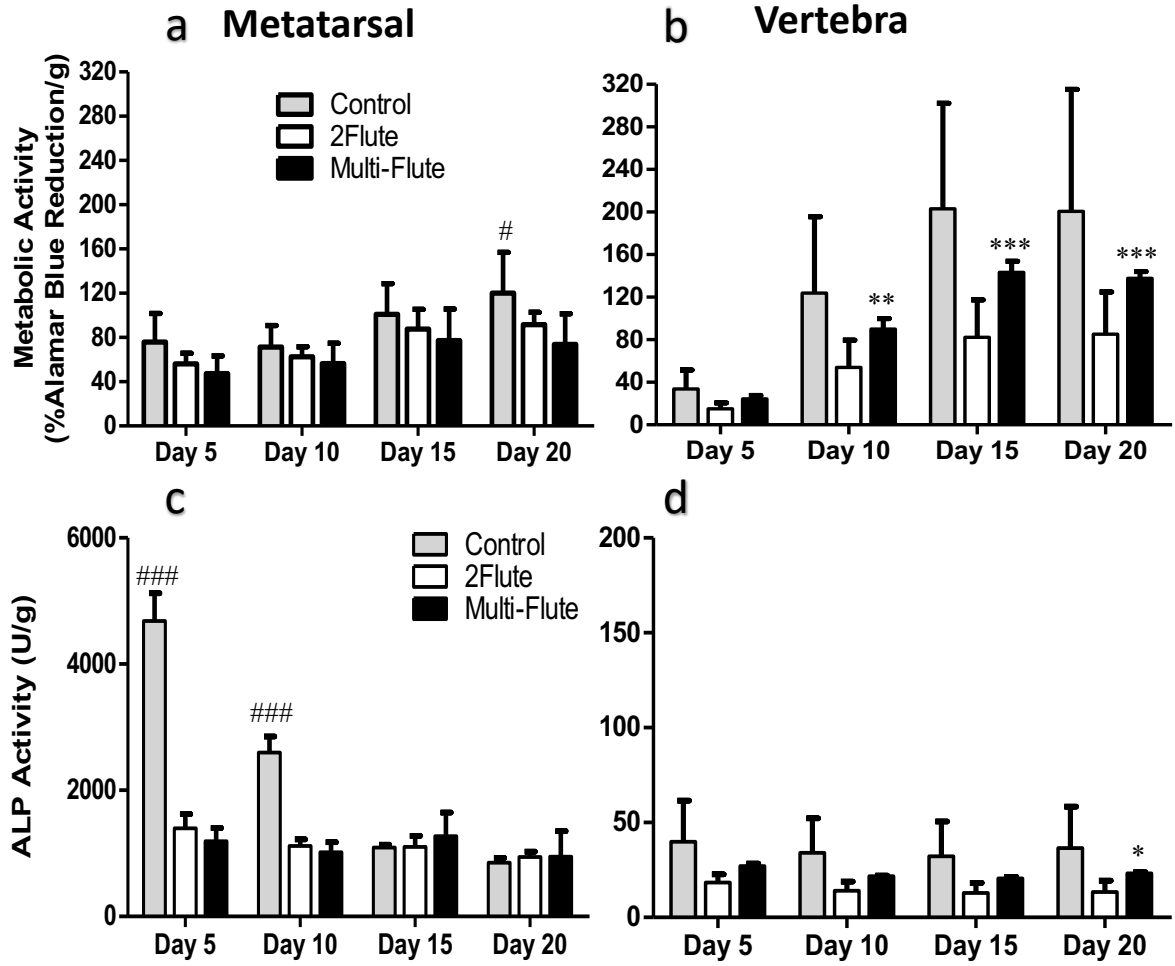

Figure 3.9: (a and b) Alamar Blue reduction of the cut surface from metatarsal (left) and vertebra (right). (c and d) Extracellular ALP activity of the cut surface groups. On day 20 of recovery, bone cut surface created by cutting with Multi-Flute showed significantly higher ALP activity in vertebra group. *$p<0.05$, **$p<0.01$, ***$p<0.001$; significance of 2Flute compared to Multi-Flute. #$p<0.05$, ###$p<0.001$; control compared to both 2Flute and Multi-Flute groups.

On day 44 of recovery, live (green, white arrows) and dead (red, yellow arrows) cells were seen on the cut surface of all groups (Fig 3.10a). When images were quantified, more viable cells were seen on the cut surface created by Multi-Flute, compared to 2Flute groups and control groups (Fig 3.10b). This was not significant, but the trend was higher in the Multi-Flute group.

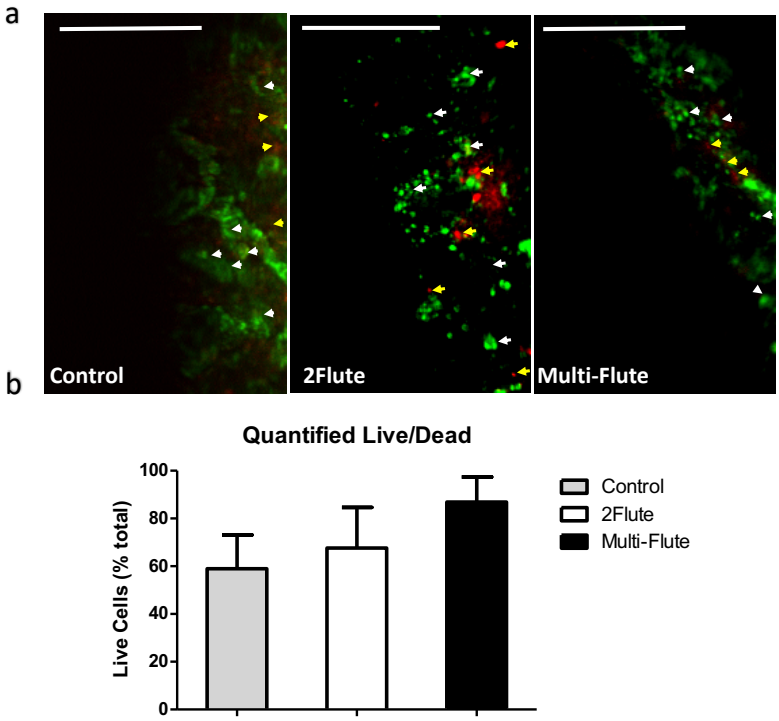

Figure 3.10: (a) Live (green, white arrows) and dead (red, yellow arrows) cells were observed. (b) In comparison to control and 2Flute groups, the cut surface created by cutting with Multi-Flute design had a higher trend for percentage of live cells to total cell count. Scale bar is 100 µm.

3.4. Discussion

Surgeons tend to avoid high speed cutting tools, because they generate high temperature that can thermally damage bone and leave behind necrotic tissue. The study in this Chapter has shown although high speed surgical cutting (without irrigation) generated increased surface temperatures in excess of 80°C, whereas dissipated temperatures were less than 35°C, bone

dust and the cut surface still have osteogenic potential, because only cells in the superficial region experience these high temperatures for very short durations (<1.33 seconds). Interestingly, the Multi-Flute bur generated higher temperature for longer durations, but the dissipated temperature in the bone still remained lower than 30°C throughout the cutting. Furthermore, the percentage of heated surface area was significantly lower with Multi-Flute cutting, because the cooling was quick after contact with the bur. Here it is reported that the regenerative potential was significantly higher in the Multi-Flute group for both bone dust and the cut surface. Thermal damage (cell apoptosis) was exacerbated in the Multi-Flute group, but only identified in the superficial resected surface and did not dissipate deep into the bone. Duration of temperature elevations and heat shock were also exacerbated during cutting with the Multi-Flute bur, but these spikes in temperature rise also cooled faster, whereby thermal necrosis was only 107.7 µm deep compared to the 182.4 µm depth observed in the cut surface resected with a 2Flute bur. These findings of enhanced mineralisation in the bone dust and the cut surface might seem surprising. Alamar blue reduction is a measurement of metabolic activity and it is commonly used to determine viability of cells exposed to stress conditions (Kuttenberger, Polska, and Schaefer 2013). It is believed that the decrease in metabolic activity at recovery day 10 is due to cells dying after 5 days of recovery, which was observed in the DNA results. However, it has been previously reported that thermal damage activates tissue regeneration (Dolan et al. 2015; Dolan et al. 2016). It is proposed that the higher temperature elevation and duration above 80°C during cutting with Multi-Flute increased the percentage of positive apoptotic cells, and thereby initiated an earlier healing response pathway than that for the 2Flute group. The Live/Dead images revealed cells dying in cut surface resected by a 2Flute bur, which was surprising after 44 days of recovery. Cells in the cut surface were not characterised in this study, further investigation is needed in order to determine which cell type was dying at later recovery days. It is proposed that the deeper necrotic tissue zone, observed

on the cut site resected with a 2Flute bur, resulting from slower cooling time had affected cell viability later during recovery. The clinical expectation of a necrotic tissue zone is initiated by angiogenesis in the area of necrosis, then bone remodelling takes place, whereby necrotic bone is resorbed by osteoclasts, paving the way for osteoblasts to lay down new bone (Shah et al. 2015).

A limitation in this study was that different bones for the temperature study (Femur and scapula for cortical and cortico-cancellous bone, respectively) and ex-vivo culture study (metatarsal and vertebra bone) was used for investigation, and so the generated temperature could be influenced by inherent differences in the mineral density distribution. Cutting on high bone density (>2 g/cm^2) generates more heat, because there is longer drill time leading to higher frictional heat (Eriksson 1984; Toews et al. 1999). However, to ensure similarity in temperature elevations, cutting only took place on the shaft of the femur, where mineral distribution is expected to be similar to the metatarsal. Moreover, it was not expect that this would influence the comparison between the different tool designs. Another limitation of this study was that irrigation was not included, although it is commonly used in surgery to minimise temperature elevations (Matthes et al. 2018) and is recommended by the manufacturers to minimise heat generation, because it was important to understand the influence of bur design on temperature elevation and bone regeneration without the influence of irrigation cooling. However, even with manual irrigation *surface* temperatures generated by surgical burs have been reported to elevate within the range reported here (100 - 249.7°C) (Matthes et al. 2018). Different irrigation methods affect heat generation (Matthes et al. 2018; Xu et al. 2014; Sener et al. 2009; Gehrke et al. 2016; Livingston et al. 2015), and further investigation is needed to fully understand the influence of irrigation on post-operative bone regeneration. It should also be noted that, as indicated by a previous study, there are discrepancies between temperature readings from a thermal camera and a thermocouple (Livingston et al. 2015). Therefore, the absolute

temperature reading on the surface is not the same as the reading inside the bone. Neither temperature measurement approaches are fully reflective of the temperatures arising because there are added variables, such as the surrounding environment, whether there are spaces between the bone and thermocouple (thermocouple) or the fluctuation in ambient temperature (FLIR camera). Finally, this experimental approach cannot distinguish the effect arising due to the mechanical forces applied during cutting, such as thrust force and torque created by the cutting flutes. It is well known that mechanical stimulation and thermal stimulation can separately enhance osteogenesis (Chung and Rylander 2012; Rauh et al. 2011; Sittichockechaiwut et al. 2009). However, previous in vivo work using a thermal probe (without mechanical forces) at 47°C and 60°C on a rat tibia for short durations of 30 seconds and 1 minute also reported that thermally damaged cell death initiated a healing response (Dolan et al. 2016). In surgical cutting, it is not easy to separate the role of each stimulation factor on post-operative bone regeneration. Further investigation is needed to fully understand the separate influences of mechanical and thermal stimulation on the osteogenic potential of surgically cut bone dust and the cut surface.

In the study conducted in this Chapter, temperature elevations increased more than 80°C on the cut surface during cutting with 2Flute and Multi-Flute surgical burs, which is much higher than temperatures previously used or investigated in either in vitro or in vivo studies (Dolan et al. 2012; Dolan et al. 2015; Dolan et al. 2016; Chung and Rylander 2012). *Surface* temperatures generated by surgical burs have been reported to be higher than 80°C, even as high as 249.7°C with manual irrigation on human spine (Matthes et al. 2018), whereas a maximum *surface* temperature of 141°C was reported when a diamond bur was used for cutting with no irrigation on porcine spine (Hosono et al. 2009). *Surface* temperature measured by a FLIR thermal camera can be unreliable due to outside factors affecting the reading from the bone cut surface, such as the camera's focal point or the temperature in the room. However, a

mean *surface* temperature elevation of 71.1±14.7°C was reported when no irrigation was used during cutting on sheep cervical vertebrae (Livingston et al. 2015). It should be noted that this study (Livingston et al. 2015) used a standard light pressure on their bur, which prevented excessive frictional heat.

Here it is report that tissue necrosis occurred as far as 182.4 µm (2Flute) and 107.7 µm (Multi-Flute) away from the cut surface when cutting with a high speed drill, which is less than that previously reported, whereby empty lacunae was observed up to 300 µm away from the drill site, where temperature was measured at 75°C with a thermocouple 500 µm away (Karaca, Aksakal, and Kom 2011). Previous work involving bone chips cut from different design burs have reported no significant difference in osteogenic capacity between different diameter size burs (3 mm, 4 mm, 5 mm, 6 mm) (Ye et al. 2013; Roth AA 2017). Both of these studies were carried out using primary cells isolated from surgically cut bone dust, where cells were devoid of their bone matrix, and identified mineralisation by qualitative immunostaining alone at later time points (Roth AA 2017) than those investigated in our study. Here, this is the first study to report significant differences in temperature elevations, thermal damage, and tissue osteogenic response, measured using quantitative assays, between two different surgical bur designs (2Flute and Multi-Flute).

Temperature elevation above the cell death threshold has been shown in vitro (Dolan et al. 2012; Dolan et al. 2015) and in vivo (Dolan et al. 2016) to cause thermally induced cell apoptosis leading to an osteogenic response in bone cells, but these studies used temperatures up to 60°C, which was considered an extreme temperature based on studies using an optical thermal chamber to stimulate heat generation and study recovery in rabbit tibia (Eriksson and Albrektsson 1984; Eriksson, Albrektsson, and Magnusson 1984; Eriksson and Albrektsson 1983). The study conducted in this Chapter report that cutting with a high speed bur generates superficial temperatures that increase by more than 80°C for short durations, and that thermally

induced cell apoptosis occurs. This study proposes that this apoptosis triggered an osteogenic response in ex-vivo bovine bone.

In contrast to previous osteogenic studies using bone dust harvested from human patients, (Roth AA 2017; Ye et al. 2013; Eder et al. 2011), temperature elevation was characterised during cutting, in order to understand heat generation on bone and influence on mineralisation. The temperature characterisation has shown that the superficial cooling rate increases as the generation of heat gets higher, and as a result, the percent of heated cut surface was lower. The study conducted in this Chapter is the first to characterise heat generated during cutting with a high speed bur, and then use this characterisation to understand the osteogenic response in ex-vivo bovine bone.

Orthopaedic surgeons have always viewed temperatures >47°C as a negative factor for bone regeneration. For this reason, surgical tools are designed with the aim of maintaining temperatures below this threshold in order to limit osteonecrosis. However, such low temperatures are not always achieved in surgery, even when irrigation is used (Matthes et al. 2018). High temperature and cell death is unavoidable during high speed surgical cutting, but the study conducted in this Chapter has shown that in fact temperature elevations can be exploited to enhance post-operative bone regeneration. It has already been shown in vitro and in vivo that thermally induced cell death initiate proliferation and tissue repair in thermally damaged bone (Dolan et al. 2015; Dolan et al. 2016). Temperatures >47°C can lead to recruitment of heat-shock proteins and upregulation of osteogenic factors to promote cell survival during thermal stress conditions (Chung and Rylander 2012). The study conducted in this Chapter have shown that ex vivo bone exposed to high superficial temperature can still survive and have osteogenic capabilities. This study could change the thinking of surgeons who avoid using these high speed tools for fear of excessive osteonecrosis. To convince them, more clinical surgical studies using high speed tools are needed. These studies should not be limited

to just osteonecrosis investigation, but should further include the osteogenic response during recovery days, which includes using quantitative PCR to determine osteogenic gene expression (COX2, RANKL, OPG, VEGF).

3.5. Conclusion

High speed cutting with surgical burs generate temperatures that increase more than 80°C for short durations at the cut surface, but temperatures in the bone remain below the threshold for cell death. This high temperature induced superficial cells to undergo apoptosis, creating necrotic tissue, and it is proposed that the thermally induced cell death triggered an osteogenic response in ex-vivo bovine bone dust and the cut surface. This study also proposes that bone exposed to high superficial temperature during high speed cutting can survive and have osteogenic capabilities.

Chapter 4 : The ex-vivo osteogenic capacity of surgically cut bone surfaces is enhanced using continuous irrigation by a device, whereas bone dust is preserved for osteogenesis when a manual intermittent irrigation is used during cutting

4.1. Introduction

High speed surgical cutting tools generate heat (Dolan, Vaughan, Niebur, Casey, et al. 2014; Matthes et al. 2018) and induce temperature elevations in the bone tissue that exceeds 47°C (Dolan et al. 2012; Dolan et al. 2015; Karaca, Aksakal, and Kom 2011; Eriksson and Albrektsson 1983; Eriksson 1984; Eriksson and Albrektsson 1984; Eriksson, Albrektsson, and Magnusson 1984). It has been shown that temperatures generated above 47°C can induce thermal necrosis and apoptosis, leading to osteogenic paracrine signalling from apoptotic cells (osteocytes) to nearby surviving cells (Dolan et al. 2015; Dolan et al. 2016). Most recently it has been reported that thermally induced cell death can initiate osteogenesis by bone cells in vitro and in vivo (Chung and Rylander 2012; Dolan et al. 2012; Dolan et al. 2015; Dolan et al. 2016). An in vitro study investigated the role of thermal stress on MC3T3 cells (pre-osteoblast) by subjecting them to temperature elevations (40°C, 42°C and 44°C) for short durations of (4, 8 minutes). Gene expression analysis of heat shock proteins, HSP47 and HSP70, and bone-related proteins, osteopontin (OPN) and osteocalcin (OCN) were carried out at 8, 24, and 72 hours after thermal conditioning (Chung and Rylander 2012). They reported an upregulation in HSP47, HSP70, OPN and OCN gene expression after thermal stress conditioning at 44°C, indicating that MC3T3 cells underwent an osteogenic response when experiencing a slight increase in temperature compared to physiological temperature (37°C). However this study

investigated temperatures below the threshold temperature for cell death (47°C). The study conducted in Chapter 3 has reported that temperature increases (relative to bone temperature) exceed 80°C for short durations, using a thermal camera during cutting with high speed surgical burs of different designs (2Flute, Multi-Flute) on bovine bone surfaces (Chapter 3). The study also reported higher temperature elevation and apoptotic cells in the cut surface resected with Multi-Flute bur (Chapter 3). Interestingly, the bone dust and the cut surfaces resected with the Multi-Flute exhibited an enhanced ex-vivo osteogenic response and this was proposed to be associated with higher thermally-induced cell apoptosis (Chapter 3). However, this study was not conducted in the presence of irrigation, which is commonly used alongside of high speed cutting, and so the osteogenic response in cells subjected to the same cutting conditions in surgery is not fully understood.

Post-operative bone regeneration can be influenced by duration of temperature elevation (Dolan et al. 2012; Eriksson and Albrektsson 1983; Eriksson, Albrektsson, and Magnusson 1984; Eriksson and Albrektsson 1984). An in vitro study compared the influence of heat treated MLO-Y4 cells on Balb/c MSCs and MC3T3 cells, using moderate temperature elevations (45ºC, 47ºC, and 60ºC) for short durations (30 seconds and 1 minute), and they reported an increase in extracellular and intracellular ALP activity and calcium content in Balb/c and MC3T3 cells receiving conditioned media from heat treated MLO-Y4 compared to control (MLO-Y4 cells with no heat treatment) (Dolan et al. 2012). In comparison to control groups (37ºC), heat-treated MC3T3 cells in groups subjected to 60ºC for 30 seconds and 1 minute durations had an immediate necrotic response to heat shock and showed an increase in intracellular ALP activity (Dolan et al. 2012). Another study heat treated (41 - 44°C) human mesenchymal stem cells (MSCs) from bone marrow of iliac crest of patients (25 - 30 years) for one hour duration, and reported an increase in ALP activity and calcium content after 8 days of culture (Norgaard, Kassem, and Rattan 2006). These studies chose durations to reflect the

usage time of cutting tools, yet this is not always consistent between surgical procedures or even between surgeons and is highly dependent on the duration of the procedure. However, the duration of heat shock (>47°C) on bone surgically cut using burs and irrigation methods still remains unknown, and the effect of heat exposure time on post-cutting bone regeneration is still not known.

Using irrigation during high speed cutting is a common practice during orthopaedic surgery, in order to minimise temperature elevations and limit cell death and osteonecrosis. Different irrigation approaches are used; manual irrigation is applied by a surgical assistant whereas automated irrigation is delivered by a pumped device with constant continuous flow of liquid onto the cut site. Parameters such as feed rate, spindle speed, irrigation temperature, and irrigation flow rate have been explored to determine the effect of irrigation on temperature elevation during cutting with a high speed orthopaedic twist drill (Sener et al. 2009; Hosono et al. 2009; Sharawy et al. 2002). One study explored the effect of continuous irrigation temperature at 10°C and 25°C on heat elevation at different drilling depths (3 mm, 7 mm, and 12 mm) on 37°C bovine mandibles (Sener et al. 2009). Temperature was measured by a thermoresistor (0.5 mm away) and it was reported to decrease below 37°C during drilling at a rotational speed of 800 rpm when irrigation at 10°C and 25°C was incorporated (Sener et al. 2009). Another study exploring temperature elevation during cutting on porcine spinal lamina using steel and diamond tip burs and varying irrigation flow rate (180ml/hr and 540 ml/hr delivered using an irrigation device), reported a significant increase in temperature when a diamond bur was used compared to a steel tip bur, both without irrigation (Hosono et al. 2009). They also reported a decrease in temperature when irrigation (540 ml/hr) was used with a diamond bur, compared to not irrigating with the same bur (Hosono et al. 2009). These studies focused on irrigation parameters affecting heat generation, but they did not further explore the influence of manual and continuous irrigation, used during high speed cutting, on ex-vivo bone

regeneration. These different methods likely influence temperature elevations during cutting, but this has never been quantified.

A study compared temperature generation during spinal fusion surgery using high speed cutting with diamond burs in the presence of manual and continuous irrigation, and the temperature as measured by a thermal camera for manual and continuous irrigation was reported to be between 88.4°C and 249.7°C, and 75.5°C and 194.2°C, respectively (Matthes et al. 2018). The surgical cutting temperature was significantly decreased in the presence of continuous irrigation, in comparison to using manual irrigation with a syringe (Matthes et al. 2018). Another study investigated temperature elevation using a FLIR camera (superficial) and thermocouple (deep) during surgical decortication of porcine vertebra, and they also reported a significant decrease in temperature when continuous irrigation (43.3±6.25°C) was delivered by a 10 mL syringe, in comparison to no irrigation (71.1±14.7°C) (Livingston et al. 2015). However, these studies did not further investigate bone cell recovery from such temperatures generated during high speed cutting, and so the influence of irrigation on bone cells' regenerative capacity remains unknown.

Bone cells are exposed to temperature elevations during cutting with a high speed device, and the regenerative capacity of these cells at the cut surface is vital for bone healing. One study reported maximum temperature elevations (54.84°C) at the endosteal cut surface during cutting of ovine metatarsal bone using a surgical saw (150 mm/min) (Dolan, Vaughan, Niebur, Casey, et al. 2014). The duration that the endosteal cut surface exceeded the cell death threshold (47°C) was reported to be 38 seconds, whereas the temperate also dissipated to bone tissue up to 620 μm from the cut surface and remained above the cell death threshold for 20 seconds (Dolan, Vaughan, Niebur, Casey, et al. 2014). Computational modelling predicted that these elevated temperatures could be experienced by osteocyte cells embedded in the matrix (Dolan, Vaughan, Niebur, Casey, et al. 2014). Another study assessed cell viability at the cut

surface using histological staining to report osteonecrosis induced by cutting with a high speed orthopaedic drill (Karaca, Aksakal, and Kom 2011). An increase in empty lacunae at the cut surface were observed to be associated with temperatures between 60°C and 79°C, measured by thermocouples (0.5 mm away) (Karaca, Aksakal, and Kom 2011). Although these studies explored thermal exposure of cells at (and in proximity to) the cut surface, the influence of irrigation parameters on temperature elevations at the surface, and the regenerative capacity of the cut surface is not yet fully understood.

Therefore, the hypothesis that "Surgical cutting with manual irrigation induces higher temperatures, when compared to cutting with continuous irrigation, but the ex-vivo osteogenic potential of autograft bone dust is enhanced" was tested in this Chapter. The overall objective of the study conducted in this Chapter was to compare the cellular response in bone dust and the cut surface after resection with high speed cutting while using manual and continuous irrigation. The first specific objective of this study was to determine the relative *surface* (FLIR camera) and *dissipated* (thermocouple) temperature elevation during cutting with surgical burs (2Flute, Multi-Flute). Specifically the study sought to compare temperature elevations in the presence of manual irrigation, representative of a surgeon's assistant applying irrigation with a syringe, and continuous, where temperature fluctuations is minimised by an automated irrigation device. Thermal exposure time to damaging levels was assessed by quantifying the duration of *surface* temperature above the cell death threshold (47°C). The extent of potential tissue volume damage was assessed by quantifying the cooling rate and percent heated cut surface. The second specific objective of this study was to determine the role of this temperature elevation on thermal damage by investigating osteogenic capacity of bone dust and the cut surface during recovery days post cutting using ex-vivo cell culture techniques (Alamar blue, ALP activity, Alizarin red), and to compare this response between manual and continuous irrigation.

4.2. Materials and Methods

4.2.1. Bone harvest

Freshly harvested porcine spine samples (Rosderra Irish Meats, Edenderry, Offaly, n=3) were obtained, where cutting took place in the spinal lamina located in the lumbar region (L1-L6) of the spine (4 samples from each porcine animal). A scalpel blade was used to cut through the vertebra disc, ensuring that the vertebra body and lamina bones were not damaged. Soft tissue was removed using osteotomy tools (Stryker, Kalamazoo, Michigan) and scalpels, ensuring that the periosteum was completely removed from the lamina and spinal processes.

4.2.2. Surgical Cutting

All cutting was conducted with a high speed πDrive drill (Stryker, Kalamazoo, Michigan) at a rotational speed of 75,000 rev/min using a clockwise hand motion with either a 2Flute or Multi-Flute bur (both from Stryker, Kalamazoo, Michigan) until 20 cc of bone dust was collected. Surgical cutting was conducted in combination with either (a) manual or (b) continuous irrigation, wherein the irrigation solution was phosphate buffered saline (PBS) containing 5% Antimycotic Antibiotic solution (AAS, both Sigma). Manual irrigation was delivered with a 50 ml syringe, and this represents a surgical assistant applying irrigation while a surgeon is cutting. Cutting with manual irrigation was conducted by cutting for 30 seconds, then irrigate cut surface and repeat until 20 cc of bone dust was collected. Continuous irrigation was conducted using an irrigation sleeve, (Stryker, Kalamazoo, Michigan) attached to the πDrive drill to provide continuous irrigation on the surface throughout the cutting process (Fig. 4.1a), whereby the flow rate of the irrigation solution (14 ml/minute) was controlled using an irrigation cassette and console (both Stryker, Kalamazoo, Michigan). Thus, the four conditions in this study are as follows: Multi-Flute Manual (MM), 2Flute Manual (2M), Multi-Flute Continuous (MC), and 2Flute Continuous (2C).

4.2.3. Surface Temperature determined by FLIR camera

Temperature analysis was conducted during surgical cutting of porcine spinal lamina using a Forward-Looking Infrared Radiometer thermal camera (FLIR, FLIR T440) to measure surface temperature (Fig. 4.1a and d). The FLIR camera took images at a frame rate of 7.5 frames/second, where emissivity of 0.95 (Feldmann 2016) and the Ar1 setting was to define the area for temperature measurement (27 mm x 31 mm, Fig. 4.1a). The *surface* temperature data was analysed to quantify (1) the maximum relative temperature during 60 seconds of cutting (relative to initial wet bone temperature), (2) the duration of temperature exposure to bone at temperature elevations above 47°C, and (3) the cooling rate, which was the differential in one second. The initial temperature of the bone in the intended cut surface prior to cutting was used to quantify the *relative* increase in temperature. FLIR images were further processed using ImageJ software to quantify the percent heated surface area and the total cut surface area. All temperature measurements for each condition were repeated 3 times (replicates) for 3 different animals.

4.2.4. Dissipated temperature determined by thermocouple

A K-type thermal couple (Agilent) was embedded into the centre of the porcine lamina to measure dissipated temperature (Fig. 4.1b) into a pre-drilled hole, prepared using a πDrive drill with a router attachment (both Stryker, Kalamazoo, Michigan), with thermal paste (Sigma) filling the spaces between the thermocouple and bone (Fig. 4.1b, yellow line). Cutting was conducted in the vicinity of the thermocouple, whereby the borderline of the cut surface was between 0.24 mm and 0.56 mm (Fig 4.1c) from the thermocouple, whereas the FLIR camera was pointed at the cut site. Data from the thermocouple was analysed to quantify the maximum dissipated temperature elevation during cutting in the presence of irrigation and temperature increase relative to bone temperature before cutting. For all temperature analysis, the duration of cutting was 60 seconds, and data is expressed as mean ± standard deviation.

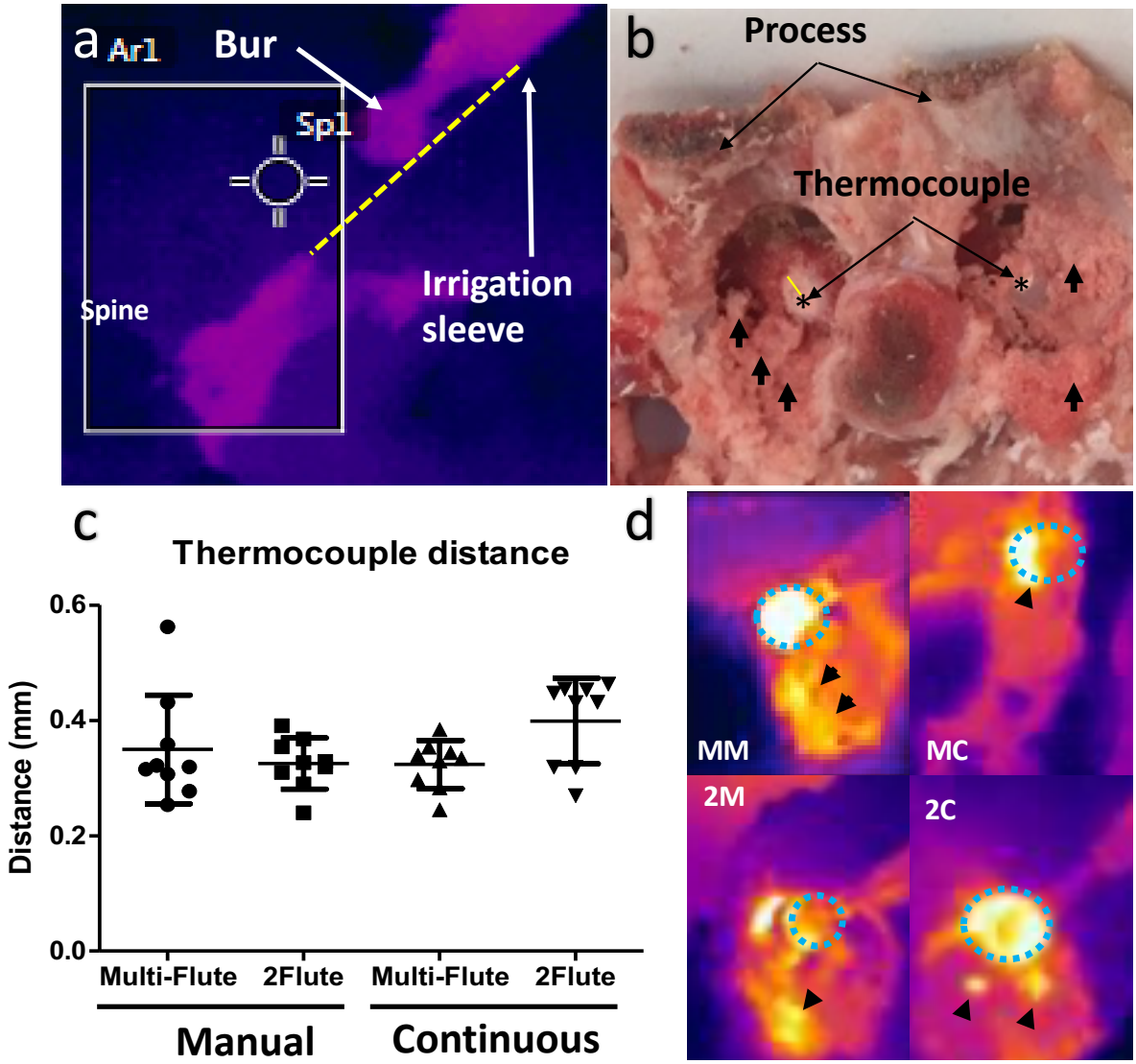

Figure 4.1: (a) Thermal camera image of irrigation sleeve. (b) Gross image of porcine spine showing clogging (black arrows), the location of the thermocouple and distance between edge of the cut surface and thermocouple (yellow line). (c) Graph of distance of thermocouple. (d) Thermal camera images also showing clogging of bone dust on the cut surface during cutting (black arrows).

4.2.5. Ex-vivo culture

The (1) bone dust was collected into 50 ml falcon tubes, and (2) the cut surfaces were further processed into bone cores (5 mm x 5 mm x 2 mm) using the router attachment (Stryker, Kalamazoo, Michigan) with copious continuous irrigation for ex-vivo culture. Control cores of the same dimensions were also prepared using a router, but contained no cut surface created by the burs (2Flute, Multi-Flute). All samples were transferred into a 50 ml falcon tube

containing 5% AAS in phosphate buffered saline solution (PBS). Using a vortex to remove fats and unwanted soft tissue, all bone dust and the cut surface groups were washed 3-5 times with sterile PBS. Afterwards, all bone dust and bone cut surface samples were cultured in cell culture media at 37°C, 5% CO_2 for ex-vivo cell culture experiments for up to 65 days for bone dust groups and 55 days for the cut surface groups, when experiment was terminated.

Bone dust, and the cut surface samples were cultured in Dulbecco Modified Eagle Medium Glutamax media (Biosciences) and Hyclone Nutrient Ham's/F12 (ThermoFisher) (DMEM/F12, 1:1 ratio), supplemented with 10% foetal bovine serum (FBS), 2% antimycotic antibiotic streptomycin solution, 50 µM Ascorbic acid, 1% w/v Dexamethasone, and 20 mM β-Glycerol phosphate (all Sigma). The media was changed twice per week or two days before collecting media for alkaline phosphatase (ALP) assay (Sigma). For all ex-vivo groups, metabolic activity and extracellular ALP activity was quantified on days 1, 10, 15, and 20. For bone dust groups, calcium was quantified on days 55 and 65, while calcium was quantified on days 41 and 55 in the cut surface groups. All data is expressed as mean ± standard deviation.

4.2.6. Thermal damage in bone

Thermally induced damage in the bone dust was investigated using an antibody for cleaved caspase 3, a marker of cell apoptosis, as described previously (Dolan et al. 2016). The cleavage of pro-caspase 3 activates extrinsic and intrinsic cell apoptosis pathways, whereby cell morphology changes, and cell blebbing occurs due to lysis of cellular and nuclear membrane, leading to the release of cellular content. On recovery day 1, bone dust groups were fixed with 10% neutral buffered formalin solution (Sigma) and then decalcified in 0.5M ethylenediaminetetraacetic acid (EDTA, Sigma) for five days or until a decalcification test was negative for calcium. Following this, bone dust samples were embedded in Histogel (Thermo Fisher), processed in an automated Tissue Processor (Leica) overnight, embedded in paraffin

wax and sectioned at 4 μm using a microtome (Leica). Sectioned samples were mounted on a glass slide and deparaffinised overnight in an oven at 60°C. Sections were blocked for 30 minutes using 1% bovine serum albumin (BSA, Sigma) to prevent non-specific binding, then followed by overnight incubation with cleaved caspase 3 antibody (Cell Signalling) at a concentration of 1:100. Samples were washed with 1% BSA and stained with Alexa Fluor 488 (Thermo Fisher) at a concentration of 1:700 for 1 hour at room temperature in the dark, then counterstained with mounting media containing 4',6'-diamidino-2-phenylindole (DAPI, Sigma), and imaged using a confocal laser scanning microscope (Olympus Fluoview 100 system) at 40x magnification. Images were processed using ImageJ software to quantify positive and negative apoptotic cells. To quantify intensity of cleave caspase 3, images were further processed by ImageJ as previously described by (Geoghegan, Hoey, and McNamara 2019), whereby more intensity indicate increase in concentration of activated caspase 3 signalling molecule, which leads to DNA fragmentation and cell blebbing.

4.2.7. Metabolic activity in bone dust and the cut surface

An Alamar Blue assay (Bioscience, DAL 1100) was conducted on ex-vivo bone dust and the cut surface groups to measure the metabolic activity of cells through glycolysis, according to previous protocol (Kuttenberger, Polska, and Schaefer 2013). Briefly, bone dust and the cut surface were washed 3 times with 2% AAS/PBS solution, then incubated in 10% v/v Alamar Blue reagent in DMEM/F12 media in an incubator (37°C, 5% CO_2) for 4 hours. Absorbance values were measured using a microplate reader (BioTek Synergy HT), and Alamar Blue reduction was quantified for each condition group and normalised to DNA content (bone dust) and weight (cut surface), expressed as %/μg and %/g, respectively.

4.2.8. Alkaline phosphatase activity in bone dust and the cut surface

Alkaline phosphatase (ALP) activity is an early mineralisation marker and an indication of osteoblastic differentiation. An ALP assay is commonly used to quantify extracellular ALP content in media, using a calorimetric test for *p*-nitrophenyl phosphate (*p*-NPP) as a phosphate substrate. Extracellular ALP activity for bone dust and the cut surface groups were quantified according to a previous protocol (Dolan et al. 2012). Briefly, media from the bone dust and the cut surface groups were collected on recovery days, where 40 µl of media from each sample group was added to 50 µl of 5mM pNPP solution (Sigmafast) and 40 µl of water in a 96-well plate, which was then incubated at room temperature for 1 hour, to which 20 µl of 3M NaOH was added to stop reaction of ALP enzyme (all Sigma). Absorbance values were measured at 405 nm using a microplate reader (BioTek Synergy HT). Using a standard curve of 0-80 nM of p-NPP content, ALP activity was calculated in milli-units (mU), then normalised to DNA content and expressed as milli-units per µg of DNA (mU/µg) for bone dust groups and weight for the cut surface groups (mU/g).

4.2.9. Calcium content assay in bone dust and the cut surface

Calcium deposition is a late stage mineralisation marker for osteogenesis. To determine the calcium deposition from the cells derived from the surgically cut bone dust and the cut surface, cell outgrowths were expanded and seeded at a concentration of 100 x 10^3 cells/well in a 24-well plate. Time points were chosen based on first passage of cells in the first repeat, then the same time point was used for all repeated experiments. Calcium content was quantified by Alizarin red staining, as previously described (Dolan et al. 2016). Briefly, cells were washed twice with PBS, then stained with 40 µM Alizarin red S (Sigma) for 20 minutes at room temperature on an orbital shaker at 350 rpm. Afterwards, cells were washed with PBS until the liquid was clear, indicating the full removal of unbound Alizarin red S (AR). AR-calcium complex was de-stained in 10% w/v cetylpyridinium chloride (Cpl, Sigma) by incubating at

room temperature for 20 minutes on an orbital shaker (350 rpm) and quantified. Absorbance values were measured using a microplate reader (BioTek Synergy HT) at 562 nm. Calcium content was calculated, normalised to DNA content (both bone dust and the cut surface), and expressed as micro-molar per microgram (μM/μg).

4.2.10. DNA content in bone dust

DNA content was quantified using a Hoechst assay, as previously described (Dolan et al. 2012). Briefly, bone dust and cells were washed twice with PBS and then 500 μl of lysis buffer solution, containing 1% Triton X (Sigma) in Hoechst buffer (100mM Tris, 2M NaCl, and 10mM EDTA, all Sigma), was added and placed into a -80°C freezer. Samples were subjected to 3 cycles of freeze-thawing in lysis buffer. For cell samples, a cell scraper was used to detach and lyse the cells. Lysate solution was transferred into a 1.5 ml Eppendorf tube and frozen at -20°C until use for Hoechst assay. The Hoechst assay was carried out by aliquoting 20 μl of lysate for each group in triplicates into a 96-well plate. Two hundred microlitre of DNA working solution, containing 0.01% Hoechst 33258 dye in Hoechst buffer, was added into each well, ensuring homogenous mixture. Using a microplate reader (BioTek Synergy HT), fluorescence was measured and DNA content was quantified and used to normalise Alamar blue reduction, extracellular ALP activity and calcium data.

4.2.11. Statistical analysis

Temperature data, ex-vivo metabolic activity (Alamar Blue), ALP activity and calcium (quantified Alizarin red) data were analysed using Graphpad (version 5) software, and values are represented as mean ± standard deviation. A two-way ANOVA was used with Bonferroni's post-test to compare between manual and continuous irrigation groups, and between 2Flute and Multi-Flute groups. A student t-test was used to analyse apoptosis images with significance at $p<0.05$. All experiments were repeated 3 times with 3 replicates.

4.3. Results

4.3.1. Higher surface and dissipate temperature elevations occur during cutting in the presence of manual irrigation

Relative surface temperature was significantly higher with manual irrigation in comparison to continuous irrigation for both Multi-Flute ($p<0.01$) and 2Flute cutting ($p<0.05$) (Fig. 4.2a, Table 4.1). For the manual group, the relative temperature was significantly higher ($p<0.01$) when a Multi-Flute was used for cutting, compared to cutting with the 2Flute design (Table 4.1). However, with continuous irrigation there was no significant ($p=0.1398$) difference in temperature elevation between cutting with the 2Flute and Multi-Flute bur (Fig. 4.2a, Table 4.1).

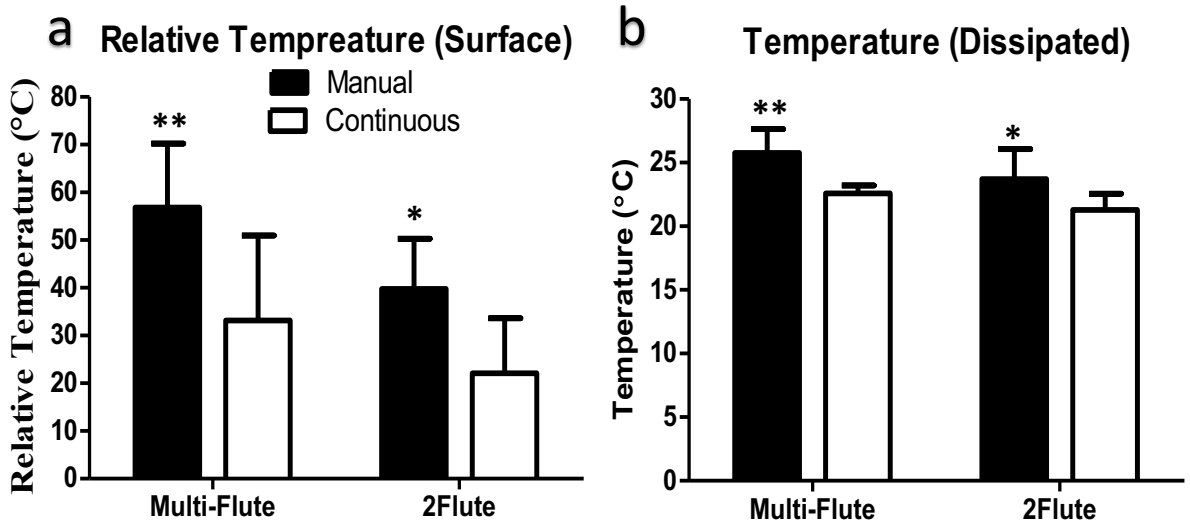

Figure 4.2: (a) Relative surface temperature was significantly higher during manual irrigation in both 2Flute and Multi-Flute groups. (b) Dissipated temperature was higher during manual irrigation, compared to automated. * $p<0.05$; ** $p<0.01$; *** $p<0.001$ Manual vs Continuous

The dissipated temperatures inside the bone remained below 30°C for all cutting conditions (Fig. 4.2b, Table 4.2). The dissipated temperature was significantly higher ($p<0.05$) when manual irrigation was used, in comparison to continuous groups (Fig. 4.2b, Table 4.2). This significance was observed in both Multi-Flute ($p<0.01$) and 2Flute ($p<0.05$) groups. Moreover,

the increase in dissipated temperature was also significantly higher ($p<0.05$) during manual irrigation compared to continuous (Table 4.2). When comparing bur designs during continuous irrigation, the increase in dissipated temperature was significantly ($p=0.014$) higher when using a Multi-Flute for cutting (Table 4.2).

Table 4.1: Maximum Surface Temperature (Thermal Camera)

Thermal Camera n=9	Cutting	2Flute	Multi-Flute	p-value*	p-value#
Relative Temperature	Manual	39.75±10.55 °C	56.85±13.41 °C	0.00613 (MF)	0.008784
	(Range)	(21.27 °C – 53.54 °C)	(38.38 °C – 79.47 °C)		
	Continuous	22.07±11.55 °C	33.15±17.92 °C	0.00378 (2F)	0.139823
	(Range)	(7.6 °C – 36.18 °C)	(12.17 °C – 54.26 °C)		

*p-value shows significance of manual versus continuous, #p-value shows significance of 2Flute versus Multi-Flute

The cooling rate was significantly faster with manual compared to continuous irrigation for the 2Flute groups (Fig. 4.3a). When cutting in the presence of continuous irrigation, the cooling rate was significantly faster when a Multi-Flute was used for cutting (Fig. 4.3a). The elevated temperature (>47°C) duration was significantly ($p<0.001$) longer during manual irrigation when compared to continuous for the Multi-Flute groups (Fig. 4.3b). The percent heated surface was also higher during manual irrigation in comparison to using continuous irrigation (Fig. 4.3c) for both the Multi-Flute ($p<0.01$) and 2Flute ($p<0.001$) groups.

Table 4.2: Maximum Dissipated Temperature (Thermal Couple)

Thermal Couple n=6	Cutting	2Flute	Multi-Flute	p-value*	p-value#
Mean Maximum Temperature	Manual	23.72±2.35 °C	25.75±1.88 °C	0.0078 (MF)	0.056
	Continuous	21.29±1.26 °C	22.59±0.62 °C	0.058 (2F)	0.132
Mean Temperature Increase	Manual	7.29±2.61°C	8.84±2.15 °C	0.029 (MF)	0.29
	Continuous	4.458±0.94 °C	6.195±1.08 °C	0.045 (2F)	0.014

*p-value shows significance of manual versus continuous, #p-value shows significance of 2Flute versus Multi-Flute

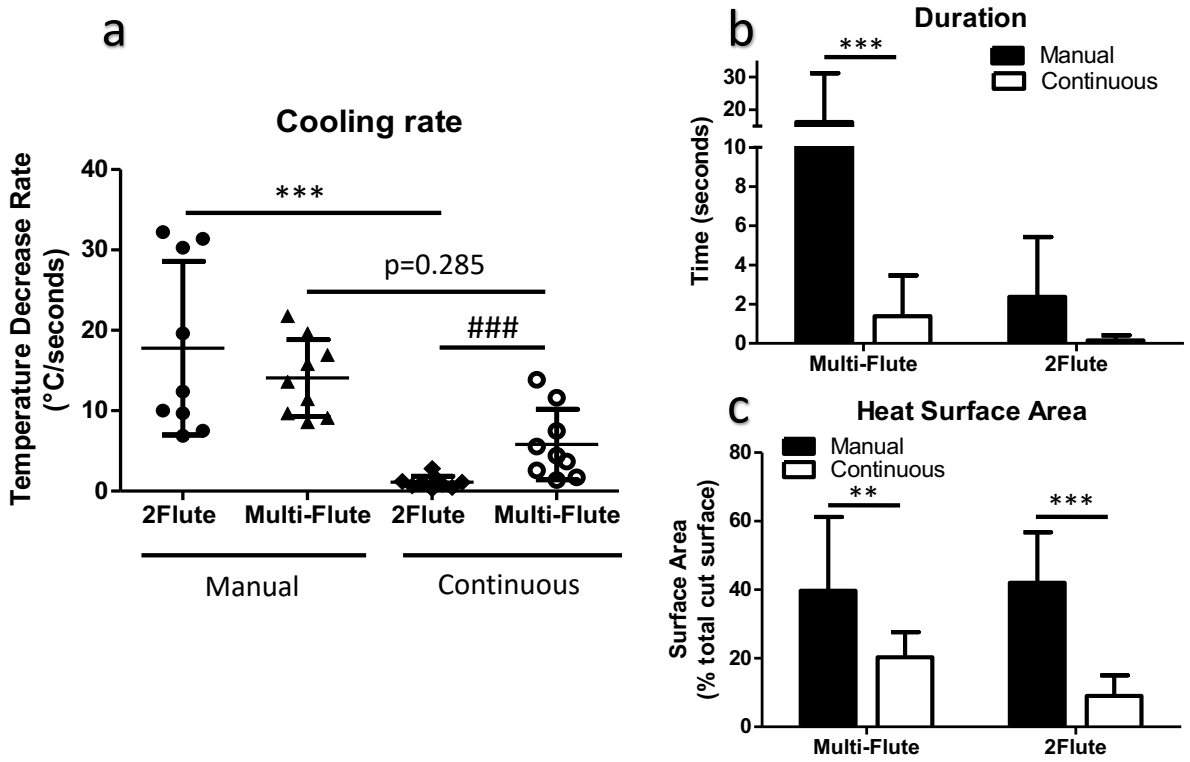

Figure 4.3: (a) Cooling rate during cutting in the presence of manual and continuous irrigation. (b) Duration time of exposure to temperatures >47°C during cutting with manual and continuous irrigation using 2Flute and Multi-Flute burs. (c) Percent heated cut surface was higher during manual irrigation. ** $p<0.01$; *** $p<0.001$ Manual vs Continuous; ### $p<0.001$ 2Flute vs Multi-Flute.

4.3.2. Cell apoptosis and metabolic activity within bone dust and at the cut surface do not differ due to cutting with manual and continuous irrigation

Caspase positive and negative cells were observed in all bone dust (Fig. 4.4) and the cut surface groups (Fig. 4.5). For both bone dust and the cut surface groups, there was no significant difference in positive staining for apoptotic cells between the manual and continuous groups (Fig. 4.4 and Fig. 4.5). Significantly higher negative apoptotic cells were observed than positive cells in both bone dust and the cut surface groups (Fig. 4.4c and Fig. 4.5c). Cleaved caspase 3 was more prominent in bone dust resected with manual irrigation, whereby fluorescence intensity for cleaved caspase 3 (activated cell death) was higher compared to continuous irrigation groups (Fig. 4.4d). Necrotic region (DAPI-negative) on surface of cut site was

quantified, and the trend was higher in cut surface resected with a manual irrigation approach during cutting with high speed burs (Fig. 4.5e).

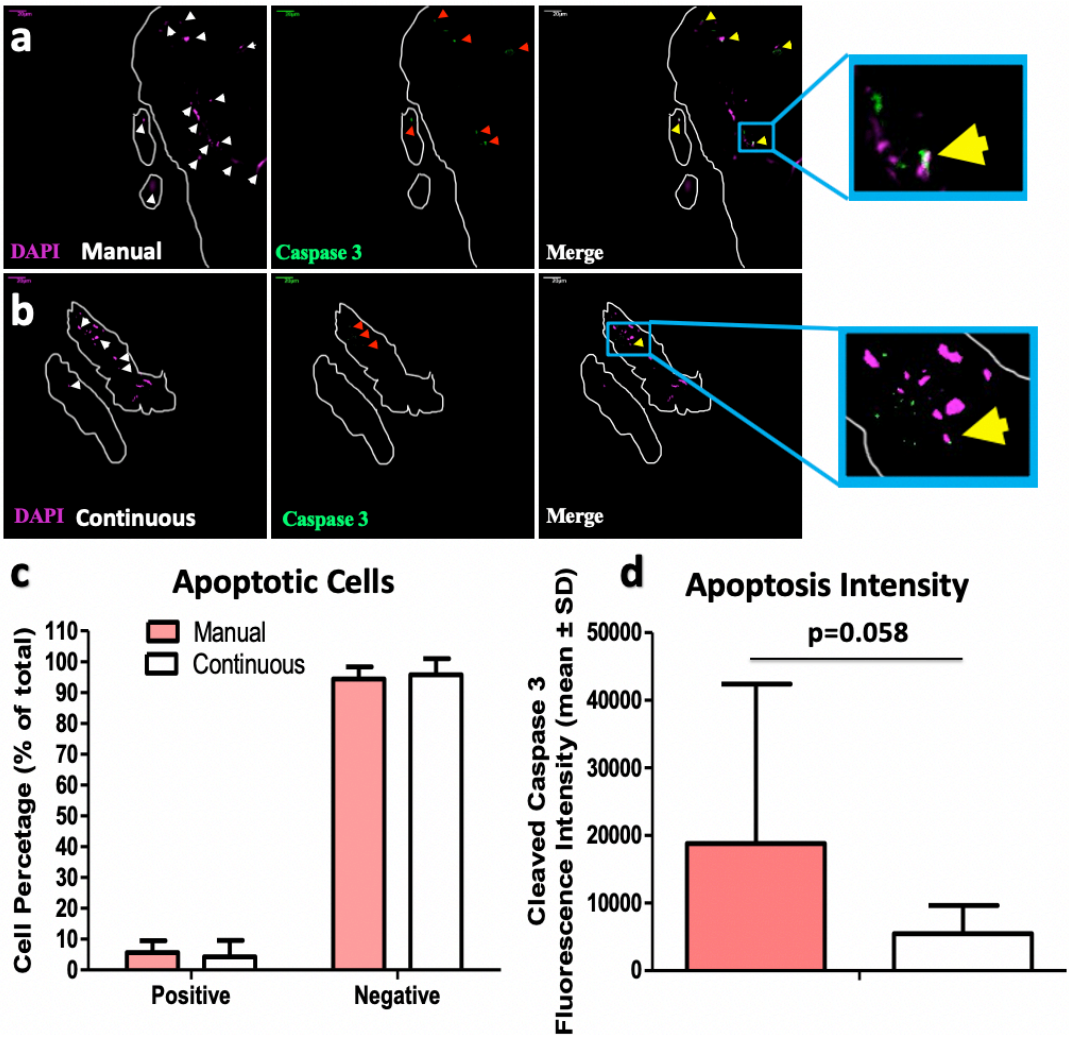

Figure 4.4: Fluorescence image of cleaved caspase 3 on recovery day 3 on bone dust resected during (a) manual irrigation and (b) continuous irrigation. White line indicates shape of bone dust, white arrows indicate DAPI stain for cell nucleus, red arrow indicates caspase 3, and yellow arrows indicated caspase positive cells. (c) Graph showing percentage of positive and negative apoptotic cells. (d) Quantified apoptosis intensity of images from bone dust resected in the presence of manual and continuous irrigation. Scale bar is 20 µm.

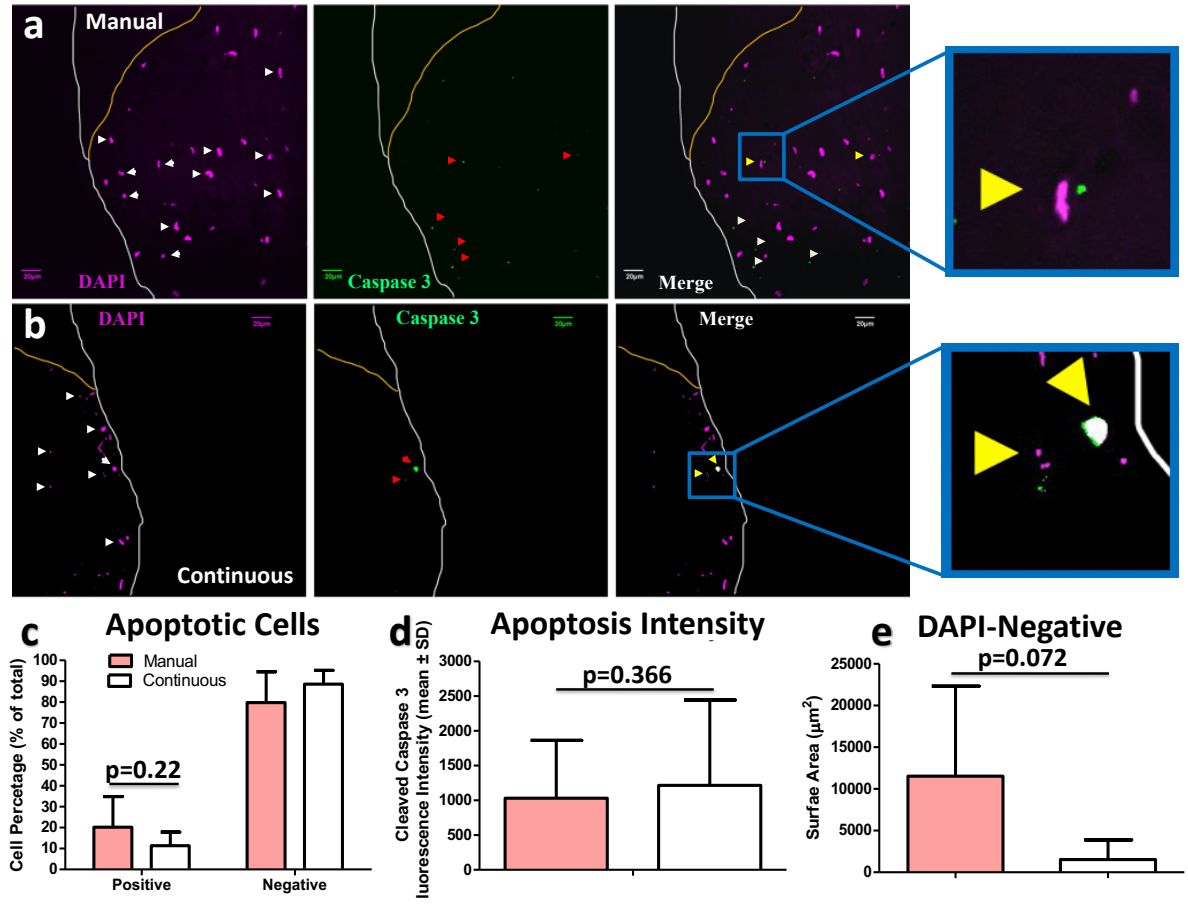

Figure 4.5: Fluorescence image of cleaved caspase 3 on recovery day 1 on the cut surface resected during (a) manual irrigation (n=557) and (b) continuous irrigation (n=444). White line indicates border of the cut surface and yellow lines indicate DAPI negative area, white arrows indicate DAPI stain for cell nucleus, red arrow indicates caspase 3, grey arrows indicate apoptotic bodies, and yellow arrows indicate caspase positive cells. (c) Graph showing percentage of positive and negative apoptotic cells. (d) Quantified apoptosis intensity of images from the cut surface resected in the presence of manual and continuous irrigation. (e) Quantified area of DAPI-negative region on surface of cut site, where the trend is higher in cut surface resected with a manual irrigation approach. Scale bar is 20 μm. The n represents the total cell count for manual and continuous irrigation.

Metabolic activity (Alamar Blue reduction) increased on day 10 and decreased afterwards in bone dust groups, whereas reduction remained the same (>50%) for all time points in the cut surface groups (Fig. 4.6). Moreover, there was no significant difference in metabolic activity between manual and continuous irrigation groups, observed in both bone dust and the cut surface groups (Fig. 4.6).

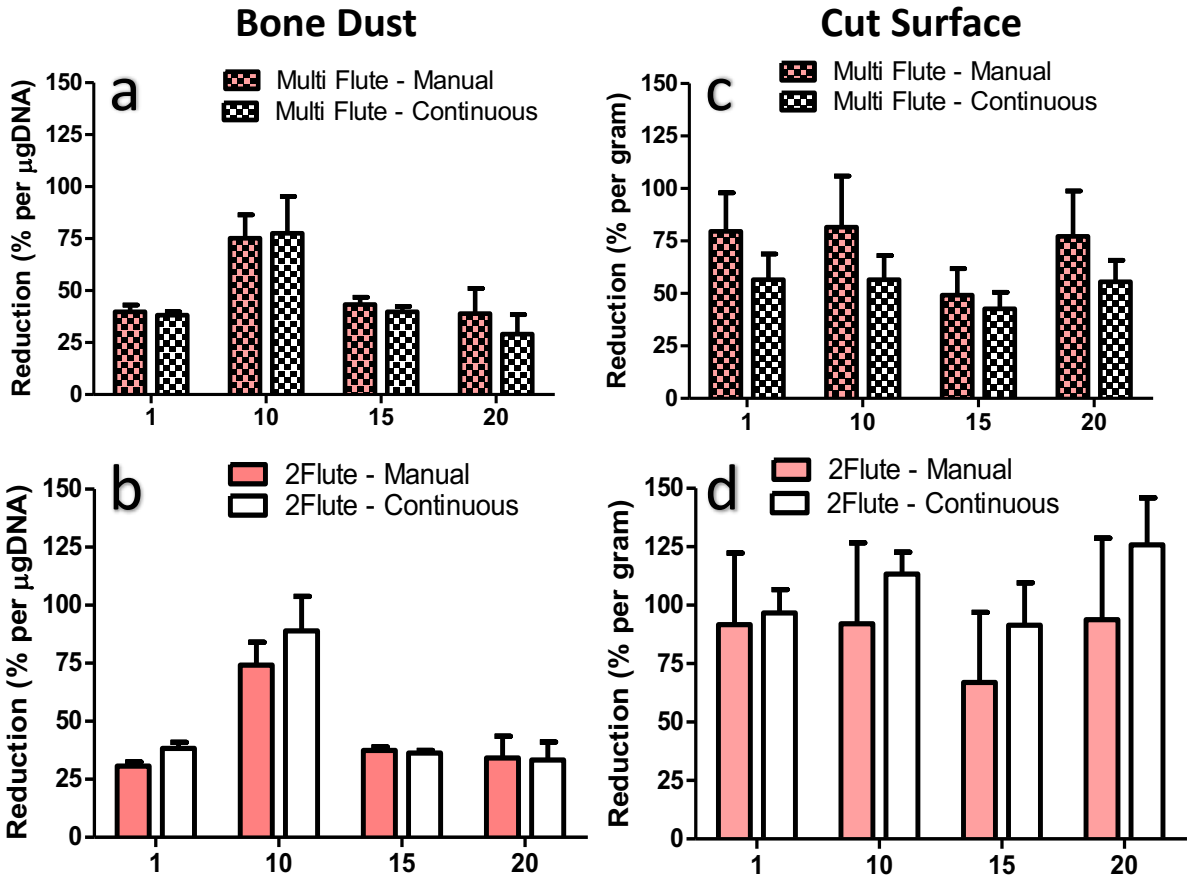

Figure 4.6: Alamar Blue reduction of (a-b) bone dust and (c-d) the cut surface during 20 days of recovery, where there was no significant difference between manual and continuous irrigation.

4.3.3. The osteogenic capacity of bone dust is higher when resected in the presence of manual irrigation compared to continuous irrigation

In bone dust groups, extracellular ALP activity decreased after recovery day 1 and increased after day 10 (Fig. 4.7). The manual irrigation group had significantly higher ALP activity on recovery day 1, compared to continuous irrigation groups on the same day for both the 2Flute ($p<0.001$) and Multi-Flute ($p<0.05$) bur cutting conditions (Fig. 4.7a). The results demonstrate that there was no significant difference between manual and continuous irrigation cutting groups on recovery days 10, 15 and 20 (Fig. 4.7a).

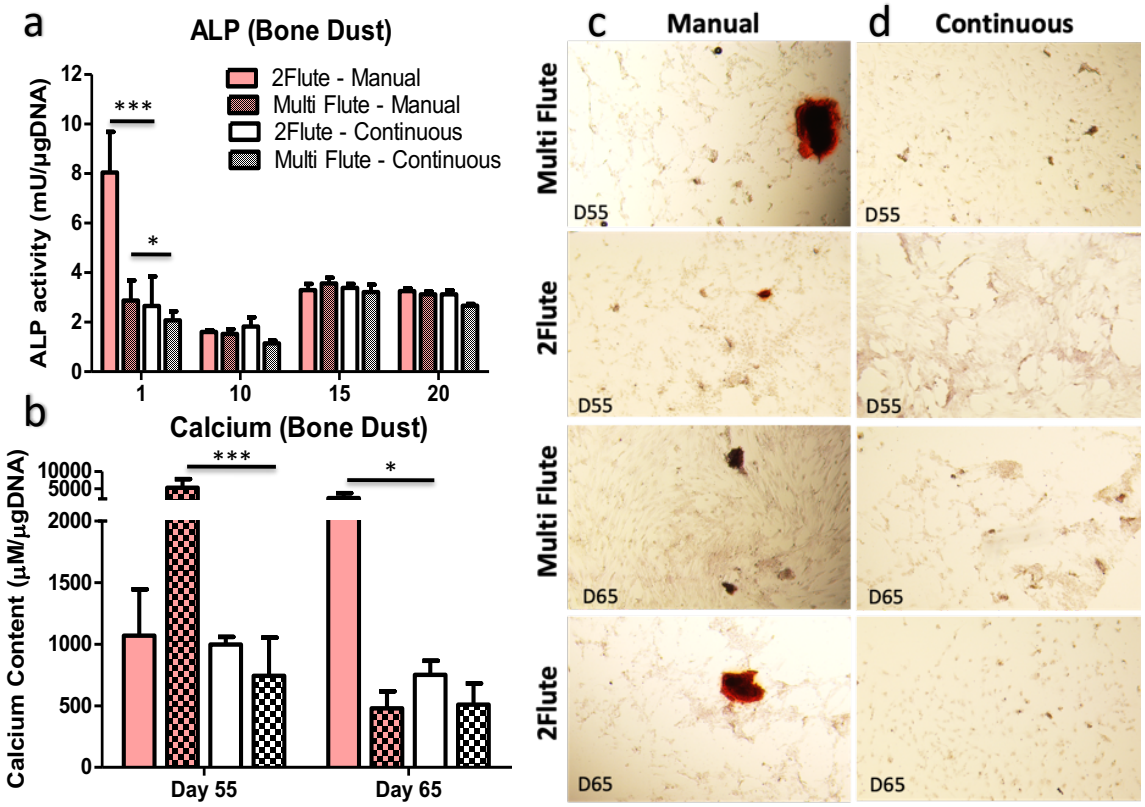

Figure 4.7: (a) Extracellular ALP activity and (b) calcium content of bone dust resected with manual and continuous irrigation. Images (5x magnification) of Alizarin red stain of calcium deposits (stained red) of cells from bone dust resected with (c) manual and (d) continuous irrigation. *p<0.05; *** p<0.001 comparing either 2Flute - Manual vs 2Flute – Continuous or Multi-Flute – Manual vs Multi-Flute – Continuous.

The calcium content was significantly higher in manual irrigation groups, compared to its continuous counterpart (Fig. 4.7b-d). This significance was seen on recovery day 55 ($p<0.001$) in Multi-Flute group and recovery day 65 ($p<0.05$) in 2Flute group (Fig. 4.7b).

4.3.4. The osteogenic capacity of the cut surface is higher following cutting with continuous irrigation compared to manual irrigation

Extracellular ALP activity was highest on recovery day 1 for all groups, except the Multi-Flute manual (MM) group, then activity decreased afterwards on recovery days 10, 15, 20 (Fig. 4.8a). The cut surface resected in the presence of continuous irrigation had significantly higher ALP activity on recovery days 1 ($p<0.001$) and 20 ($p<0.05$) for both the Multi-Flute and 2Flute groups, when compared to manual irrigation groups (Fig. 4.8a). Moreover, for the Multi-Flute groups, the cut surface resected in the presence of continuous irrigation also showed

significantly higher ($p<0.05$) ALP activity on recovery day 15, in comparison to resection with manual irrigation (Fig. 4.8a). Moreover, at day 1, ALP activity was significantly higher in ($p<0.05$) cut surface resected with 2Flute bur using a manual irrigation approach when compared to the cut surface resected with Multi-Flute with the same irrigation approach (Fig. 4.8a).

The calcium content was significantly higher in continuous irrigation groups compared to manual groups, whereby significance was seen on recovery day 41 ($p<0.05$) and 55 ($p<0.001$) in Multi-Flute and day 55 ($p<0.001$) in 2Flute groups (Fig. 4.8b-d). Moreover, calcium content was also higher in cut surface resected with 2Flute bur using a manual irrigation approach when compared to the cut surface resected with Multi-Flute with the same irrigation approach at day 41 ($p<0.05$) and 55 ($p<0.01$) (Fig. 4.8b).

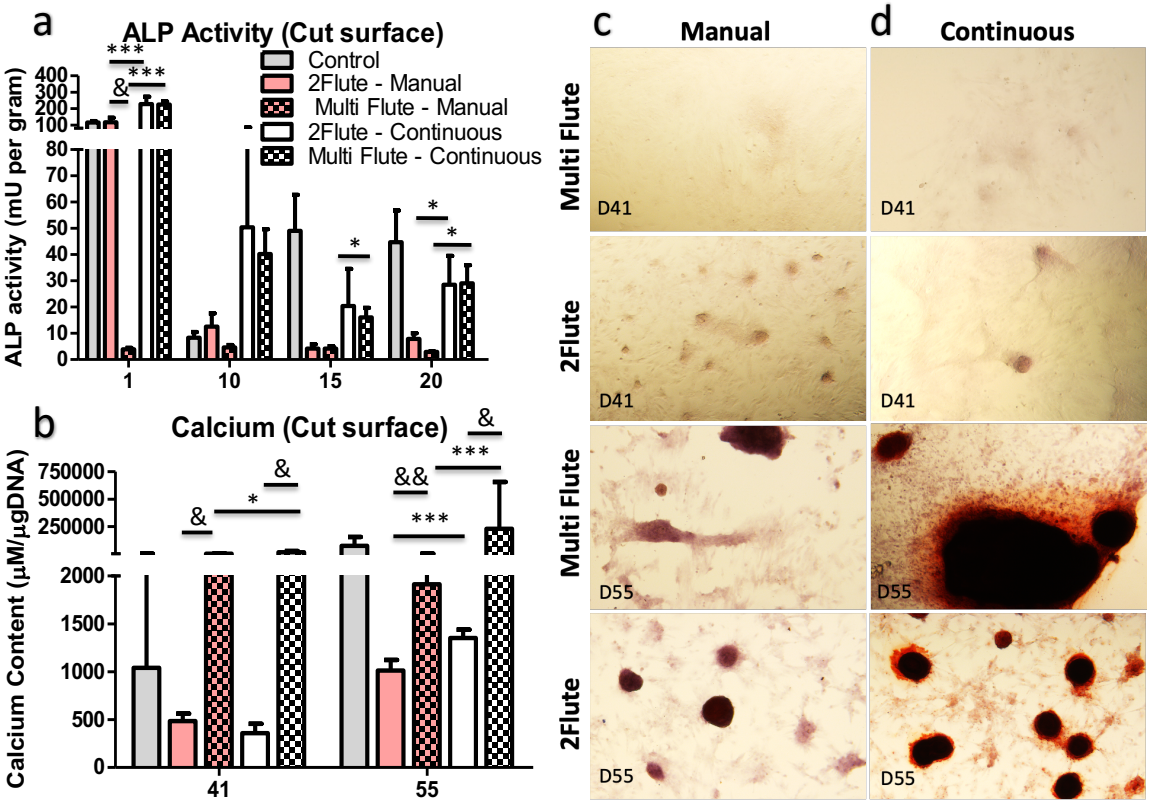

Figure 4.8: (a) Extracellular ALP activity and (b) calcium content of the cut surface resected with manual and continuous irrigation. Alizarin red images (5x magnification) of calcium deposits (stained red) in cells from the cut surface resected with (c) manual and (d) continuous irrigation. * $p<0.05$; *** $p<0.001$ Manual vs Continuous, & $p<0.05$; && $p<0.01$ 2Flute vs Multi-Flute

4.4. Discussion

One of the main factors affecting post-operative bone regeneration is heat generated during cutting with high speed tools. In this study the relative *surface* temperature increase arises during cutting of porcine spine lamina with high speed burs in the presence of manual and continuous irrigation (< 39°C, < 22°C respectively). The study conducted in this Chapter reveal that both irrigation approaches maintain dissipated temperatures within the bone tissue (0.5 mm from the cut surface) below 30°C. The cooling rate at the cut surface was faster during manual irrigation, whereas the rate decreased when continuous irrigation was used during cutting. Cell apoptosis was induced in both the bone dust and the cut surface ex-vivo samples by heat generated during cutting with both irrigation methods. However, this was not substantially high in comparison to the cell apoptosis observed in the study conducted in Chapter 3. It is proposed that both irrigation approaches limited the temperature elevations during high speed cutting, and thereby prevented excessive cell death to occur at the cut surface. Fluorescent intensity was higher in bone dust groups compared to the cut site groups. It is proposed that exposure to both mechanical and thermal damage during the cutting process lead to a more prominent cleavage of Caspase 3 signalling molecule in the bone dust groups. Moreover, metabolic activity was not significant when comparing manual and continuous irrigation groups, and it changes during recovery days. Although, Alamar Blue is not a perfect representation of cell viability, because non-proliferating healthy cells may not reduce Alamar Blue. Interestingly, the regenerative capacity of the cut surface was preserved when continuous irrigation was used for cutting with two different surgical bur designs, whereas cells in bone dust resected with manual irrigation, which also generated higher temperature, had the highest calcium content.

There are a number of limitations regarding this study that require consideration. Firstly, this study measured bone surface temperature in the presence of manual and continuous irrigation using a thermal camera, which can be limited due to the surrounding ambient temperature. However, relative temperature was referenced to temperature on the bone before cutting took place. Secondly, recording surface temperature elevation with the thermal camera using irrigation was also limited, and this was resolved by irrigating the bone before cutting and use this temperature as a reference. Thirdly, accumulation of bone dust occasionally occurred on the surface, which might increase heat generation, and this was exacerbated during cutting in the presence of manual irrigation (Fig. 4.1b and d, black arrows). This was quickly addressed by immediately removing the build-up of bone dust on the cut surface using irrigation. Moreover, measuring dissipated temperature with a thermocouple was also limited by the space between the bone and thermocouple, which was mitigated by using thermal paste to fill in the holes. Finally, the effect due to the mechanical forces applied during cutting, such as thrust force and torque created by the cutting flutes, may have played a role in cellular damage, especially in the bone dust groups, which experienced both mechanical and thermal damage. However, whereby the study conducted in Chapter 3 implemented histological evaluation on similar cutting experiments and showed intact tissue and lamellar structure on the cut surface and so mechanical damage at the surface might be minimal (Chapter 3). Moreover, it is well known that mechanical stimulation (Rauh et al. 2011; Sittichockechaiwut et al. 2009) and thermal stimulation (Dolan et al. 2015; Dolan et al. 2016; Chung and Rylander 2012) can separately enhance osteogenesis. In surgical cutting, the role of each stimulation factor on post-operative bone regeneration is indistinguishable. Further investigation is needed to fully understand the influences of mechanical and thermal stimulation both separately and together on the osteogenic potential of surgically cut bone dust and the cut surface.

The study conducted in this Chapter report relative surface temperatures lower than 80°C, with a range of 21.27°C-79.47°C and 7.6°C-54.26°C for manual and continuous irrigation respectively. This is lower than absolute temperatures previously reported with manual and continuous irrigation during bony decompression surgery on human patients, whereby the absolute maximum temperature range was 75.5°C - 194.2°C and 88.4°C - 249.7°C for manual and continuous irrigation respectively (Matthes et al. 2018). However, it should be noted that (Matthes et al. 2018) did not reference their temperature to initial bone temperature. Another study reported a surface temperature increase of 14.6±6.1°C with continuous saline irrigation, using a 10 mL syringe, on ovine cervical spine (Livingston et al. 2015), which is lower than the relative temperature of 22.07±11.55°C (2Flute) and 33.15±17.92°C (Multi-Flute) in the continuous irrigation group, which is reported here. However, they used a standard light pressure on the bur during cutting, which explains their lower temperature compared to results reported here. Moreover, they reported a dissipated temperature of 22.0±1.9°C with continuous irrigation (Livingston et al. 2015), which is similar to results reported here, the dissipated temperature result of 21.29±1.26°C (2Flute) and 22.59±0.62°C (Multi-Flute) for continuous irrigation.

The study in this Chapter has reported enhanced mineralisation in bone dust resected in the presence of manual irrigation, where cutting also exposed cells in bone dust to higher temperature elevations compared to continuous irrigation groups. A previous bone dust study, which did not report use of irrigation, reported a significantly higher viability (cell count after 3 weeks of culture) in cells from bone dust produced by 2Flute compared to Multi-Flute groups (Roth et al. 2018). In comparison, the study conducted in this Chapter has shown no difference in viability (metabolic activity) between the 2Flute and Multi-Flute groups during 20 days of recovery. This previous bone dust study also reported similar qualitative expression of ALP and Alizarin Red staining between cells derived from bone dust produced by 2Flute and Multi-

Flute, whereas similar results of quantified ALP activity between cells derived from bone dust resected with 2Flute and Multi-Flute were observed in this Chapter. This is the first study to investigate osteogenesis in bone dust autograft resected with manual irrigation and compare it to continuous irrigation, whereby bone dust exposed to higher relative temperature (manual irrigation) also showed higher mineralisation (quantified Alizarin Red). It has previously been reported that high speed cutting with no irrigation method generated relative surface temperatures higher than 80°C and induced thermal damage in bone dust autograft, which enhanced mineralisation response in cells (Chapter 3). In the study conducted in this Chapter, mineralisation was also enhanced in bone dust group that was exposed to higher temperature (manual irrigation).

Previous studies investigating the effect of irrigation on the cut surface have focused on mechanical and irrigation parameters, such as temperature of liquid, flow rate, forces affecting heat generation and tissue viability and integrity using histological staining (Isler et al. 2011; Haddad et al. 2014), but they did not determine the cellular response to temperature generated by cutting in the presence of irrigation. An in vivo study in rabbits, using a high speed carbide bur at 35,000 rev/min for cutting with 6°C of continuous irrigation, reported a higher trend for bone fusion rate at the cut surface (ulnohumeral) compared to using no irrigation method (Haddad et al. 2014). Similar to these results, here it is reported that the cut surface resected with continuous irrigation exhibited higher osteogenic response than the cut surface resected in the presence of manual irrigation. Another study on Spraque-Dawley rats explored the effect of cutting (burs) using no irrigation compared to cutting with continuous irrigation at different temperatures (4°C, 25°C) on new bone formation, bone necrosis, and presence of infection using histologic evaluations (Isler et al. 2011). According to their histological images, they reported a significantly higher new bone formation with less infection and necrosis at the cut surface resected using (4°C and 25°C) continuous irrigation, when

compared to no irrigation. Both of these in vivo studies provided an insight into the influence of using continuous irrigation to minimise temperatures during surgical cutting with burs and enhance new bone formation. However, to the best of our knowledge, no study has been conducted to compare irrigation approaches (manual with continuous) to determine the irrigation parameters that influence post-surgical regeneration following cutting with surgical burs.

Understanding the effect of cutting tool parameters, such as spindle speed (revolutions per minute), feed rate (chip thickness or mm/min), magnitude of thermal elevation (°C) and blade sharpness, on temperature elevation will inform approaches to alleviate thermal damage (Eriksson and Albrektsson 1983; Matthews and Hirsch 1972a; Xu et al. 2014; Lee, Chavez, and Park 2018). One study reported a drill speed higher than 70,000 rpm can generate lower temperature (74°C), compared to a drill speed of 27,000 rpm ,which generated a temperature of 105°C measured by a thermocouple 0.75 mm away on bovine cortical bone (Abouzgia and James 1997). Here, in the study conducted in this Chapter, manual and continuous irrigation approaches are shown to affect heat generation during high speed cutting, where a drill speed of 75,000 rev/min was used. Moreover, results from this study has shown that inside the bone, dissipated temperatures (0.5 mm away) were between 20°C and 30°C during cutting in the presence of manual and continuous irrigation respectively, and this dissipated temperature did not significantly increase compared to the referenced bone temperature (16.64 ± 0.753°C). Temperatures generated during cutting with manual irrigation are highly variable, because using a syringe does not create a constant cooling on the cut surface.

It has been proposed that heat generation >47°C will induce tissue damage, and as a consequence may limit bone healing (Eriksson and Albrektsson 1983; Eriksson, Albrektsson, and Magnusson 1984; Eriksson 1984; Eriksson and Albrektsson 1984). Previous cut surface studies have only used histology to explore tissue damage and regenerative capacity. The study

conducted in this Chapter further explored the regenerative capacity at the cut surface by investigating the cellular response to cutting with surgical burs in the presence of different irrigation methods. Surgeons are wary about using high speed cutting instruments because it can induce excessive necrosis and cell death. In this study, temperatures generated by surgical burs in the presence of continuous irrigation did exceed the threshold for cell death (>47°C), but only for a short duration (<4 seconds). Moreover, the cut surface was preserved for regeneration when continuous irrigation was used in combination with high speed cutting with surgical burs. It is proposed that heat shock created during cutting with this irrigation method initiated an earlier mineralisation response. Thus it is proposed that continuous irrigation might be favourable for surgical applications that rely on preservation of the cut surface for post-surgical healing, whereas manual irrigation might be a beneficial approach for cases where harvesting and preservation of the osteogenic capacity of autograft bone dust is required.

4.5. Conclusion

The study conducted in this Chapter reveals that temperatures generated by surgical burs at the cut surface exceeded the threshold for cell death, but only for short durations. Importantly the cut surface was preserved for regeneration when continuous irrigation was used in combination with high speed cutting with surgical burs. It was also observed that cut surface resected with a Multi-Flute design bur using both irrigation approaches also showed higher calcium content at day 41 and 55 compared to ones resected with a 2Flute design, and this corroborates with the study conducted in Chapter 3. In contrast an enhanced osteogenic response occurred in bone dust resected in the presence of manual irrigation, and this was associated with heat shock created during cutting with this irrigation method. Our study can be used to inform surgical irrigation for surgical procedures using high speed burs whereby continuous irrigation might be preferred for post-surgical healing of the cut surface, whereas manual irrigation enhances the osteogenic capacity of autograft bone dust.

Chapter 5 : Early and long-term mineralisation in porcine autograft bone dust surgically cut with a high speed bur using an ex-vivo bioreactor

5.1. Introduction

Spinal laminectomy during posterolateral fusion is performed to allow posterior access to the intervertebral disc space, such that the disc can be resected to place a supporting spinal cage and bone graft material with the aim of achieving interbody fusion. Larger bone chips (>112,000 μm^2) are typically resected using manual instrumentation, such as a rongeur, while bone dust is produced using a high speed bur and is subsequently much smaller (<66,000 μm^2) in comparison (Kim et al. 2016; Epstein 2017; Perez-Cruet et al. 2013). The in vitro and ex-vivo osteogenic potential of bone dust for dental and orthopaedic applications has been studied using in vitro cell culture approaches (Roth et al. 2018; Kuttenberger, Polska, and Schaefer 2013; Eder et al. 2011; Ye et al. 2013). One study compared the osteogenic potential of bone dust (cut with high speed bur) with iliac bone chips (harvested with rongeur), and reported a significantly higher cell viability and alkaline phosphatase activity in bone chips compared to bone dust groups, although there was no difference in mineralisation (Alizarin red staining) between the groups (Ye et al. 2013). Another study compared the osteogenic potential of human laminectomy bone chips and bone dust, and reported that bone dust had a poorer osteogenic potential (osteoblast yield and Alizarin red staining) by 3 weeks post-surgery compared to bone chips, which was proposed to be associated with the preservation of lamellar tissue structure (Eder et al. 2011).

Cutting tools induce thermal and mechanical damage by creating necrotic tissue and microcracks at the superficial cut surface (Karaca, Aksakal, and Kom 2011; Xu et al. 2014).

The influence of orthopaedic twist drilling parameters (drill speed, drill force, drill diameter, and feed rate) on temperature elevation has been investigated in bovine cortical bone using a T-type thermocouple situated 0.5 mm away from drill site (Karaca, Aksakal, and Kom 2011) and compared tissue necrosis and tissue damage at the cut surface (drill site) by histology. It was reported that higher drill force, lower drill speed, and higher feed rate led to lower magnitude of temperature elevation, visually less necrotic tissue (empty lacunae) and higher tissue damage at the drill site. Another study also compared the influence of drilling parameters (drilling speed, feed rate) on temperature elevation, measured by a thermal camera, in a study using a twist drill in porcine humerus bone under dry and irrigated conditions (Xu et al. 2014). They reported that higher feed rate and lower drill speed led to lower temperature elevation during dry cutting, whereas irrigation minimised temperature elevation and mitigated the influence of feed rate and drill speed parameters (Xu et al. 2014).

The regenerative capacity of bone dust is influenced by temperature elevation generated during high speed cutting. Interestingly, thermally induced cell apoptosis has been shown to enhance in vitro, in vivo, and ex-vivo osteogenesis in bone (Chung and Rylander 2012; Dolan et al. 2012; Dolan et al. 2015; Dolan et al. 2016) (Chapter 3 and 4). The study conducted in Chapter 3 has shown that temperature elevations during high speed cutting (Multi-Flute and 2Flute Bur) occur for short durations and are associated with cell apoptosis (Chapter 3). In the same study an ex-vivo culture approach was used to study the osteogenic potential of the bone dust and the cut surface after cutting, and reported that the cutting approach that led to the highest temperature resulted in an enhanced osteogenic response (confirmed by ALP activity and calcium) (Chapter 3). The differences in osteogenic potential of bone dust and bone chips might be associated with heat exposure, which differs between the two whereby temperature elevations during high speed cutting with burs expose bone dust to temperatures above 60°C (Hosono et al. 2009) while cutting with rongeurs does not expose bone chips to heat generation.

It should be noted that the study (Chapter 3) was conducted under in vitro static conditions. However, autograft bone chips and dust experience mechanical forces such as compression and torsion in vivo (Kim et al. 2016), for example when implanted between the vertebral bodies for spinal fusion surgery (Epstein 2017; Kim et al. 2016), in gums for orthodontic surgery (McAllister and Haghighat 2007), and as a bone filler during canal wall reconstruction (Roth et al. 2018). While patients are encouraged to return to physical activity, because of the beneficial effect of loading on bone cells (osteoblasts, osteocytes, and mesenchymal stem cells) (Guo et al. 2012), the influence of mechanical stimuli on the osteogenic potential of bone dust is not fully understood.

Bioreactors are commonly used to provide an in vitro physical growth environment for cells and tissue, and can induce an upregulation of gene expression and matrix production associated with osteogenic differentiation (Matziolia et al. 2011; Freeman et al. 2017). For example, a study used porcine trabecular cores to investigate mechanotransduction in bone marrow cells under vibrational low magnitude mechanical stimulation (LMMS, 50 Hz for two 30 minutes bouts for 5 days per week), and reported higher bone formation rate (Alizarin red fluorochrome labelling) and downregulation of sclerostin expression (anti-osteoblast differentiation) in mechanically stimulated trabecular cores compared to control (Curtis et al. 2018). However, no study has implemented a bioreactor approach to assess cellular viability and the osteogenic response of bone dust exposed to the effects of surgical cutting.

Irrigation is a common practice during orthopaedic cutting with high speed cutting tools, which is implemented to minimise temperature elevation and prevent excessive cell death and tissue necrosis. Irrigation can be implemented in a manual fashion, whereby a surgical assistant applies irrigation to flush out bone debris during cutting, or using an irrigation device to automatically apply a continuous flow of irrigation while simultaneously cutting. It has been reported that heat generation during decompression surgery in a human spine is higher

in the presence of manual irrigation when compared to automated continuous irrigation (Matthes et al. 2018). The study conducted in Chapter 4 has also shown that manual irrigation can induce higher temperature elevations in porcine bone than cutting with continuous irrigation, and that this is associated with apoptosis but an enhanced cellular mineralisation response in bone dust cultured ex-vivo (ALP and quantified Alizarin red), when compared to bone dust surgically cut with continuous irrigation to minimise temperature elevation (Chapter 4). Previous studies have investigated the influence of irrigation parameters (flow rate, temperature of liquid) (Hosono et al. 2009; Sener et al. 2009; Isler et al. 2011) and bur design (Chapter 3) on temperature elevation. A study of thermal damage to nerve roots in porcine lumbar spines reported higher temperature elevation (measured by FLIR) when a diamond bur was used for cutting, when compared to using a steel fluted / cutting bur, without irrigation (Hosono et al. 2009). The study also investigated temperature arising under different irrigation flow rates, and reported that a higher flow rate applied by automated irrigation (540 ml/hour vs 180 ml/hour) significantly decreased temperature elevation when a diamond bur was used (Hosono et al. 2009). However, these studies were conducted under static conditions and they did not assess the cellular response to cutting with irrigation. Thus the osteogenic capacity of surgically cut bone dust under mechanical stimulation, representative of the in vivo implantation environment, has not been explored.

Therefore, the hypothesis that "The mineralisation potential of autograft bone dust is enhanced by mechanical stimulation representative of in vivo conditions" was tested in this Chapter. The global objective of this study was to assess the mineralisation capacity of surgically cut bone dust under mechanical stimulation, representative of the in vivo implantation environment, using a custom bioreactor. Moreover, the study sought to compare the osteogenic capacity of bone dust prepared in the presence of *manual* and *continuous* irrigation and then cultured under static and mechanically stimulated conditions. The study

determined the osteogenic capacity of bone dust during post-cutting recovery using an ex-vivo cell culture approach with a mechanical bioreactor and biochemical assays. The post-cutting mineralisation was also assessed by high-resolution micro-CT scanning.

5.2. Materials and Methods

5.2.1. Bone harvest

Porcine (Rosderra Irish Meats, Edenderry, Offaly) spine samples, were transported on ice to the university, where fresh lamina sections (n=3) were harvested. It was confirmed that the spinal lamina was still intact and not affected by the cutting in the slaughterhouse. Tissue samples were thoroughly sprayed with 70% ethanol immediately before transfer into a biosafety laminar flow hood. The spine was dissected using a scalpel blade to cut through the vertebral disc, ensuring that the vertebra body (C10-C12 and L1-L6) and lamina bones were not damaged. The sectioned spine samples (3 vertebrae per section) were held in a clamp during surgical cutting. Soft tissue was removed using osteotomy tools (Stryker) and scalpel, ensuring that the periosteum was completely removed from the lamina and spinous process.

5.2.2. Surgical Cutting

All cutting was conducted with a high speed πDrive drill (Stryker, Kalamazoo, Michigan) at a rotational speed of 75,000 rev/min using a clockwise hand motion. Surgical cutting was conducted in the presence of either *continuous*, with an automated irrigation sleeve (Stryker, Kalamazoo, Michigan) attached to the drill attachment, or *manual* irrigation. Manual irrigation was conducted by an assistant using a 50 ml syringe, where drops of saline were administered in a drip-drip technique by hand during cutting, and this represented the scenario in which a surgical assistant applies irrigation while the surgeon cuts. Irrigation solution was phosphate buffered saline containing 5% Antimycotic Antibiotic solution (AAS/PBS, both Sigma). Continuous flow from the irrigation sleeve was set at 8% (8 ml/minute) flow rate using an

irrigation cassette and Console (both Stryker, Kalamazoo, Michigan). The surgical bur used for all cutting was a 3 mm 2Flute bur (Stryker, Kalamazoo, Michigan), and cutting was carried out until 20 cc of bone dust for each condition (*manual* static, *manual* stimulated, *continuous* static, *continuous* stimulated) was collected with a bone collector device (Bone Vac, Stryker, Kalamazoo, Michigan) and transferred into a 50 ml falcon tube. All bone dust groups were washed with sterile PBS containing 5% AAS, then cultured in media as explained below.

5.2.3. Ex-vivo cell culture

All bone dust groups (4 replicates for each condition per animal) were cultured in Dulbecco Modified Eagle Medium Glutamax media (Biosciences) and Hyclone Nutrient Ham's/F12 (ThermoFisher) (DMEM/F12, 1:1 ratio), supplemented with 10% foetal bovine serum (FBS, Sigma), 2% antimycotic antibiotic streptomycin (Sigma), 50 μM Ascorbic acid (Sigma), 1% w/v Dexamethasone (Sigma), and 20 mM β-Glycerol phosphate (Sigma). The media was changed twice per week or on days 1 and 20 of recovery for extracellular alkaline phosphatase (ALP) activity. Bone dust constructs were cultured ex-vivo in a 24-well plate placed in an incubator set at 37°C and 5% CO_2 for 20 days, when the experiment was terminated. Static condition groups were continuously cultured in the well plates. Stimulated bone dust groups were also cultured in 24 well plates until time of stimulation.

5.2.4. Mechanical stimulation with compression bioreactor

A custom bioreactor, designed to compress with cyclic loading (Fig. 1a), was validated by applying controlled displacements to a porous scaffold and recording under high magnification (Figure 5.1a and b). The strain distribution was determined locally using a digital image correlation (DIC) technique (Verbruggen et al. 2015).

At time of stimulation, bone dust groups were transferred from well plates into a chamber. Mechanically stimulation of bone dust was carried out at the same time every day.

The cyclic loading regime was set at 0.05 Hz for 1 hour every day for 20 days. Media was added into the wells of the bioreactor, but no perfusion was used during cyclic loading for 1 hour. Bone dust constructs resected with *manual* and *continuous* irrigation during cutting then cultured in mechanical stimulation were immediately transferred back into well plates for culturing after each bout of loading.

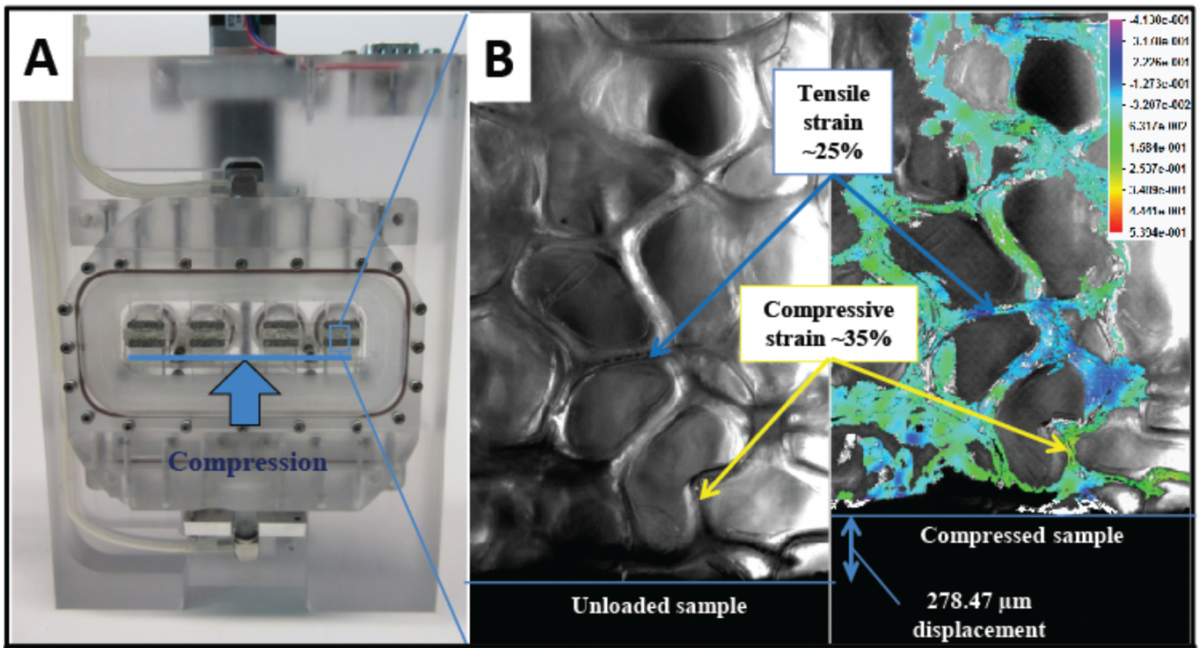

Figure 5.1: Validation of bioreactor was carried out with a porous scaffold. A) Bioreactor contained 4 chamber wells where the bone dust constructs were placed into and subjected to cyclic loading. B) Compression was verified with computational modelling.

5.2.5. Cell apoptosis

Cell apoptosis was assessed on recovery days 1 and 20, in order to investigate viability of constructs cultured under static and stimulated ex-vivo culture conditions. Cleavage of pro-caspase 3 activates extrinsic and intrinsic cell apoptosis pathways, whereby cell morphology changes, and cell blebbing occurs due to lysis of cellular and nuclear membranes, leading to the release of cellular content.

On recovery days 1 and 20, bone dust groups were fixed with 10% neutral buffered formalin solution (Sigma) and then decalcified in 0.5M ethylenediaminetetraacetic acid (EDTA, Sigma) for five days or until full decalcification. Bone dust samples were embedded in Histogel (Thermo Fisher), then processed in an automated Tissue Processor (Leica) overnight, embedded in paraffin wax and sectioned at 7 µm using a microtome (Leica). Sectioned samples were mounted on a glass slide and deparaffinised overnight in an oven at 60°C. Sections were blocked for 30 minutes using 1% bovine serum albumin (BSA, Sigma) to prevent non-specific binding, then followed by overnight incubation with cleaved caspase 3 antibody (Cell Signalling) at a concentration of 1:100. Samples were washed with 1% BSA and stained with Alexa Fluor 488 (Thermo Fisher) at a concentration of 1:700 for 1 hour at room temperature in the dark, then counterstained with mounting media containing 4',6'-diamidino-2-phenylindole (DAPI, Sigma), and imaged using a confocal laser scanning microscope (Olympus Fluoview 100 system) at 40x magnification. Images were processed using ImageJ software to quantify positive apoptotic cells.

Control porcine cells were also cultured on slides and stained with cleaved caspase 3 antibody. Positive controls were dosed with 5 µM Etoposide (Abcam), which induces cell apoptosis, whereas negative controls received no etoposide treatment.

5.2.6. Hoechst DNA Assay

DNA content was quantified as described previously with modifications (Dolan et al. 2012), in order to asses cell proliferation during recovery days. Briefly, bone dust constructs were washed twice with PBS, then lysis buffer solution, containing 1% Triton X (Sigma) was added. Then, cells in bone dust were subjected to 3 cycles of freeze-thaw to break open the cell membrane. Lysate solution was transferred into a 1.5 ml Eppendorf tube and frozen at -20°C

until use. Bone dust was wet weighed after lysate solution was fully removed, and weight was used to normalise DNA content.

Hoechst DNA assay was carried out by adding 20 µl lysate solution from each group to 200 µl DNA working solution in triplicates into a black 96-well plate. DNA working dye solution contained 2 µl Hoechst 33258 enzyme (Sigma) added to 20 mL of Hoechst buffer (100mM Tris, 2 M NaCl and 10 mM EDTA, all Sigma). Ensuring a homogeneous mixture, fluorescence was measured at an emission of 460 nm and excitation of 365 nm using a spectrophotometer (BioTek Synergy HT). DNA content was calculated with a known amount of calf thymus DNA as the standard. Quantified DNA was used to assess cell proliferation at recovery day 1 and 20, and also to normalise ALP activity.

5.2.7. Extracellular Alkaline Phosphatase Activity

Alkaline phosphatase (ALP) activity is an early mineralisation marker and an indication of osteoblastic differentiation. An ALP assay is commonly used to quantify extracellular ALP content, using a calorimetric test for *p*-nitrophenyl phosphate (*p*-NPP) as a phosphate substrate. Extracellular ALP activity for bone dust was quantified as previously described with modifications (Dolan et al. 2012). Briefly, media was changed on recovery days 1 and 20, and then collected 24 hours after stimulation as described above, where 40 µl of media from each sample group was added to 50 µl of 5 mM p-NPP solution (Sigmafast) and 40 µl of water in a 96-well plate, which was then incubated at room temperature for 1 hour, to which 20 µl of 3M NaOH was added to stop reaction of ALP enzyme (all Sigma). Absorbance values were measured at 405 nm with a microplate reader (BioTek Synergy HT). Using a standard curve of 0-80 nM of p-NPP content, ALP activity was calculated in milli-units (mU), then normalised to DNA content and expressed as milli-units per µg of DNA (mU/µg).

5.2.8. Micro computed tomography

Both static and stimulated bone dust constructs were fixed on recovery day 1 and 20 with formalin 10% neutral buffered (Sigma) for 24 hours and then scanned by micro-computed tomography (micro-CT, Scanco 100) with parameters: 14 mm holder, 45 kVp tube voltage, 200 µA intensity, A1 filter, 5 µm voxel size, 300 ms integration time, and framing averaging value of 2. Samples were scanned in air with Styrofoam and tape to hold samples in place. Constructs were evaluated using a threshold of 200 - 255 mgHA/ccm, ensuring that the threshold preview matches the grey scale image (Figure 5.2a and b). A volume of interest (VOI, cylindrical, mm^3) was 3D reconstructed and evaluated for bone volume fraction (BV/TV) and greyscale histograms, to describe bone volume and bone mineral density distribution (explained below).

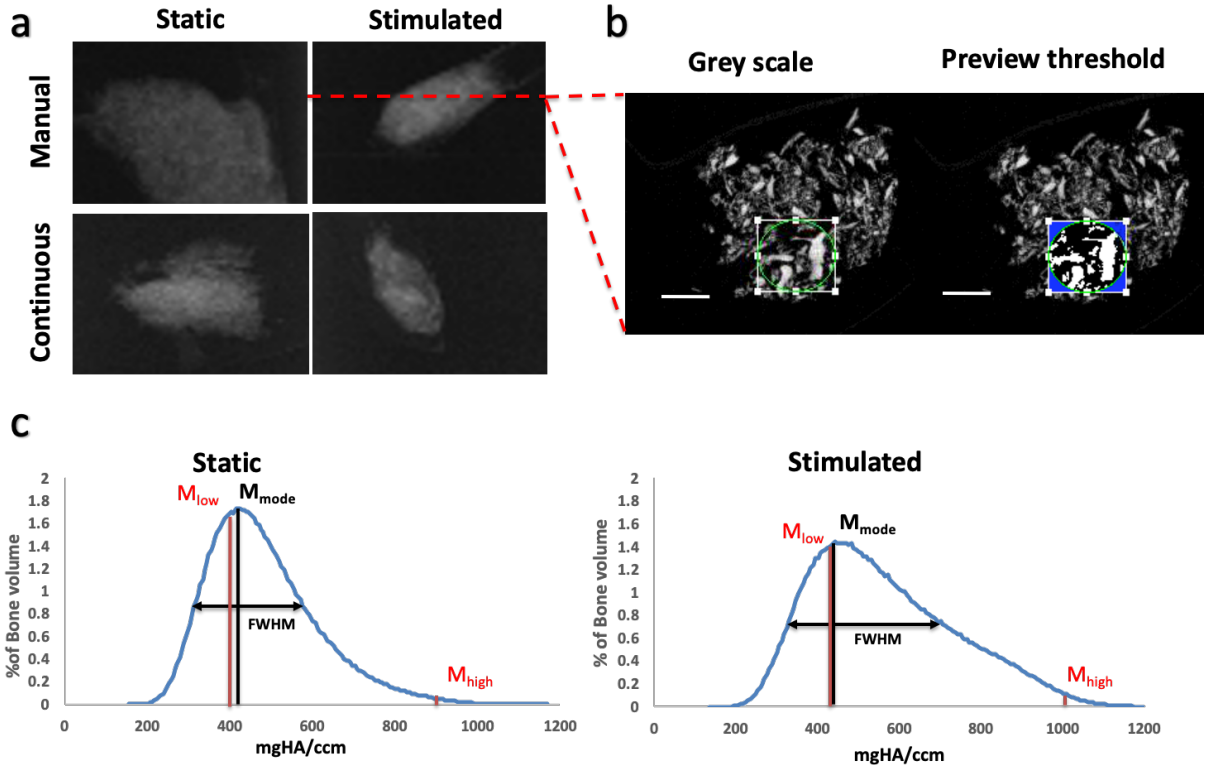

Figure 5.2: Example of grey scale image in (a) sagittal and (b) top view. Scale bar is 1 mm. (c) Example of a histogram for static and stimulated bone dust, where black line indicates most common mineral density, red lines show tissue volume at low and high mineral density, and black arrow is the full width at half max (FWHM) for heterogeneity.

5.2.9. Bone mineral density distribution analysis

Bone mineral density distribution was quantified from 3D reconstruction of VOI, using evaluation scripts in the Scanco Image Processing Language (IPL) as previously described by (O'Sullivan et al. 2020). This method assessed the amount of bone volume and bone quality at early (day 1) and late (day 20) stages of regeneration post-cutting. Raw micro-CT data files were processed to produce bone mineral density distribution (BMDD) measurements for each static and stimulated groups. Grey scale histograms were evaluated from micro-CT images in order to show frequency of occurrence of voxels at a grey level or mineral density (mgHA/ccm), see example curve in Figure 5.2c. A script was also used to characterise the full width at half maximum (FWHM) of the mineral distribution curve (mineral heterogeneity, mgHA/ccm) (Roschger et al. 2008), average weighted mineral density (M_{mean}, mgHA/ccm), the most frequent mineral density (M_{mode}, mgHA/ccm), and the bone volume at low and high mineral density (M_{low}, M_{high}, mgHA/ccm). Tissue volume at M_{low} represents immature bone, while M_{high} represents mature bone mineral. Bone volume (BV, mm^3) at low and high mineral densities were quantified below the 25^{th} and above the 75^{th}, respectively, percentile mineral density value of the baseline BMDD curves. This analysis allows for a comprehensive and quantitative description of changes in mineral composition of bone dust constructs.

5.2.10. Statistical Analysis

Data was analysed using Graphpad (version 5) software, and values are represented as mean ± standard deviation. A two-way ANOVA was used with Bonferroni's post-test to compare between *manual* and *continuous* irrigation groups, and between static and stimulated condition groups. All experiments were repeated with 3 animals, and 4 replicates for each animal.

5.3. Results

5.3.1. Cell apoptosis arises in bone dust cultured under static conditions, and the irrigation method did not influence cell death

Apoptotic cells were observed in the positive control group (Etoposide treated) (Figure 5.3a), but not in the negative control group (Figure 5.3b).

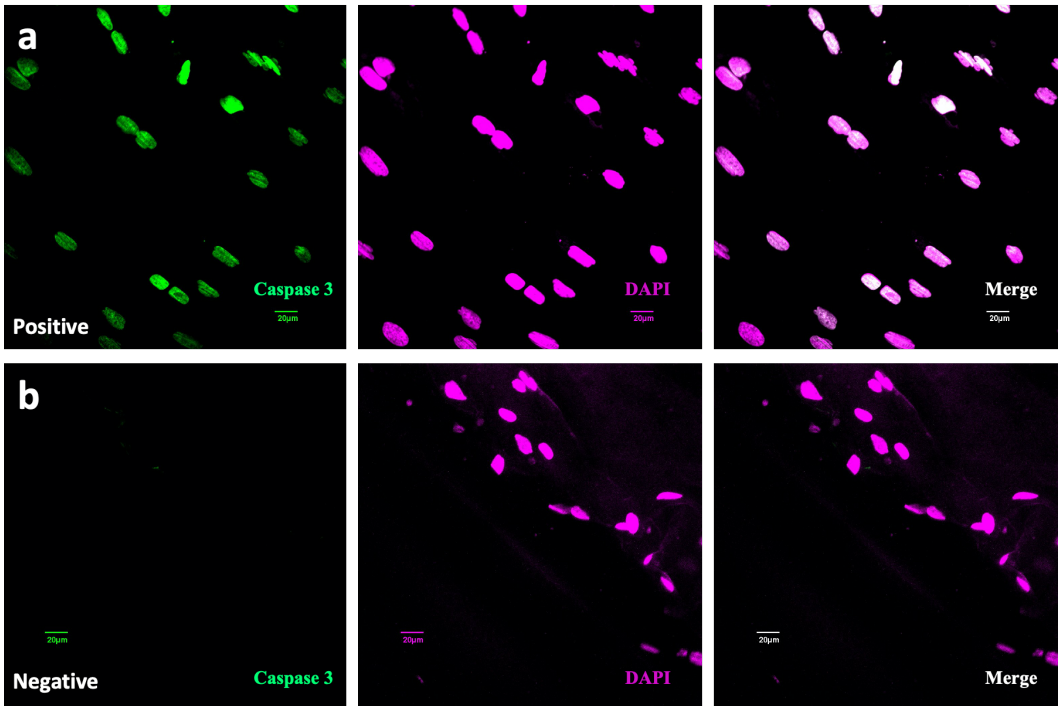

Figure 5.3: a) Positive caspase 3 control, where porcine cells were dosed with etoposide, which induces cell apoptosis. b) Negative control porcine cells did not get treatment with etoposide.

On day 1, positive apoptotic cells were observed in the *continuous* irrigation group cultured under static conditions (Figure 5.4a-b and e). Also on day 1, cell apoptosis was not observed in bone dust obtained under *manual* or *continuous* irrigation and cultured ex-vivo in the presence of mechanical stimulation (Figure 5.4c-e). On day 20, apoptotic cells were observed in bone dust cut in the presence of both *manual* and *continuous* irrigation and then cultured under static conditions (Figure 5.5a-b, e). On the other hand, no apoptotic cells were observed in bone dust cultured under mechanical stimulation by recovery day 20, regardless of the irrigation approach used during cutting (Figure 5.5c-e).

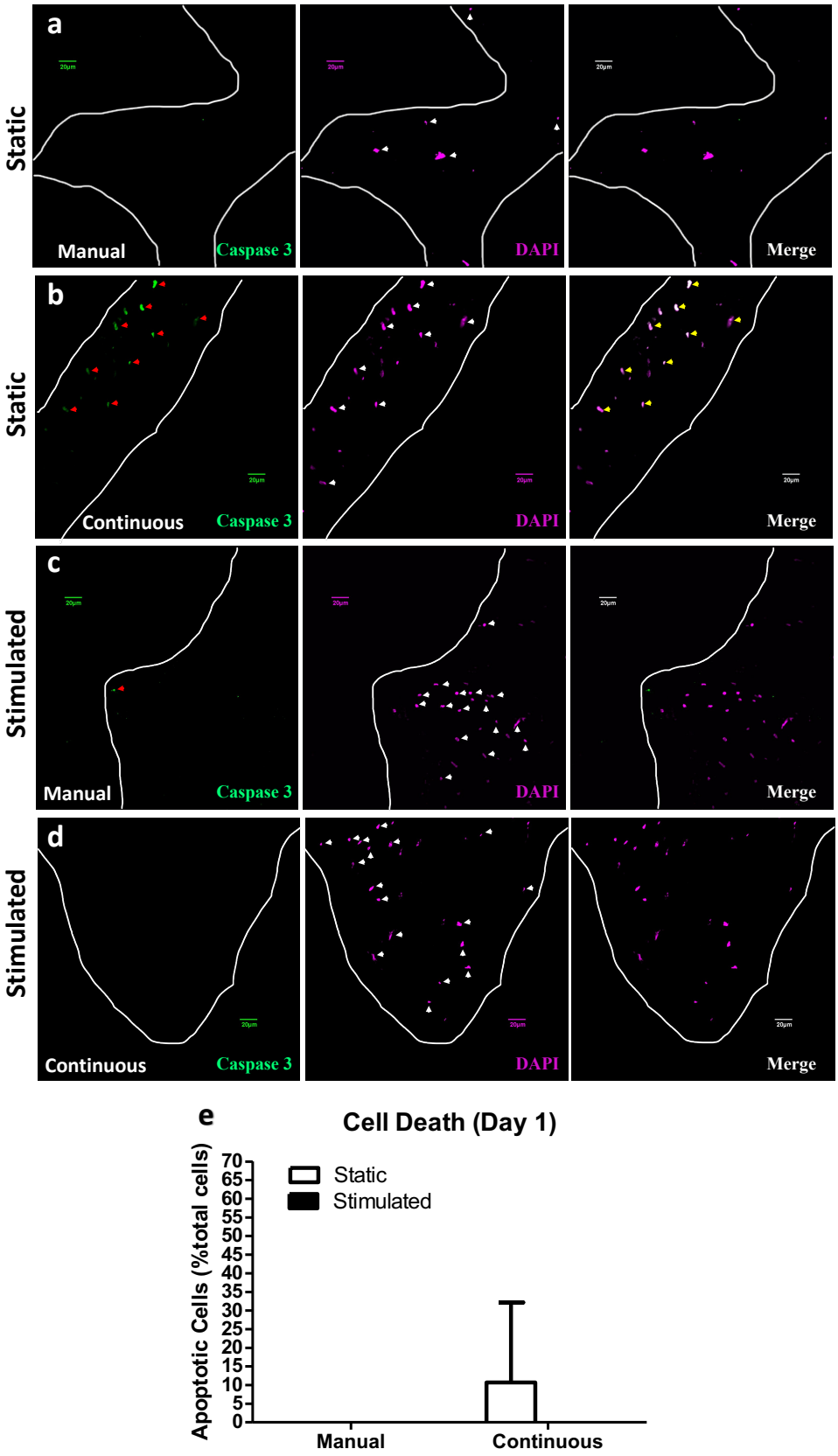

Figure 5.4: Day 1 images of apoptotic cells of bone dust in (a) static and *manual*, (b) static and *continuous*, (c) stimulated and *manual*, and (d) stimulated and *continuous* groups. White line indicates shape of construct, white arrows indicate DAPI stain for cell nucleus, red arrow indicates cleaved caspase 3, and yellow arrows indicate positive apoptotic cells. (e) Graph is quantified percentage of positive apoptotic cells normalised to total cells.

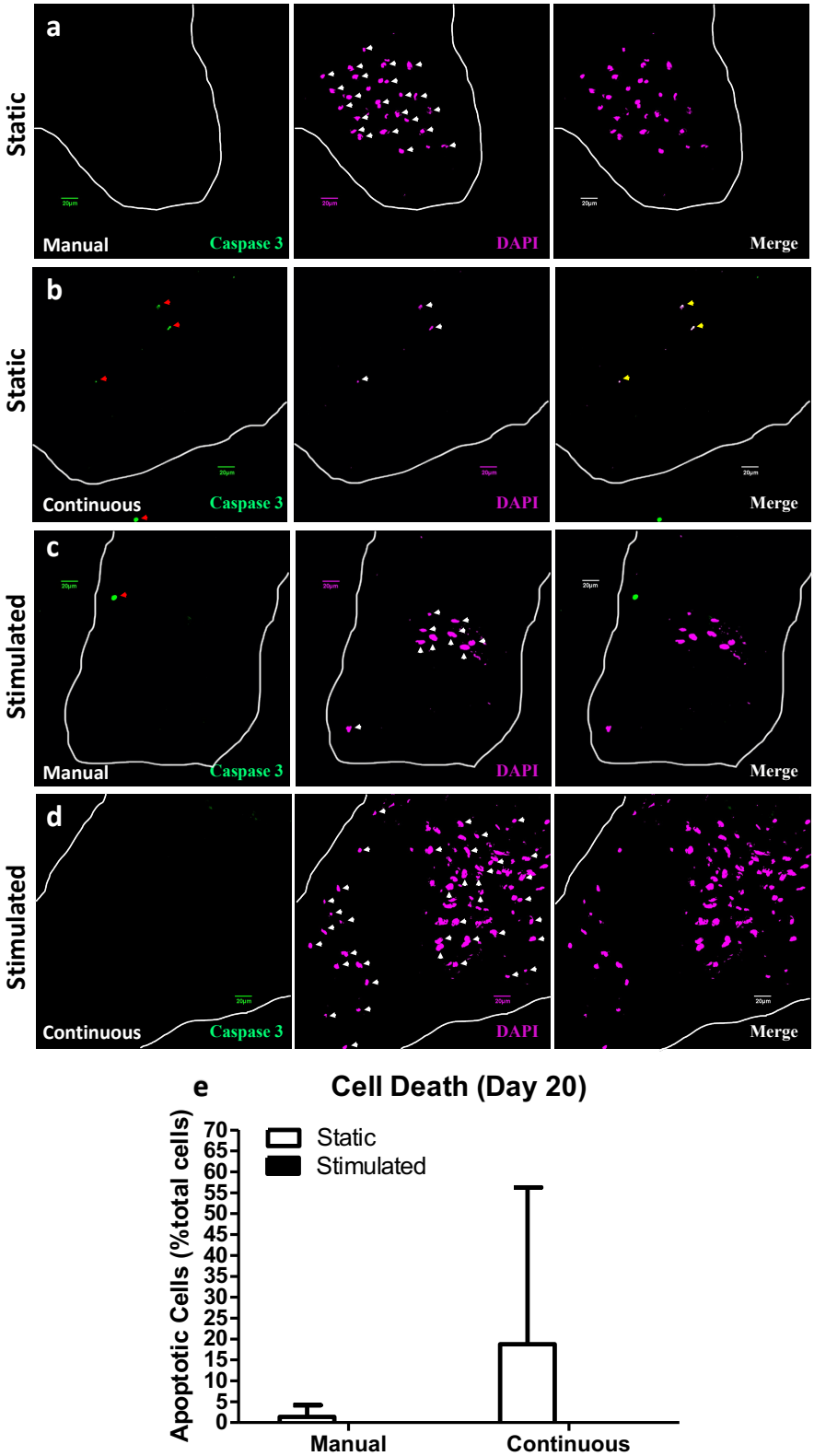

Figure 5.5: Day 20 images of apoptotic cells of bone dust in (a) static and *manual*, (b) static and *continuous*, (c) stimulated and *manual*, and (d) stimulated and *continuous* groups. White line indicates shape of construct, white arrows indicate DAPI stain for cell nucleus, red arrow indicates cleaved caspase 3, and yellow arrows indicate positive apoptotic cells. (e) Graph is quantified percentage of positive apoptotic cells normalised to total cells.

5.3.2. Cell viability was higher in mechanically stimulated bone dust, regardless of the irrigation approach used during cutting

All mechanically stimulated groups had significantly higher DNA content at recovery day 20 ($p<0.001$) than the static groups, regardless of the irrigation method used during cutting (Figure 5.6a and b, Table 1). Moreover, the DNA content in bone dust resected with either *manual* or *continuous* irrigation and then cultured under stimulated conditions was significantly higher ($p<0.001$) at day 20, compared to day 1, (day 1 vs day 20, Figure 5.6a and b, Table 2).

Table 1: Summary Results (Static vs Stimulated)

Irrigation	Viability	ALP	BV/TV	M_{mode}	M_{mean}	FWHM	M_{low} M_{high}
Manual	NS ✓	✓ ✓	✓ ✓	NS ✓	NS ✓	NS ✓	NS ✓
Continuous	NS ✓	✓ ✓	✓ ✓	NS NS	NS ✓	NS ✓	NS NS

✓ Significantly higher in stimulated (Day 1)
✓ Significantly higher in stimulated (Day 20)
NS Not significant
NS Not significant

Table 2: Summary Results (Day 1 vs Day 20)

Irrigation	Viability	BV/TV	M_{mode}	M_{mean}	FWHM	M_{low}	M_{high}
Manual	NS ✓	✓ ✓	NS ✓	NS ✓	NS NS	NS ✓	NS ✓
Continuous	NS ✓	✓ ✓	NS NS	NS NS	NS ✓	NS NS	NS NS

✓ Significantly higher at Day 20 (static)
✓ Significantly higher at Day 20 (stimulated)
NS Not significant in static
NS Not significant in stimulated

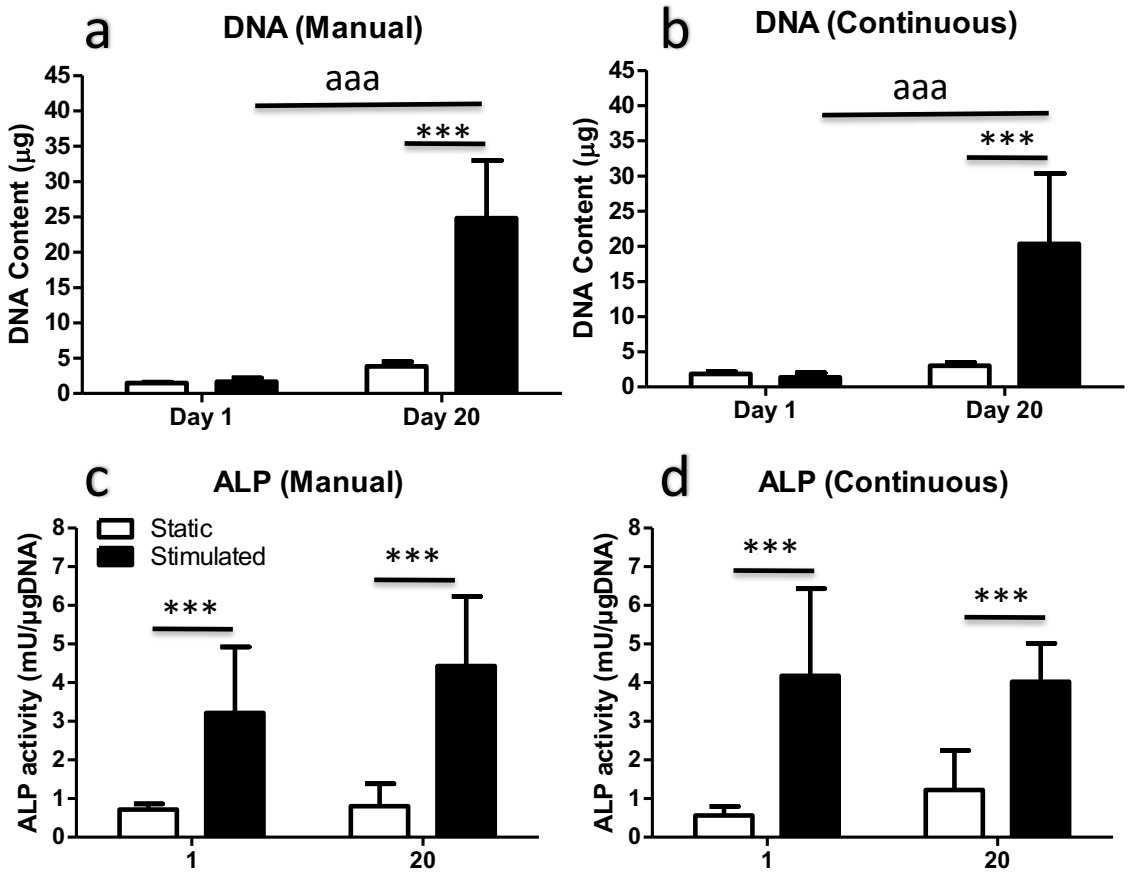

Figure 5.6: (a and b) Viability (DNA content) and (c and d) ALP activity of bone dust in *manual* and *continuous* irrigation groups. *** $p<0.001$ static vs stimulated groups; aaa $p<0.001$ day 1 vs day 20.

5.3.3. Early osteogenic response was higher in mechanically stimulated bone dust groups, regardless of the irrigation approach used during cutting

At day 1 and 20, ALP activity was significantly ($p<0.001$) higher in bone dust resected with *manual* and *continuous* irrigation and then cultured ex-vivo under mechanical stimulation, when compared to groups cultured under static conditions (Figure 5.6c and d, Table 1). The irrigation approach during cutting did not affect ALP activity at day 1 and 20 (Figure 5.6c and d). Moreover, there was no difference in ALP activity at day 20, compared to day 1, for all irrigation groups cultured in either static or stimulated conditions (Figure 5.6c and d).

5.3.4. Longer-term mineralisation was higher in mechanically stimulated groups compared to static, but no difference between manual and continuous groups

Micro CT images showed dispersed bone dust cultured under static conditions at day 1 of recovery, whereas in the mechanically stimulated groups bone dust was more compacted (Figure 5.7a), and there was no influence of the irrigation technique used during cutting on the distribution of mineral within the samples. The quantified 3D reconstructed micro-CT data at day 20 revealed a higher bone volume fraction (BV/TV) for all irrigation groups, cultured ex-vivo under either static or stimulated conditions, when compared to day 1 (Figure 5.7b, Table 2). At day 20, fusion of bone fragments were also observed in the bone dust resected with *continuous* irrigation and cultured under stimulated condition (Figure 5.7b, right). Bone volume fraction (BV/TV) was significantly higher on recovery day 1 and 20 for bone dust cultured under stimulated conditions. This was statistically significant for both *manual* ($p<0.05$) and *continuous* ($p<0.01$) irrigation groups at day 1 and 20 (Figure 5.7c and d, Table 1). Moreover, the irrigation approach did not influence the BV/TV results at day 1 and 20 (Figure 5.7c and d, Table 1). There was a significant ($p<0.001$) increase in BV/TV value at day 20 compared to day 1 of recovery, for all the groups (Figure 5.7c and d, Table 2).

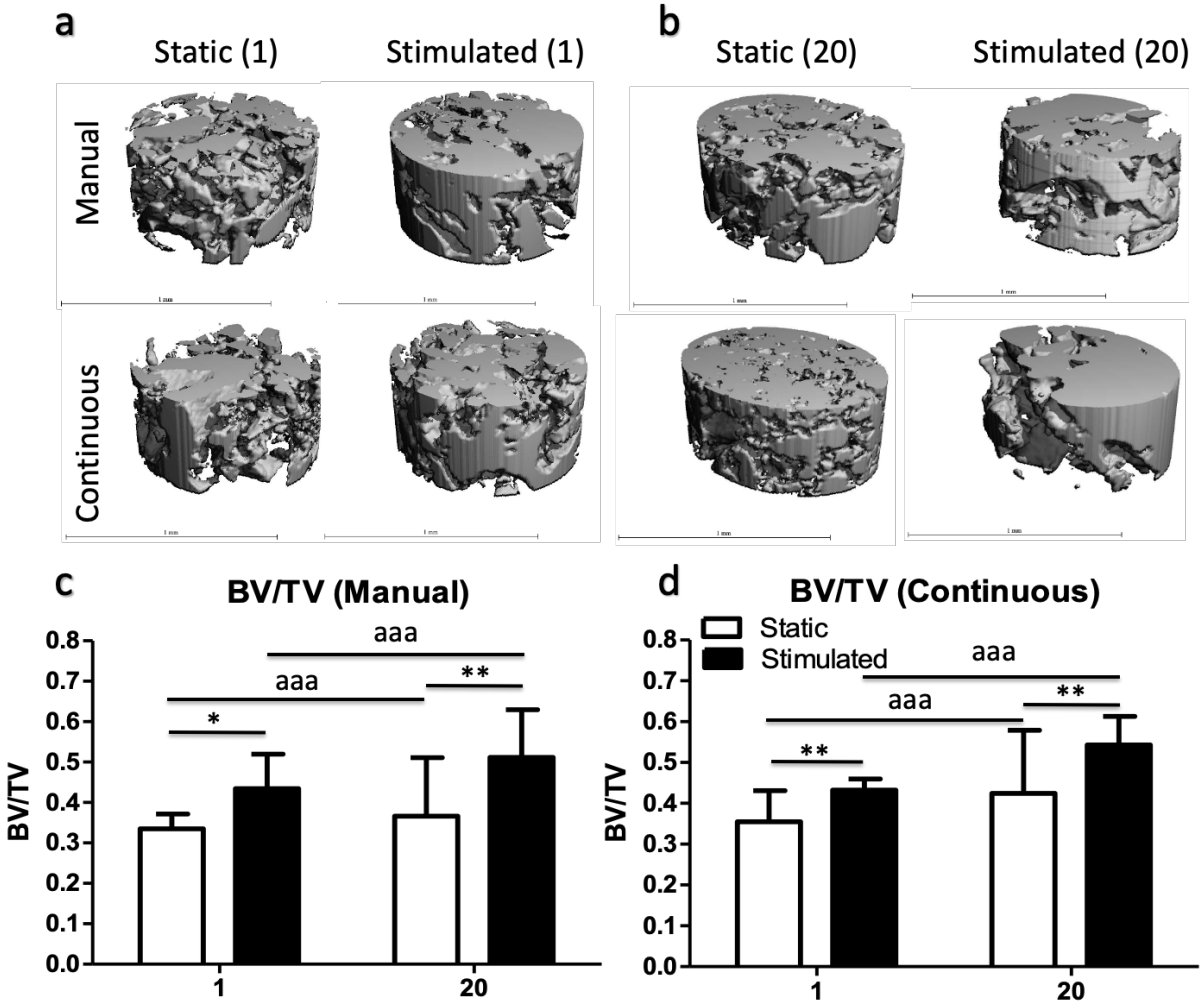

Figure 5.7: Bone volume fraction 3D reconstructed images on (a) day 1 and (b) day 20. Bone volume fraction in (c) *manual* and (d) *continuous* groups * $p<0.05$, ** $p<0.01$ static vs stimulated groups; aaa $p<0.001$ day 1 vs day 20.

5.3.5. Mineralisation enhanced in bone dust resected with manual irrigation and cultured ex-vivo under mechanical stimulation

By day 20, bone dust resected in the presence of *manual* irrigation and then cultured under stimulated conditions had a higher ($p<0.01$) peak mineralisation (M_{mode}) compared to the same irrigation group cultured under static conditions (Figure 5.8a, Table 1). Also at day 20, bone dust resected with *manual* irrigation and cultured in a mechanically stimulated condition had a significantly ($p<0.05$) higher M_{mode} compared to the *continuous* irrigation group also cultured in stimulated condition (*manual* vs *continuous*, Figure 5.8a and b). M_{mode} was significantly

($p<0.05$) increased at day 20, compared to day 1, in bone dust resected with *manual* irrigation and cultured under mechanically stimulated conditions (Figure 5.8a, Table 2).

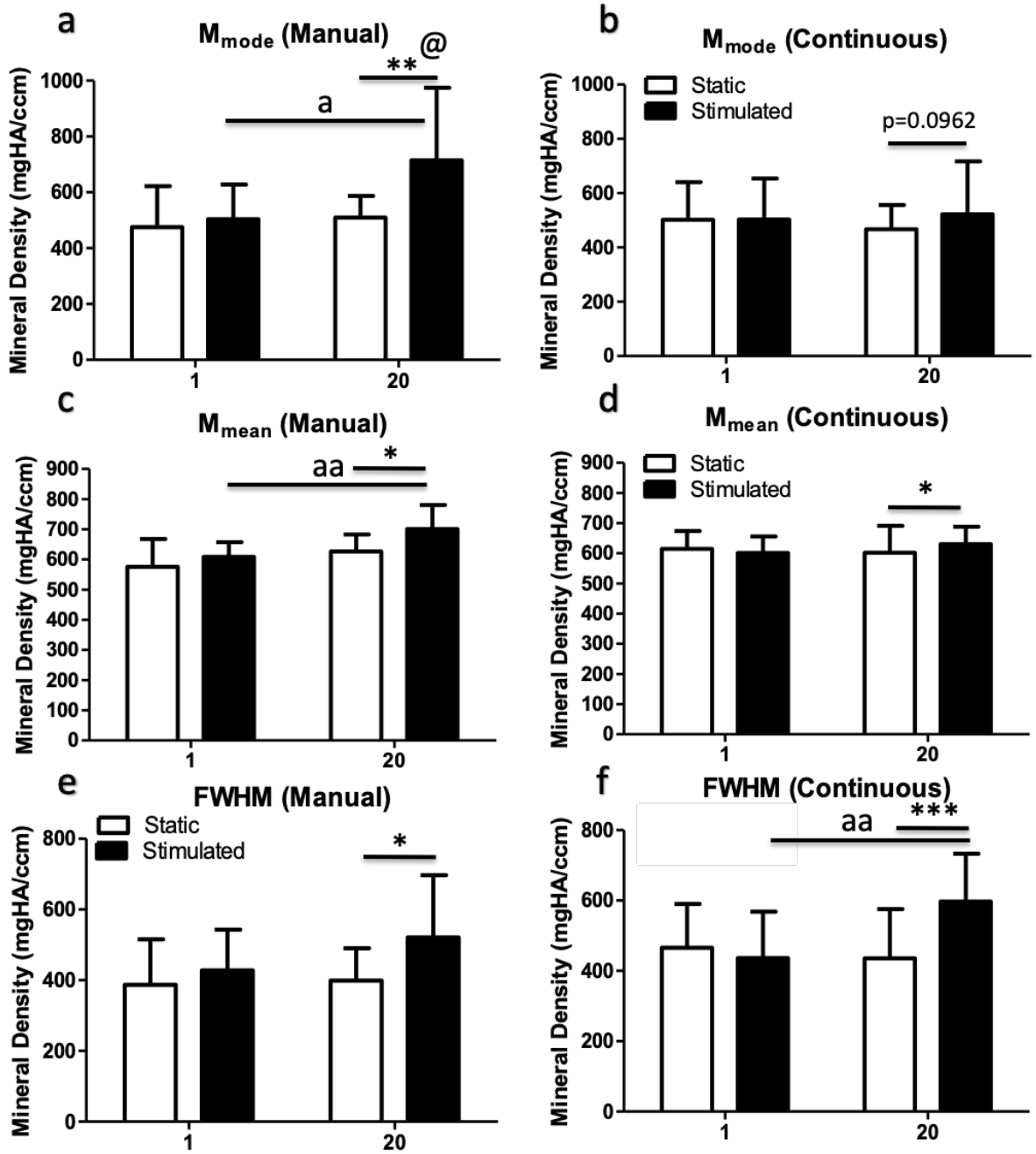

Figure 5.8: Most frequent mineral density (M_{mode}) for (a) *manual* and (b) *continuous* irrigation groups are reported as mean ± standard deviation. (c and d) Average weighted density (M_{mean}) and (e and f) heterogeneity (FWHM) for *manual* and *continuous* groups. @ $p<0.05$ *manual* vs *continuous*; * $p<0.05$, ** $p<0.01$, *** $p<0.001$ static vs stimulated groups; a $p<0.05$, aa $p<0.01$ day 1 vs day 20.

At day 20, the average weighted mineral density (M_{mean}) was significantly higher ($p<0.05$) in bone dust cultured under stimulated condition compared to the group cultured under static condition, regardless of the irrigation approach used during cutting (Figure 5.8c and d, Table 1). Under both static and stimulated conditions, there was no significant difference in M_{mean} between bone dust resected with *manual* irrigation and those resected with *continuous* irrigation at day 1 and 20 (*manual* vs *continuous*, Figure 5.8c and d). Also at day 20, compared to day 1, mean mineral density (M_{mean}) was significantly increased ($p<0.01$) in bone dust resected with *manual* irrigation and then cultured under mechanical stimulation (day 1 vs day 20, Figure 5.8c and d, Table 2).

The Full width at half max (FWHM, heterogeneity) at day 20 was significantly higher in the bone dust group cultured under stimulated conditions ($p<0.001$), compared to the group cultured under static conditions, regardless of the irrigation approach used during cutting (Figure 5.8e and f, Table 1). There was no significant difference between bone dust resected using *manual* and the group resected with *continuous* irrigation at day 1 and 20, for either static or stimulated conditions (*manual* vs *continuous*, Figure 5.8e and f). However, heterogeneity (FWHM) was significantly ($p<0.01$) higher at day 20, compared to day 1, in the bone dust group resected using *continuous* irrigation and cultured ex-vivo under stimulated conditions (Figure 5.8f, Table 2).

At day 20, bone dust resected with *manual* irrigation and cultured under stimulated conditions had a higher proportion of ($p<0.05$) immature and mature bone mineral (M_{low} and M_{high}) compared to the static counterpart (Figure 5.9a and c, Table 1). The irrigation approach did not have an effect on immature and mature bone mineral (Fig 5.9). At day 20, compared to day 1, both immature and mature bone volume (M_{low} and M_{high}) was significantly ($p<0.05$) increased in bone dust resected using *manual* irrigation and then cultured under stimulated conditions (Figure 5.9a and c, Table 2).

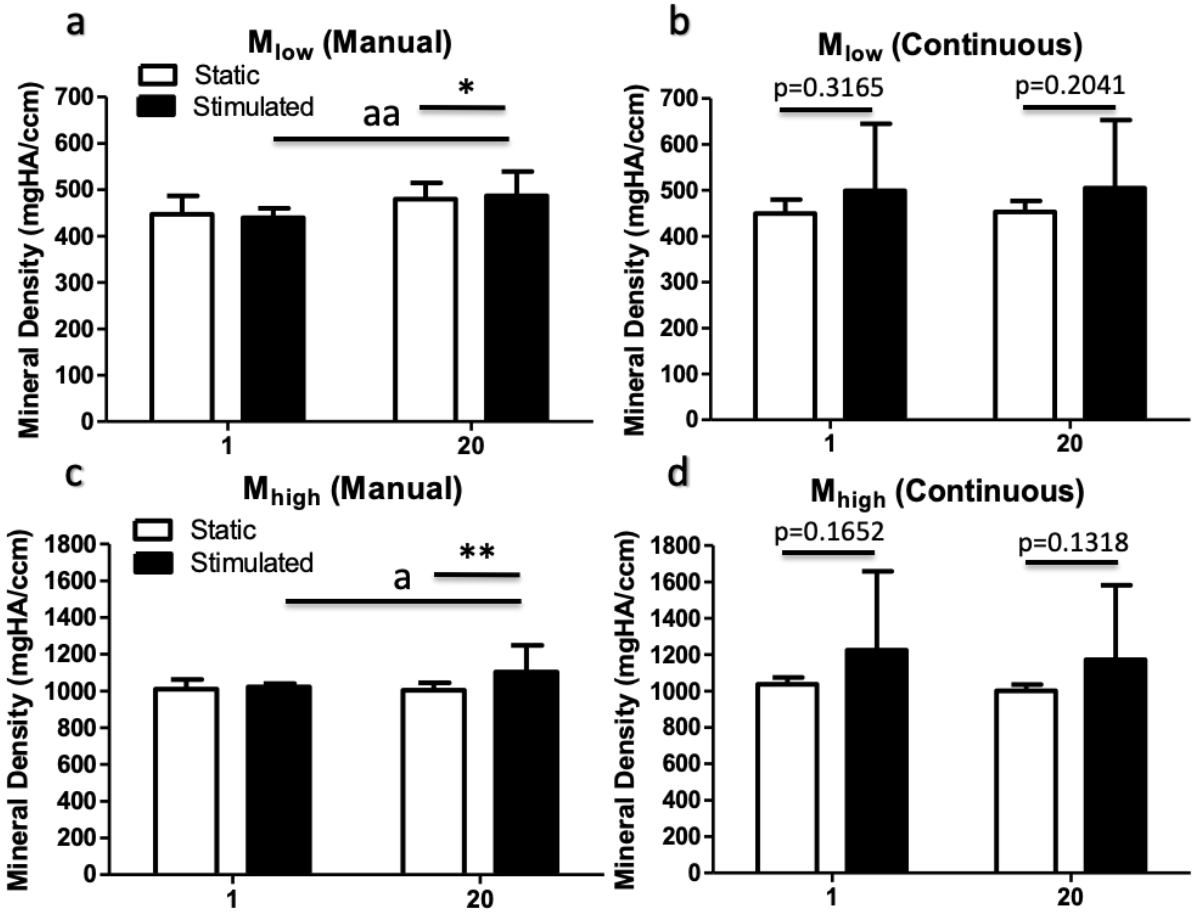

Figure 5.9: Tissue volume at (a and b) low and (c and d) high mineral density * $p<0.05$, ** $p<0.01$ static vs stimulated groups; a $p<0.05$ aa $p<0.01$, day 1 vs day 20.

5.4. Discussion

In vitro and ex-vivo studies have been conducted using cell culture techniques to assess the osteogenic potential of bone dust autograft material. Yet these studies may not fully represent the osteogenic potential of bone dust in vivo when implanted in patients, due to the absence of a mechanically active environment. The study conducted in this Chapter assessed the mineralisation capacity of surgically cut bone dust using a custom bioreactor to more closely represent the in vivo implantation environment. This study reports that the osteogenic capacity of bone dust was increased in the presence of mechanical stimulation, whereby cell apoptosis was absent. However, cell apoptosis was observed at day 20 in bone dust resected with continuous irrigation approach and cultured under static condition. In Micro-CT images, bone dust constructs cultured under static condition were still dispersed at day 20 and had higher

mechanical damage, compared to the stimulated groups, which had a solid consistency that was easy to transfer during loading regimes. This higher damage lead to cell apoptosis observed at day 20 in the bone dust cultured under static condition. Cell proliferation and early mineralisation responses from bone cells were significantly higher for mechanically stimulated bone dust when compared to those cultured under static conditions. It has also been shown that longer term mineralisation was significantly increased in bone dust subjected to compression forces during cyclic loading, whereby bone tissue volume at recovery day 20 was higher compared to bone dust in a static environment, and this increase at day 20 was significant compared to bone volume at day 1. Interestingly the irrigation method, representative of a manual approach or a continuous irrigation device, did not have an effect on mineralisation potential of bone dust under either static and stimulated conditions.

There were some limitations to this study. Firstly, the sourced spine was from porcine and so the results may not represent the outcome arising in human bone tissue. However, porcine spines are anatomically similar to humans (Abbasi and Abbasi 2019), and they have been used for regenerative and bone fusion studies (Curtis et al. 2018; Xue et al. 2005). A second limitation was that all spines were retrieved 12 hours post mortem and kept in a refrigerated room until collection, which might affect the viability of cells in the tissue before cutting experiments were conducted. However, it has been previously confirmed that cells in the vertebra were still viable following overnight refrigeration of bovine and porcine spines post-mortem (Chapter 3 and 4). Moreover, there was an increase in DNA content for both static and loaded bone dust constructs, which confirms the viability of bone cells after overnight refrigeration. A third limitation was related to the use of a bioreactor to represent loading in the human body, which is not a perfect representation of in vivo loading. However, bioreactors have been established as a tool to induce mechanical stimulation on ex-vivo bone cores, by replicating in vivo physical loading (Birmingham et al. 2015; Davies et al. 2006). Moreover,

there were some challenges in ensuring the bone dust construct remained intact during the first few cycles of cyclic loading. However, although some movement of the bone dust occurred, the construct quickly became compacted and deformation was observed visually during cyclic loading. Moreover, the bone volume and mineralisation densities were significantly higher in stimulated conditions compared to static bone dust constructs, which was expected based on previous mechanical stimulation studies (Birmingham et al. 2015; Mann et al. 2006) and confirmed that loading of the bone dust was achieved. In order to fully understand the mechanical environment's influence on mineralisation capacity of bone dust autograft, further studies are needed using ex-vivo human bone dust under varying loading conditions within bioreactors.

The study conducted in this Chapter is the first to assess the osteogenic potential of stimulated bone dust autograft, which was cut with a high speed surgical bur, in a mechanically loaded environment. A previous in vitro and ex-vivo bone dust study was conducted under static conditions, and it was reported that bone chips (cut with rongeurs) were superior in osteogenic response compared to bone dust (cut with high speed bur) (Eder et al. 2011; Ye et al. 2013). The study conducted by (Ye et al. 2013) assessed human autograft bone dust on days 7, 14 and 21 post-surgery, and reported higher ALP activity and Alizarin red staining in bone chips compared to bone dust, under static conditions (Ye et al. 2013). In comparison to their results (ALP activity at day 21: 0.95 ± 0.46 mM pNPP/mg protein) for bone dust cut with a 3 mm bur, results in the study conducted in this Chapter for ALP activity at day 20, also cut with a 3 mm bur and under static conditions, was comparable (0.802 ± 0.581 mM/µgDNA (*manual*) and 1.223 ± 1.018 mM/µgDNA (*continuous*)). Another study investigated the osteogenic potential of human bone shavings (dust) for spinal fusion, and they reported an osteoblast yield of 1.73 x 10^5 cells/g bone (equivalent to 1.34 µg/g bone) at week 3 (21 days). In comparison, the study conducted in this Chapter reported a higher DNA content of 5.992 ± 5.88 µg/g for

the *manual* and 5.671 ± 5.3 µg/g for the *continuous* groups at day 20 in the bone dust cultured under static conditions.

The micro-CT data in the study conducted in this Chapter has characterised bone dust mineral distribution during recovery days in a mechanical environment, and it was shown that mineralisation was increased when bone dust was subjected to compression loading. In comparison to static constructs, results from the study conducted in this Chapter show that low mineral density (25^{th} percentile, M_{low}), high mineral density (75^{th} percentile, M_{high}), heterogeneity (FWHM), and most frequent mineral density (M_{mode}) were higher in mechanically stimulated bone dust. Similarly, a study on hydrogel constructs mechanically stimulated within a hydrostatic pressure vessel also reported higher volume of most frequent mineral density and low mineral density compared to its static counterpart (Naqvi et al. 2020). Moreover, their heterogeneity (FWHM) was also higher in mechanically stimulated constructs compared to their static constructs, which is similar to the results of this study, where there was higher heterogeneity in stimulated bone dust compared to static conditions. A clinical study of lumbar non-instrumented fusion rate using lamina autograft (59 patients), combined with Nanoss and bone marrow aspirate, reported bone fusion at 6 months post-operatively in a patient with grade 1 degenerative spondylolisthesis, whereby fusion of bone fragments were visually observed in a 3D-CT scan of the L4-L5 vertebrae (Epstein 2017). Similarly, the results from the study conducted in this Chapter of 3D reconstructed micro-CT images of bone dust constructs at day 20 also show a fusion of bone fragments, especially in mechanically stimulated groups, when compared to more dispersed bone fragments at day 1. Studies have been conducted on mechanically stimulated bone cores (Mann et al. 2006; Birmingham et al. 2015; Birmingham et al. 2016), where mechanically stimulated osteogenic potential have been assessed using a bioreactor. In one study, a mechanically loaded (cyclic loading) human trabecular bone core (cut with low speed diamond drill) showed an increase in viability,

assessed by lactate dehydrogenase (LDH) activity, and higher positive staining of ALP (histochemical Fast Blue and Naphthol-ASMX stain) on bone surface when subjected to loading and prefusion, compared to unloaded groups (Mann et al. 2006). Similarly, the ex-vivo cell culture analysis in the study conducted in this Chapter show that viability and extracellular ALP activity was increased in mechanically stimulated (cyclic loading) bone dust compared to static bone dust, and this was observed in both irrigation groups.

In conclusion, the mechanical environment existing in vivo does influence the mineralisation response in autograft bone dust. This is the first study conducted to investigate the mineralisation potential of surgically cut bone dust in a mechanical environment representing the site of implantation, which is relevant to implantation in a vertebral site where bone dust autograft would experience compression loading. Previous clinical studies of bone dust have assessed long term (>4 months) bone fusion between the vertebrae with the addition of a scaffold or demineralised bone matrix (DMBM) (Epstein 2017; Kim et al. 2016). They did not assess the immediate mineralisation response taking the mechanical environment of implant site into account. The study conducted in this Chapter is the first to assess and characterise the mineralisation potential of bone dust cultured under a mechanically stimulated environment, using an ex-vivo cellular technique and micro-CT analysis. This is relevant to fully understand the potential of bone dust to regenerate in the site of implantation, where mechanical loading is experienced continuously. This approach could be used for further assessment of bone dust intended for different sites of implantation with varying loading conditions, such as compression and torsional forces between two vertebra or inside gums under a dental implant. Bone dust are a unique autograft, because they are subjected to both thermal and mechanical stress during and after resection, which also influences their regenerative capacity to heal. The study conducted in this Chapter has unique clinical relevance

because it further informs surgeons the important role of a mechanical environment in a site of implantation when assessing mineralisation potential of autograft bone dust.

Chapter 6 : Discussion and Conclusion

6.1. Introduction

This Chapter summarizes the main findings of the Thesis, where the influence of high speed cutting on post-operative bone regeneration, by the surgically cut bone surface and bone dust material for autografting applications, has been explored. The osteogenic response of autograft bone dust in a mechanical environment representative of in vivo conditions was also investigated. The relationship between the individual Chapters and previous studies are shown in a schematic in Figure 6.1, and this will be discussed in more detail in Section 6.3. Key findings are discussed in context to other relevant studies in the field, and implications as a result of this Thesis for the field of bone regeneration and high speed surgical cutting are explored. Recommendations for further studies and future work are also discussed in Section 6.4.

6.2. Main Findings of Thesis

The studies conducted during the course of this PhD Thesis focused on the ex-vivo cellular response to surgical cutting with a high speed bur. Heat generated by cutting with surgical burs with 2Fute and Multi-Flute designs were measured by a thermal camera and thermocouple, to assess surface and dissipated temperature respectively. Thermal damage and osteogenic responses by ex-vivo bone dust and the cut surface samples were investigated to determine the relationship between their regenerative potential and *surface* and *dissipated* temperature elevations. Next a study was conducted to determine the effect of cutting with different irrigation approaches, mimicking those used during surgery, on the osteogenic potential of ex-vivo bone dust and the cut surface, and to determine its association with temperature elevations arising during cutting in the presence of irrigation. Autograft bone dust are re-introduced into

patients to enhance healing at the cut site, but in these environments mechanical forces are exerted onto the autograft. Therefore, the final study investigated the osteogenic response in autograft bone dust in a mechanical environment representative of in vivo conditions. The key contributions of each hypothesis are summarised below.

Hypothesis 1: A Multi-Flute surgical cutting tool bur generates higher temperature at the superficial surface than a 2Flute bur design

The first study, presented in Chapter 3 of this Thesis, demonstrated that *surface* temperature elevations was in excess of 80°C during high speed cutting with a 2Flute and Multi-Flute design bur where no irrigation was used, whereas *dissipated* temperatures were less than 40°C. Moreover, the Multi-Flute design generated significantly higher *surface* temperature compared to the 2Flute design bur. These findings support Hypothesis 1. Although higher temperature was observed during dry cutting with the Multi-Flute bur, there was a faster cooling rate at the cut surface immediately after contact with the bur, which also resulted in a lower percentage of heated cut surface when compared to the 2Flute design. By observing these high temperature elevations at the surface, but not dissipated inside the bone, this Chapter provided an insight into heat dissipation during dry cutting with high speed surgical burs. In particular, this Chapter reveals an increase in heat generation (>80°C) at the surface but it does not induce a substantial heat shock inside the bone. This was corroborated by a study that was conducted by (Malvisi et al. 2000) using an E-type thermocouple 1 mm away to measure temperature elevations in bovine bone heated to 37°C by a heating element, and they reported temperatures below 46°C, which was a 10°C increase during dry cutting with a milling tool similar to a surgical bur.

The difference in temperature elevation between dry cutting with a 2Flute and Multi-Flute has not been reported before the studies of this PhD thesis. The results in this Chapter

provided essential information regarding the relationship between *dissipated* heat generation and induced *surface* temperature elevations during high speed cutting with surgical burs.

Hypothesis 2: Bone surfaces and autograft dust exposed to temperature elevations induced by high speed cutting undergo cell apoptosis, which enhances the osteogenic response ex-vivo

The first study of this Thesis also investigated the regenerative capacity in ex-vivo bone in response to temperatures above 60°C for short durations, which was induced during cutting with a high speed bur. Although heat generation reached in excess of 80°C, bone dust and the cut surface still had osteogenic potential, because only the cells on the *surface* were affected by these high temperature elevations for short durations (<1.33 seconds). Cell apoptosis was exacerbated in the cut surface prepared by a Multi-Flute cutting tool compared to the cut surface prepared using a 2Flute. Tissue necrosis was observed as far as 182.4 μm (2Flute) and 107.7 μm (Multi-Flute) away from the cut surface. Interestingly, the cut surface resected with the Multi-Flute tool also had higher osteogenic potential, whereby ALP activity and mineralisation was higher than that of the cut surface generated using a 2Flute device. As such, these results provided evidence to support Hypothesis 2. Surgeons avoid using high speed cutting tools because of concerns regarding the potential for excess osteonecrosis. This Chapter provides evidence that although high speed surgical round burs may generate high surface temperatures above the threshold for cell death (>47°C), enhanced osteogenesis is in fact observed in the cut surface resected with 2Flute and Multi-Flute designs, because the dissipated temperatures remain below 47°C and cells deep inside the bone and away from the cut surface are not exposed to temperature elevations.

Hypothesis 3: Surgical cutting with manual irrigation induces higher temperatures, when compared to cutting with continuous irrigation, but the ex-vivo osteogenic potential of autograft bone dust is enhanced

The second study, presented in Chapter 4 of this Thesis, quantified the influence of irrigation approaches on temperature elevations arising during high speed cutting. The results of this Chapter revealed that both *surface* and *dissipated* temperature elevations were higher during cutting in the presence of manual irrigation, which replicated the surgical scenario in which a surgical assistant applies irrigation to the cut surface, when compared to continuous irrigation with an irrigation device attached to the cutting instrument. Relative *surface* temperature elevations only increased to 60°C, while dissipated temperatures remained below 30°C, during high speed cutting with 2Flute and Multi-Flute design burs with either irrigation approach. However, the cooling rate was faster, and the percentage of heated surface was higher in the cut surface resected in the presence of manual irrigation in comparison to continuous. Interestingly, there was a lower percentage of positive apoptotic cells in both the cut surface and bone dust resected in the presence of both manual and continuous irrigation methods, and also no significant difference was observed in metabolic activity between all of the irrigation groups. However, bone dust exposed to the higher increase in temperature elevation (manual group) also showed higher mineralisation response, whereby ALP activity and calcium content were significantly higher, supporting Hypothesis 3. This study revealed that although *surface* temperatures did not increase to the same level as cutting with no irrigation (>80°C, Chapter 3), the slight increase in temperature still induced a mineralisation response in bone dust resected in the presence of manual irrigation.

The results of Chapter 4 also showed for the first time that the cut surface was preserved for osteogenesis when continuous irrigation was used during high speed cutting with surgical burs. The study conducted in Chapter 4 is the first to report a difference of osteogenic response

in bone surgically cut in the presence of different irrigation methods (manual vs continuous). Previous work have reported differences in new bone formation (histological analysis) between the cut surface resected with no irrigation or prepared using continuous irrigation (Isler et al. 2011; Haddad et al. 2014).

Hypothesis 4: The mineralisation potential of autograft bone dust is enhanced by mechanical stimulation representative of in vivo conditions

All previous bone dust and bone chip autograft studies have been assessed in static conditions by culturing in a tissue flask or well plates (Roth AA 2017; Ye et al. 2013; Eder et al. 2011; Kuttenberger, Polska, and Schaefer 2013; Gao et al. 2018). All of these studies have made considerable contributions to the understanding of osteogenic potential of bone dust. However autograft bone dust is harvested with the intention of re-implantation, commonly into an in vivo environment that induces mechanical stimulation, such as the intervertebral spaces that induce compressional and torsional forces. Therefore, in vitro studies under static conditions do not fully represent the cellular response in vivo, where a mechanical environment exists and is known to be critical to bone biology. The final study (Chapter 5) sought to address this gap in the field of bone dust regeneration and demonstrated that the osteogenic response in autograft bone dust is enhanced by mechanical stimulation representing in vivo conditions, and this is independent of the irrigation method used during surgical cutting. Interestingly, cell death was not observed in bone dust resected with irrigation and then cultured under mechanically stimulated conditions, and a significant increase in osteogenic potential was also observed. Longer-term mineralisation as assessed by Micro-CT scans revealed a significant increase in bone volume by day 20. All of these findings support Hypothesis 4 of the Thesis. The study conducted in Chapter 5 is the first to report the osteogenic potential of autograft bone dust in a mechanical environment setting representative of in vivo.

These findings are further considered in the context of current understanding of temperature elevations during high speed cutting, the thermal damage and cellular response associated with these heat generations.

6.3. Insight and implications for the field of surgical cutting

The findings of this Thesis provide an insight into tissue and thermal damage in bone surgically cut with a high speed bur, and a further understanding of the association of temperature elevation to the osteogenic potential of ex-vivo bone. Moreover, the results in this Thesis have important implications for the field of post-operative bone regeneration and surgical cutting research. The occurrence of temperature elevations during surgical cutting with a high speed bur is explored. The osteogenic response in ex-vivo bone contributes to the understanding of bone healing after surgical cutting.

Although heat generation on the superficial cut surface reached above 47°C, it did not dissipate deep into the bone. The thermal diffusivity of bone is low and is associated with bone mineral density surrounding the osteocytes (Dolan, Vaughan, Niebur, Casey, et al. 2014), therefore heat generated by high speed surgical burs is only felt by cells on the cut surface. Moreover, it has been shown that using a drill speed above 27,000 rpm decreases temperature elevation during cutting (Abouzgia and James 1997). Until now, temperature elevations representing orthopaedic cutting have been explored using artificial induction of temperature to investigate bone cell response to moderate temperatures (<60°C) (Dolan, Vaughan, Niebur, Casey, et al. 2014; Dolan et al. 2015; Dolan et al. 2016; Eriksson and Albrektsson 1984; Eriksson and Albrektsson 1983; Eriksson, Albrektsson, and Magnusson 1984). However, high speed cutting with surgical burs has been shown to generate temperatures above 60°C (Gao et al. 2018; Hosono et al. 2009; Livingston et al. 2015; Matthes et al. 2018), even with manual irrigation during decompression surgery, temperatures can reach up to 249°C (Matthes et al.

2018). While all of these studies have added new knowledge to the field regarding temperature elevations arising during orthopaedic cutting, the precise osteogenic response to surgical cutting under different conditions previously remained unknown. The temperature analysis in Chapter 3, built upon previous temperature parameter studies, measured the temperature elevation on the *surface* and *dissipated* inside the bone during high speed cutting with burs, whereby *surface* temperatures were in excess of 80°C for very short durations (<1.33 seconds), but *dissipated* temperatures remained below 35°C. These results are corroborated by previous studies, where temperatures measured using a thermocouple remains below 47°C (Shin and Yoon 2006) during cutting with a round bur, which suggests that temperature elevation does not dissipate substantially into bone and therefore only affect the cells on the surface.

High speed surgical burs generate temperatures in excess of 80°C on the surface, but this thermal damage on the surface led to a thermally induced cell apoptosis and an enhanced bone regeneration, whereby the bur design that generated higher temperature (Multi-Flute) also created bone dust with increased mineralisation potential (Chapter 3). The results of Chapter 3 also revealed that osteonecrosis occurs at the surface up to 182.4 μm deep, but the necrotic tissue did not negatively affect the osteogenic capacity of the ex-vivo bone dust or the cut surface groups. Previous studies assessed osteonecrosis (histological staining) caused by surgical cutting with orthopaedic drills, but these studies did not assess the cellular response post-cutting (Karaca, Aksakal, and Kom 2011; Isler et al. 2011; Haddad et al. 2014). Chapter 4 built upon previous studies of bone dust (Roth AA 2017; Eder et al. 2011; Ye et al. 2013) and the cut surface (Karaca, Aksakal, and Kom 2011; Xu et al. 2014; Matthes et al. 2018) to specifically compare ex-vivo osteogenic responses under different irrigation methods, which are commonly used in surgery during high speed cutting with surgical burs.

The regenerative capacity of autograft bone dust is vital for success of laminectomy surgery, and the location of implantation site is also important to consider. These locations

present varying mechanical environments, which can also influence bone regeneration, because bone cells responds positively to mechanical forces such as compression, hydrostatic pressure, torsion, and fluid flow shear stress (Birmingham et al. 2015; Matziolia et al. 2011; Freeman et al. 2017). Chapter 5 adds knowledge beyond that established in previous bone dust studies (Roth AA 2017; Ye et al. 2013; Eder et al. 2011; Kuttenberger, Polska, and Schaefer 2013) by assessing the osteogenic potential of bone dust in a mechanical environment representative of in vivo. This Chapter also compared the ex-vivo osteogenic response between irrigation methods using micro-CT analysis, and have shown that the type of irrigation method used during surgical cutting does not influence long-term mineralisation in autograft bone dust. It should be noted that surgical cutting conducted in Chapters 4 and 5 were carried out with different size burs. A 6 mm size was used in the study conducted in Chapter 4 while a 3 mm size bur was used for cutting in the study conducted in Chapter 5, which might explain the differences observed with respect to the influence of irrigation. In a preliminary temperature analysis conducted in the study of Chapter 3, cutting with a 3 mm bur led to lower heat generation compared to cutting with a 6 mm bur. No difference in mineralisation response was observed between manual and continuous irrigation groups in the study conducted in Chapter 5, and this might be explained by the fact that the temperature elevation during cutting with a 3 mm bur did not increase sufficiently to induce a thermal healing response.

The ex-vivo experiments conducted in this PhD provide an insight into the thermally induced osteogenic response of bone dust and the cut surface prepared by surgical cutting with different surgical flute designs (Chapter 3), cutting in the presence of different irrigation approaches (Chapter 4), and the mineralisation response of autograft bone dust in a mechanical environment representative of in vivo (Chapter 5). The individual studies reported in this Thesis add new knowledge to the field of surgical cutting, shedding further light on the current understanding of autograft bone dust and the cut surface resected by surgical burs, as shown in

Figure 6.1. When analysed together, these findings provide a novel insight into the post-operative bone tissue response to resection in different cutting conditions, as discussed further in the following section.

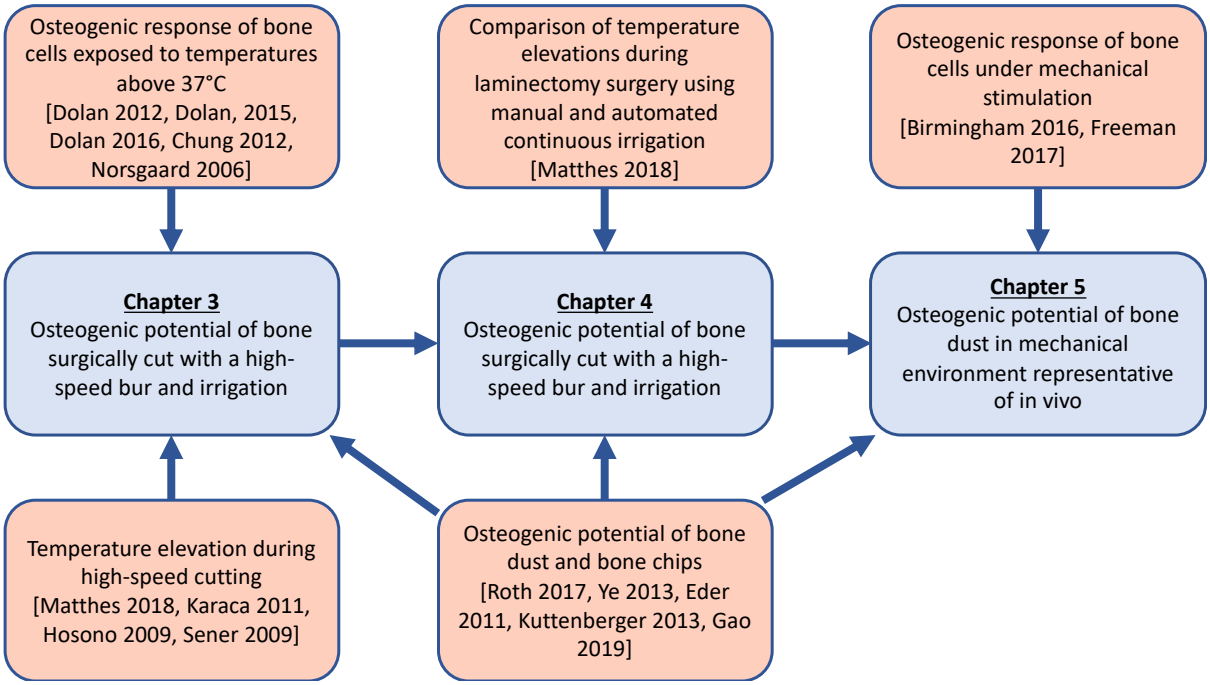

Figure 6.1 Schematic of work conducted as part of this PhD thesis in context with previous studies.

The findings of Chapters 3 and 4 provide an understanding of temperature elevations during cutting with a high speed bur on the surface and inside the bone during different cutting conditions where different flute designs and irrigation methods were used. Temperature findings were then correlated to cell culture results in order to understand the osteogenic response of autograft bone dust and the cut surface, as shown in Figure 6.2. Moreover, the findings showed the importance of a mechanical environment representative of in vivo on the mineralisation potential of autograft bone dust, also shown in Figure 6.2. Based on the results of this Thesis, post-operative bone regeneration is influenced by both thermal and mechanical stimulation. Surgical cutting induces temperature elevation and mechanical damage (bone dust

group) during cutting with surgical burs. Temperature elevations during cutting with no irrigation were in excess of 80°C, which is corroborated by a study conducted in clinical settings where temperatures were well above this during cutting with manual irrigation on human patients undergoing laminectomy surgery (Matthes et al. 2018). Moreover, mechanical stimulation during recovery days also enhance mineralisation in autograft bone dust. This corroborates with other regenerative studies using trabecular bone cores (Birmingham et al. 2015; Birmingham et al. 2016) or stem cells (Freeman et al. 2017; Matziolia et al. 2011) to assess mineralisation of bone cells in a mechanical environment representative of in vivo. These findings add further understanding of mineralisation potential in bone dust and the cut surface created by surgical burs, and can be used to improve designs of future surgical burs, irrigation device, or consideration of bone dust implantation site.

Autograft bone dust differ from other graft materials such as de-cellularised bone allograft, because autograft dust contain the native growth factors and cells needed for bone healing. Unlike allografts, there is no risk of a foreign body response to autograft dust, which has been shown to be both osteoconductive and osteo-inductive (Kuttenberger, Polska, and Schaefer 2013). These properties make bone dust a better graft material, and therefore, understanding the influence of cutting bur design on post-operative bone regeneration is crucial. The clinical implication of this Thesis is to inform both surgeons and engineers on the cutting flute design (2Flute, Multi-Flute) and irrigation approach (manual, continuous) to use during cutting with surgical burs, whereby the results of post-operative bone regeneration is enhanced. Based on the results outlined in Chapters 3 and 4 of this Thesis, the recommendation is to use a Multi-Flute bur design for resection and to use a manual irrigation approach for surgeries where the intention is to use autograft bone dust for bone fusion. But if the intention is to preserve the cut site, then cutting with a Multi-Flute design and using a continuous automated irrigation approach may be better.

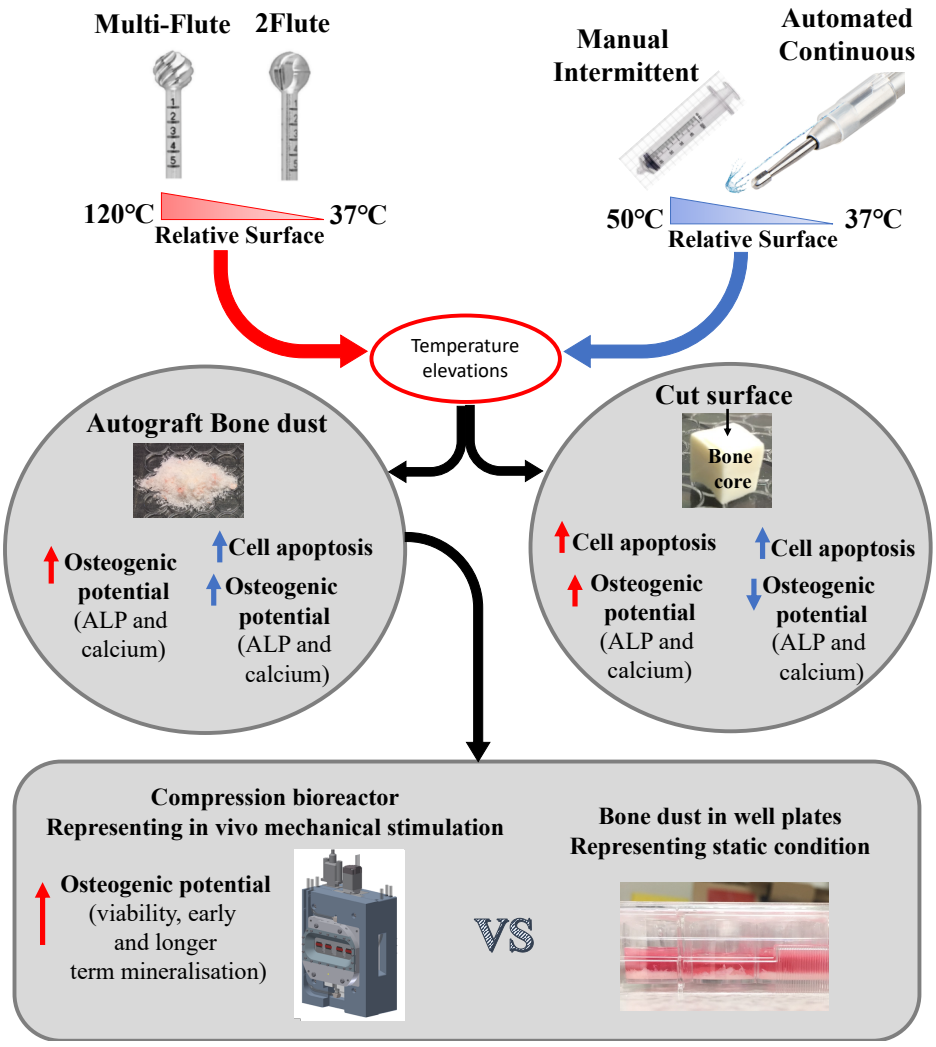

Figure 6.2 Schematic of bone response to surgical cutting with a high speed bur.

6.4. Recommendations for Future Work

The studies described in this Thesis has shed further light on the influence of high speed surgical burs on post-operative bone regeneration. The following recommendations are made for future research based on the findings of this Thesis;

6.4.1. Temperature elevations in bone surgically cut with high speed drills and oscillating saws

Temperature elevations during high speed surgical cutting is a major factor in the ability of bone tissue to recover from damage. High speed surgical cutting tools can be designed to minimise temperature elevations and prevent excessive osteonecrosis by studying the

parameters that induce heat generation (Matthews and Hirsch 1972a; Karaca, Aksakal, and Kom 2011; Saha, Pal, and Albright 1982; Sener et al. 2009). The studies in this Thesis have evaluated the temperature elevation induced by different cutting flute designs in burs and different irrigation methods. Investigation into temperature elevations was only assessed in surgical burs. Currently, there is no assessment of *surface* temperature elevations during high speed cutting with drills. It would be interesting to conduct the same assessment as conducted in this for orthopaedic drills. This surgical instrument would not fit the criteria for a moving heat object and therefore, heat generation is expected to be higher. Gathering surface temperature data would be challenging, however, as the cutting instrument would interfere with FLIR results because it remains in front of the cut surface during this process. From the time the instrument is moved out of frame the *surface* temperature would have significantly decreased, which cooling rate results in Chapter 3 would suggest. To overcome this challenge, cutting should take place where the drill is visible and the middle section of the bone has been exposed to the camera lens. Embedding thermocouples in the bone would also add understanding of heat dissipation during cutting.

6.4.2. In vivo osteogenic potential of the cut surface

Another suggestion for future work based on the results of this Thesis is an in vivo study to assess post-operative bone regeneration. Surgical burs were used on porcine spines, therefore a porcine animal study would be suitable to use these burs on. Results from studies conducted in Chapters 3 and 4 have laid out the cellular response to temperature elevations induced by surgical cutting with burs in different cutting conditions. However, an animal study would give a more representative understanding of the cellular response in vivo. Osteogenic potential can be assessed using histological staining with hematoxylin and eosin, immunostaining with cleaved caspase 3 antibodies, and quantitative polymerase chain reaction (qPCR) to quantify gene expression of osteogenic genes, such as COX2, OPG, RANKL, Il-1a, M-csf, and bone

sialoprotein (BSP). Methods adapted from (Dolan et al. 2016) could be employed to assess expression of osteogenic genes in vivo. The methods used to assess temperature analysis in Chapters 3 and 4 could be employed to quantify temperature elevations during cutting, in order to establish a correlation between heat generation and in vivo osteogenic capacity of surgically cut bone.

6.4.3. Influence of thermal and mechanical stimulation induced by high speed cutting

It is difficult to separately assess thermal and mechanical stimulation that is induced during surgical cutting, because the cutting tool simultaneously induces both. Osteogenic potential of thermally induced cells has been fully assessed in vitro and in vivo (Dolan et al. 2012; Dolan et al. 2015; Dolan et al. 2016). Mechanical stimulation of bone cells have also been assessed in vitro and ex vivo (Matziolia et al. 2011; Birmingham et al. 2015; Freeman et al. 2017). However, the comparison between thermal and mechanical stimulation has not been conducted to determine which stimulation would benefit post-operative bone regeneration. For mechanical stimulation, a device that simulates physical chattering on bone would need to be used to represent cutting with surgical burs or oscillating saws. For thermal stimulation, a thermal probe could be used to induce temperature elevation, and this is easily controlled. Alternatively, an in vitro study could be conducted by exposing bone cell lines, such as MC3T3 cells or MLO-Y4 cells, to thermal stress conditions, and compare this group to cell lines cultured under mechanical stimulation using a bioreactor.

6.4.4. Regenerative capacity in diseased bone

The studies conducted in this Thesis were carried out on healthy bone resected from slaughtered animals. However, patients undergoing surgery may be osteoarthritic, osteoporotic, or diabetic, where bone quality is low (O'Sullivan et al. 2020; Parle et al. 2020). For example, bone mineral content is decreased in osteoporotic patients compared to healthy

bone, where the fine balance between bone forming cells and bone resorbing cells has been compromised. This compromised interaction between osteoblasts and osteoclasts will influence the ability of bone to heal. A study could be designed to address this by using methods and results from Chapters 3, 4, and 5. Diseased human femoral heads could be obtained from patients undergoing hip surgery, or bone dust samples could be taken from patients undergoing lumbar spinal fusion surgery. Temperature analysis from Chapters 3 and 4 could be employed to assess temperature elevations during cutting with different design burs (2Flute and Multi-Flute) and different cutting conditions (no irrigation, manual, continuous) on human femoral bone (cancellous region). A collaboration with a spinal surgeon will be needed to carry out a study using bone dust directly from patients. Methods from the study conducted by (Matthes et al. 2018) will need to be used to measure the temperature elevation during cutting, then bone dust from patients will need to be harvested and assessed for ex-vivo osteogenic potential, categorising patients depending on whether they were healthy and or had diseased bone (osteoporotic, diabetic). Comparing these results with the ones reported in this Thesis will provide a complete understanding of the influence of temperature elevation on post-operative bone regeneration in humans.

6.5. Conclusion

In conclusion, this Thesis has presented experimental studies performed throughout the course of the author's PhD studies to investigate the influence of temperature elevation and mechanical stimulation in surgically cut bone under different cutting conditions. Together, these studies provide (1) an insight into the osteogenic response of bone tissue resected with different design burs and different irrigation approaches during cutting, and (2) uncovers how the mechanical environment that arises in vivo might influence the osteogenic capacity of autograft bone dust. Experimental design was established to determine temperature elevations during cutting with surgical burs and no irrigation, and this temperature was correlated to the

ex-vivo cell culture study where viability, ALP activity and calcium content were assessed. The established methods for temperature analysis and cell culture were then implemented to assess osteogenic potential of bone cut with different irrigation approaches, manual and continuous irrigation. Finally, to fully understand the osteogenic potential of bone dust implanted in a site representing in vivo, the autograft was cultured under static and stimulated conditions to assess early and long-term mineralisation. A compression bioreactor was used to stimulate bone dust constructs, and this represented the intervertebral disc space, which is the implantation site for lumbar interbody spinal fusion. This Thesis provides an ex-vivo understanding of regenerative tissue response to surgical cutting with burs and the osteogenic recovery in a mechanical environment representative of in vivo, and as such, the information elucidated from this body of work will inform future surgical instrument design to improve post-operative bone tissue regeneration.

References

Abbasi, H., and A. Abbasi. 2019. "Using Porcine Cadavers as an Alternative to Human Cadavers for Teaching Minimally Invasive Spinal Fusion: Proof of Concept and Anatomical Comparison." *Cureus* 11 (11). doi: 10.7759/cureus.6158.

Abouzgia, M. B., and D. F. James. 1997. "Temperature rise during drilling through bone." *International Journal of Oral & Maxillofacial Implants* 12 (3):342-353.

Aerssens, J., S. Boonen, G. Lowet, and J. Dequeker. 1998. "Interspecies differences in bone composition, density, and quality: Potential implications for in vivo bone research." *Endocrinology* 139 (2):663-670. doi: 10.1210/en.139.2.663.

Albright, J.A., T.R. Johnson, and S. Saha. 1978. *Principals of internal fixation in orthopaedic mechanics: procedures and devices*: Academic Press.

Ashkenazi, A., and V. M. Dixit. 1998. "Death receptors: Signaling and modulation." *Science* 281 (5381):1305-1308. doi: 10.1126/science.281.5381.1305.

Aubin, JE. 2001. "Regulation of osteoblast formation and function." *Reviews in Endocrine and Metabolic Disorders* 2:81-94.

Augustin G, Davila S, Mihoci K, Udiljak T, Vedrina DS, Antabak A. 2008. "Thermal osteonecrosis and bone drilling parameters revisted." *Arch Orthop Trauma Surg* 128:71-77. doi: 10.1007/s00402-007-0427-3.

Beere, H. M., B. B. Wolf, K. Cain, D. D. Mosser, A. Mahboubi, T. Kuwana, P. Tailor, R. I. Morimoto, G. M. Cohen, and D. R. Green. 2000. "Heat-shock protein 70 inhibits apoptosis by preventing recruitment of procaspase-9 to the Apaf-1 apoptosome." *Nature Cell Biology* 2 (8):469-475.

Betts, J Gordon, Kelly A Young, James A Wise, Eddie Johnson, Brandon Poe, Dean H Kruse, Oksana Korol, Jody E Johnson, Mark Womble, and Peter DeSaix. 2013. "Anatomy and Physiology." OpenStax. https://openstax.org/books/anatomy-and-physiology/pages/6-5-fractures-bone-repair.

Birmingham, E., T. C. Kreipke, E. B. Dolan, T. R. Coughlin, P. Owens, L. M. McNamara, G. L. Niebur, and P. E. McHugh. 2015. "Mechanical Stimulation of Bone Marrow In Situ Induces Bone Formation in Trabecular Explants." *Annals of Biomedical Engineering* 43 (4):1036-1050. doi: 10.1007/s10439-014-1135-0.

Birmingham, E., G. L. Niebur, L. M. McNamara, and P. E. McHugh. 2016. "An Experimental and Computational Investigation of Bone Formation in Mechanically Loaded Trabecular Bone Explants." *Annals of Biomedical Engineering* 44 (4):1191-1203. doi: 10.1007/s10439-015-1378-4.

Bonewald, L. F. 2002. "Osteocytes: a proposed multifunctional bone cell." *Journal of musculoskeletal & neuronal interactions* 2 (3):239-41.

Bonewald, L. F. 2011. "The Amazing Osteocyte." *Journal of Bone and Mineral Research* 26 (2):229-238. doi: 10.1002/jbmr.320.

Bonewald, L. F., and M. L. Johnson. 2008. "Osteocytes, mechanosensing and Wnt signaling." *Bone* 42 (4):606-615. doi: 10.1016/j.bone.2007.12.224.

Bonfoco, E., D. Krainc, M. Ankarcrona, P. Nicotera, and S. A. Lipton. 1995. "APOPTOSIS AND NECROSIS - 2 DISTINCT EVENTS INDUCED, RESPECTIVELY, BY MILD AND INTENSE INSULTS WITH N-METHYL-D-ASPARTATE OR NITRIC-OXIDE SUPEROXIDE IN CORTICAL CELL-CULTURES." *Proceedings of the National Academy of Sciences of the United States of America* 92 (16):7162-7166. doi: 10.1073/pnas.92.16.7162.

Borges, J. C., and C. H. I. Ramos. 2005. "Protein folding assisted by chaperones." *Protein and Peptide Letters* 12 (3):257-261. doi: 10.2174/0929866053587165.

Boyce, B. F., and L. P. Xing. 2008. "Functions of RANKL/RANK/OPG in bone modeling and remodeling." *Archives of Biochemistry and Biophysics* 473 (2):139-146. doi: 10.1016/j.abb.2008.03.018.

Boyle, W. J., W. S. Simonet, and D. L. Lacey. 2003. "Osteoclast differentiation and activation." *Nature* 423 (6937):337-342. doi: 10.1038/nature01658.

C., Cowin. S. 1990. "Structural adaption of Bones." *Applied Mechanics Review* 43:126-133.

Campbell, J. J., D. A. Lee, and D. L. Bader. 2006. "Dynamic compressive strain influences chondrogenic gene expression in human mesenchymal stem cells." *Biorheology* 43 (3-4):455-470.

Carter, D. R. 1984. "MECHANICAL LOADING HISTORIES AND CORTICAL BONE REMODELING." *Calcified Tissue International* 36:S19-S24. doi: 10.1007/bf02406129.

Chao, E. Y., and N. Inoue. 2003. "Biophysical stimulation of bone fracture repair, regeneration and remodelling." *Eur Cell Mater* 6:72-84; discussion 84-5. doi: 10.22203/ecm.v006a07.

Chen, E. M., D. T. Xue, W. Zhang, F. Lin, and Z. J. Pan. 2015. "Extracellular heat shock protein 70 promotes osteogenesis of human mesenchymal stem cells through activation of the ERK signaling pathway." *Febs Letters* 589 (24):4088-4096. doi: 10.1016/j.febslet.2015.11.021.

Cheng, Z. H., J. Wang, Q. X. Zheng, Y. C. Wu, and X. D. Guo. 2015. "Anterolateral Radical Debridement and Interbody Bone Grafting Combined With Transpedicle Fixation in the Treatment of Thoracolumbar Spinal Tuberculosis." *Medicine* 94 (14). doi: 10.1097/md.0000000000000721.

Chicheportiche, Y., P. R. Bourdon, H. D. Xu, Y. M. Hsu, H. Scott, C. Hession, I. Garcia, and J. L. Browning. 1997. "TWEAK, a new secreted ligand in the tumor necrosis factor family that weakly induces apoptosis." *Journal of Biological Chemistry* 272 (51):32401-32410. doi: 10.1074/jbc.272.51.32401.

Chinnaiyan, A. M. 1999. "The apoptosome: heart and soul of the cell death machine." *Neoplasia* 1 (1):5-15. doi: 10.1038/sj.neo.7900003.

Choi, Youngsil, Hyunjung Kim, Heesung Chung, Ji-Sun Hwang, Jin- A. Shin, Inn-Oc Han, and Eok-Soo Oh. 2010. "Syndecan-2 regulates cell migration in colon cancer cells through Tiam1-mediated Rac activation." *Biochemical and Biophysical Research Communications* 391 (1):921-925. doi: 10.1016/j.bbrc.2009.11.165.

Chung, E., and M. N. Rylander. 2012. "Response of preosteoblasts to thermal stress conditioning and osteoinductive growth factors." *Cell Stress & Chaperones* 17 (2):203-214. doi: 10.1007/s12192-011-0300-8.

Chung, U. I., H. Kawaguchi, T. Takato, and K. Nakamura. 2004. "Distinct osteogenic mechanisms of bones of distinct origins." *Journal of Orthopaedic Science* 9 (4):410-414. doi: 10.1007/s00776-004-0786-3.

Clarke, B. 2008. "Normal Bone Anatomy and Physiology." *Clinical Journal of the American Society of Nephrology* 3:S131-S139. doi: 10.2215/cjn.04151206.

Corporation, REOTEMP Instrument. "Thermocouple info." https://www.thermocoupleinfo.com/index.htm.

Cowin, S. C. 1983. "THE MECHANICAL AND STRESS ADAPTIVE PROPERTIES OF BONE." *Annals of Biomedical Engineering* 11 (3-4):263-295. doi: 10.1007/bf02363288.

Cowin, S. C., S. Weinbaum, and Y. Zeng. 1995. "A CASE FOR BONE CANALICULI AS THE ANATOMICAL SITE OF STRAIN GENERATED POTENTIALS." *Journal of Biomechanics* 28 (11):1281-1297. doi: 10.1016/0021-9290(95)00058-p.

Cowin, SC. 1989. *Bone Mechanics Handbook*: Taylor & Francis.

Cowin, SC. 2001. *Bone Mechanics Handbook*: CRC Press LLC.

Crowley, L. C., and N. J. Waterhouse. 2016. "Detecting Cleaved Caspase-3 in Apoptotic Cells by Flow Cytometry." *Cold Spring Harb Protoc* 2016 (11). doi: 10.1101/pdb.prot087312.

Curtis, K. J., T. R. Coughlin, D. E. Mason, J. D. Boerckel, and G. L. Niebur. 2018. "Bone marrow mechanotransduction in porcine explants alters kinase activation and enhances trabecular bone formation in the absence of osteocyte signaling." *Bone* 107:78-87. doi: 10.1016/j.bone.2017.11.007.

Dallas, S. L., M. Prideaux, and L. F. Bonewald. 2013. "The Osteocyte: An Endocrine Cell . . . and More." *Endocrine Reviews* 34 (5):658-690. doi: 10.1210/er.2012-1026.

Davidson, S. R. H., and D. F. James. 2000. "Measurement of thermal conductivity of bovine cortical bone." *Medical Engineering & Physics* 22 (10):741-747. doi: 10.1016/s1350-4533(01)00003-0.

Davidson, S. R. H., and D. F. James. 2003. "Drilling in bone: Modeling heat generation and temperature distribution." *Journal of Biomechanical Engineering-Transactions of the Asme* 125 (3):305-314. doi: 10.1115/1.1535190.

Davies, C. M., D. B. Jones, M. J. Stoddart, K. Koller, E. Smith, C. W. Archer, and R. G. Richards. 2006. "Mechanically loaded ex vivo bone culture system 'Zetos': Systems and culture preparation." *European Cells & Materials* 11:57-75. doi: 10.22203/eCM.v011a07.

Davies, G. 2006.

Delaine-Smith, R. M., and G. C. Reilly. 2011. "THE EFFECTS OF MECHANICAL LOADING ON MESENCHYMAL STEM CELL DIFFERENTIATION AND MATRIX PRODUCTION." *Vitamins and Hormones: Stem Cell Regulators* 87:417-480. doi: 10.1016/b978-0-12-386015-6.00039-1.

Dolan, E. B., M. G. Haugh, D. Tallon, C. Casey, and L. M. McNamara. 2012. "Heat-shock-induced cellular responses to temperature elevations occurring during orthopaedic cutting." *Journal of the Royal Society Interface* 9 (77):3503-3513. doi: 10.1098/rsif.2012.0520.

Dolan, E. B., M. G. Haugh, M. C. Voisin, D. Tallon, and L. M. McNamara. 2015. "Thermally Induced Osteocyte Damage Initiates a Remodelling Signaling Cascade." *Plos One* 10 (3). doi: 10.1371/journal.pone.0119652.

Dolan, E. B., D. Tallon, W. Y. Cheung, M. B. Schaffler, O. D. Kennedy, and L. M. McNamara. 2016. "Thermally induced osteocyte damage initiates pro-osteoclastogenic gene expression in vivo." *Journal of the Royal Society Interface* 13 (119). doi: 10.1098/rsif.2016.0337.

Dolan, E. B., T. J. Vaughan, G. L. Niebur, C. Casey, D. Tallon, and L. M. McNamara. 2014. "How Bone Tissue and Cells Experience Elevated Temperatures During Orthopaedic Cutting: An Experimental and Computational Investigation." *Journal of Biomechanical Engineering-Transactions of the Asme* 136 (2). doi: 10.1115/1.4026177.

Dolan, E. B., T. J. Vaughan, G. L. Niebur, D. Tallon, L. M. McNamara, and Asme. 2014. *UNDERSTANDING THE EFFECTS OF THERMAL ELEVATIONS ASSOCIATED WITH ORTHOPEDIC INTERVENTION: AN EXPERIMENTAL AND COMPUTATIONAL INVESTIGATION*, *Proceedings of the Asme Summer Bioengineering Conference - 2013, Pt B*.

Du, C. Y., M. Fang, Y. C. Li, L. Li, and X. D. Wang. 2000. "Smac, a mitochondrial protein that promotes cytochrome c-dependent caspase activation by eliminating IAP inhibition." *Cell* 102 (1):33-42. doi: 10.1016/s0092-8674(00)00008-8.

Duff, Matthew, and Joseph Towey. 2010. Two ways to measure temperature using thermocouples feature simplicity, accuracy, and flexibility. Analog Dialogue.

Eder, C., A. Chavanne, J. Meissner, W. Bretschneider, A. Tuschel, P. Becker, and M. Ogon. 2011. "Autografts for spinal fusion: osteogenic potential of laminectomy bone chips and bone shavings collected via high speed drill." *European Spine Journal* 20 (11):1791-1795. doi: 10.1007/s00586-011-1736-3.

Einhorn, T. A. 1998. "The cell and molecular biology of fracture healing." *Clinical Orthopaedics and Related Research* (355):S7-S21.

Emmett R. Costich, Philip J. Youngblood, James M. Walden. 1964. "A study of the effects of high speed rotary instruments on bone repair in dogs." *Oral Surgery Oral Medicine and Oral Pathology* 17:563-571. doi: 10.1016/0030-4220(64)90359-7.

Epstein, Nancy E. 2017. High lumbar non instrumented fusion rates using lamina autograft and Nanoss/bone marrow aspirate. Surgical Neurology International.

Eriksson, A. R., and T. Albrektsson. 1983. "TEMPERATURE THRESHOLD LEVELS FOR HEAT-INDUCED BONE TISSUE-INJURY - A VITAL-MICROSCOPIC STUDY IN THE RABBIT." *Journal of Prosthetic Dentistry* 50 (1):101-107. doi: 10.1016/0022-3913(83)90174-9.

Eriksson, A. R., T. Albrektsson, and B. Albrektsson. 1984. "HEAT CAUSED BY DRILLING CORTICAL BONE - TEMPERATURE MEASURED INVIVO IN PATIENTS AND ANIMALS." *Acta Orthopaedica Scandinavica* 55 (6):629-631. doi: 10.3109/17453678408992410.

Eriksson, A. R.; Albrektsson, T.; Albrektsson, B. 1984. "Heat caused by drilling cortical bone: temperature measured in vivo in patients and animals." *Acta Orthopaedica Scandinavica* 55 (6):629-631.

Eriksson, R. A., and T. Albrektsson. 1984. "THE EFFECT OF HEAT ON BONE REGENERATION - AN EXPERIMENTAL-STUDY IN THE RABBIT USING THE BONE-GROWTH CHAMBER." *Journal of Oral and Maxillofacial Surgery* 42 (11):705-711. doi: 10.1016/0278-2391(84)90417-8.

Eriksson, R. A., T. Albrektsson, and B. Magnusson. 1984. "ASSESSMENT OF BONE VIABILITY AFTER HEAT TRAUMA - A HISTOLOGICAL, HISTOCHEMICAL AND VITAL MICROSCOPIC STUDY IN THE RABBIT." *Scandinavian Journal of Plastic and Reconstructive Surgery and Hand Surgery* 18 (3):261-268. doi: 10.3109/02844318409052849.

F.A. Saleh, M. Whyte, and P.G. Genever. 2011. "Effects of endothelial cells on human mesenchymal stem cell activity in a three-dimensional in vitro model." *European Cells & Materials* 22:242-257. doi: 10.22203/eCM.v022a19.

Feldmann, A., P. Wili, G. Maquer, and P. Zysset. 2018. "THE THERMAL CONDUCTIVITY OF CORTICAL AND CANCELLOUS BONE." *European Cells & Materials* 35:25-33. doi: 10.22203/eCM.v035a03.

Feldmann, A., Zysset, P. 2016. "Experimental Determination of the Emissivity of Bone." *Medical Engineering & Physics* 38:1136-1138. doi: 10.1016/j.medengphy.2016.06.019.

Filvaroff, E., and R. Derynck. 1998. "Bone remodelling: A signalling system for osteoclast regulation." *Current Biology* 8 (19):R679-R682. doi: 10.1016/s0960-9822(98)70434-8.

FLIR. "How do thermal cameras work?". https://www.flir.com/discover/rd-science/how-do-thermal-cameras-work/.

Forwood, M. R., and C. H. Turner. 1995. "SKELETAL ADAPTATIONS TO MECHANICAL USAGE - RESULTS FROM TIBIAL LOADING STUDIES IN RATS." *Bone* 17 (4):S197-S205. doi: 10.1016/8756-3282(95)00292-l.

Fratzl, P., H. S. Gupta, E. P. Paschalis, and P. Roschger. 2004. "Structure and mechanical quality of the collagen-mineral nano-composite in bone." *Journal of Materials Chemistry* 14 (14):2115-2123. doi: 10.1039/b402005g.

Freeman, F. E., J. Schiavi, M. A. Brennan, P. Owens, P. Layrolle, and L. M. McNamara. 2017. "Mimicking the Biochemical and Mechanical Extracellular Environment of the Endochondral Ossification Process to Enhance the In Vitro Mineralization Potential of Human Mesenchymal Stem Cells." *Tissue Engineering Part A* 23 (23-24):1466-1478. doi: 10.1089/ten.tea.2017.0052.

Frost, H. M. 1973. "METABOLISM OF BONE." *New England Journal of Medicine* 289 (16):864-865.

Frost, H. M. 1990. "Skeletal structural adaptations to mechanical usage (SATMU): 1. Redefining Wolff's law: the bone modeling problem." *Anat Rec* 226 (4):403-13. doi: 10.1002/ar.1092260402.

Frost, HM. 1960a. "In vivo osteocyte death." *The Journal of Bone and Joint Surgery* 42:138 - 143.

Gantenbein, Benjamin, Svenja Illien-Junger, Samantha C. W. Chan, Jochen Walser, Lisbet Haglund, Stephen J. Ferguson, James C. Iatridis, and Sibylle Grad. 2015. "Organ culture bioreactors--platforms to study human intervertebral disc degeneration and regenerative therapy." *Current stem cell research & therapy* 10 (4):339-52. doi: 10.2174/1574888x10666150312102948.

Gao, R., M. Street, M. L. Tay, K. E. Callon, D. Naot, A. Lock, J. T. Munro, J. Cornish, J. Ferguson, and D. Musson. 2018. "Human Spinal Bone Dust as a Potential Local Autograft." *Spine* 43 (4):E193-E199. doi: 10.1097/brs.0000000000002331.

Garrido, C., L. Galluzzi, M. Brunet, P. E. Puig, C. Didelot, and G. Kroemer. 2006. "Mechanisms of cytochrome c release from mitochondria." *Cell Death and Differentiation* 13 (9):1423-1433. doi: 10.1038/sj.cdd.4401950.

Gaspar, D. A., V. Gomide, and F. J. Monteiro. 2012. "The role of perfusion bioreactors in bone tissue engineering." *Biomatter* 2 (4):167-75. doi: 10.4161/biom.22170.

Gehrke, S. A., J. S. Aramburu, C. P. B. Martinez, M. P. R. Fernandez, Jems de Val, and J. L. Calvo-Guirado. 2016. "The influence of drill length and irrigation system on heat production during osteotomy preparation for dental implants: an exvivo study." *Clinical Oral Implants Research* 29 (7):772-778. doi: 10.1111/clr.12827.

Geoghegan, I. P., D. A. Hoey, and L. M. McNamara. 2019. "Estrogen deficiency impairs integrin alpha(v)beta(3)-mediated mechanosensation by osteocytes and alters osteoclastogenic paracrine signalling." *Scientific Reports* 9. doi: 10.1038/s41598-019-41095-3.

Gerber, H. P., and N. Ferrara. 2000. "Angiogenesis and bone growth." *Trends in Cardiovascular Medicine* 10 (5):223-228. doi: 10.1016/s1050-1738(00)00074-8.

Guo, Y., C. Q. Zhang, Q. C. Zeng, R. X. Li, L. Liu, Q. X. Hao, C. H. Shi, X. Z. Zhang, and Y. X. Yan. 2012. "Mechanical strain promotes osteoblast ECM formation and improves its osteoinductive potential." *Biomedical Engineering Online* 11. doi: 10.1186/1475-925x-11-80.

Gupta, A., C. Lobocki, G. Malhotra, and I. T. Jackson. 2009. "Comparison of Osteogenic Potential of Calvarial Bone Dust, Bone Fragments, and Periosteum." *Journal of Craniofacial Surgery* 20 (6):1995-1999. doi: 10.1097/SCS.0b013e3181bd3010.

Haddad, S. L., A. R. Hsu, C. R. Templin, Y. P. Ren, B. Stewart, N. S. Kohli, and L. Q. Zhang. 2014. "Effects of Continuous Irrigation During Burring on Thermal Necrosis and Fusion Strength in a Rabbit Arthrodesis Model." *Foot & Ankle International* 35 (8):796-801. doi: 10.1177/1071100714535767.

Hengartner, M. O. 2000. "The biochemistry of apoptosis." *Nature* 407 (6805):770-776. doi: 10.1038/35037710.

Hill, M. M., C. Adrain, P. J. Duriez, E. M. Creagh, and S. J. Martin. 2004. "Analysis of the composition, assembly kinetics and activity of native Apaf-1 apoptosomes." *Embo Journal* 23 (10):2134-2145. doi: 10.1038/sj.emboj.7600210.

Hosono, N., T. Miwa, Y. Mukai, S. Takenaka, T. Makino, and T. Fuji. 2009. "Potential risk of thermal damage to cervical nerve roots by a high-speed drill." *Journal of Bone and Joint Surgery-British Volume* 91B (11):1541-1544. doi: 10.1302/0301-620x.91b11.22196.

Hou, Z. B., and R. Komanduri. 2000. "General solutions for stationary/moving plane heat source problems in manufacturing and tribology." *International Journal of Heat and Mass Transfer* 43 (10):1679-1698. doi: 10.1016/s0017-9310(99)00271-9.

Hsu, H. L., J. Xiong, and D. V. Goeddel. 1995. "THE TNF RECEPTOR 1-ASSOCIATED PROTEIN TRADD SIGNALS CELL-DEATH AND NF-KAPPA-B ACTIVATION." *Cell* 81 (4):495-504. doi: 10.1016/0092-8674(95)90070-5.

Isler, S. C., E. Cansiz, C. Tanyel, M. Soluk, F. Selvi, and Z. Cebi. 2011. "The Effect of Irrigation Temperature on Bone Healing." *International Journal of Medical Sciences* 8 (8):704-708. doi: 10.7150/ijms.8.704.

Jacob, C. H., and J. T. Berry. 1976. "A study of the bone machining process--drilling." *Journal of biomechanics*:343-9.

Jee, W. S. S., X. J. Li, and M. B. Schaffler. 1991. "ADAPTATION OF DIAPHYSEAL STRUCTURE WITH AGING AND INCREASED MECHANICAL USAGE IN THE ADULT-RAT - A HISTOMORPHOMETRICAL AND BIOMECHANICAL STUDY." *Anatomical Record* 230 (3):332-338. doi: 10.1002/ar.1092300306.

Joza, N., S. A. Susin, E. Daugas, W. L. Stanford, S. K. Cho, C. Y. J. Li, T. Sasaki, A. J. Elia, H. Y. M. Cheng, L. Ravagnan, K. F. Ferri, N. Zamzami, A. Wakeham, R. Hakem, H. Yoshida, Y. Y. Kong, T. W. Mak, J. C. Zuniga-Pflucker, G. Kroemer, and J. M. Penninger. 2001. "Essential role of the

mitochondrial apoptosis-inducing factor in programmed cell death." *Nature* 410 (6828):549-554. doi: 10.1038/35069004.

Kanczler, J. M., and R. O. C. Oreffo. 2008. "Osteogenesis and angiogenesis: The potential for engineering bone." *European Cells & Materials* 15:100-114. doi: 10.22203/eCM.v015a08.

Karaca, F., B. Aksakal, and M. Kom. 2011. "Influence of orthopaedic drilling parameters on temperature and histopathology of bovine tibia: An in vitro study." *Medical Engineering & Physics* 33 (10):1221-1227. doi: 10.1016/j.medengphy.2011.05.013.

Kato, Y., J. J. Windle, B. A. Koop, G. R. Mundy, and L. F. Bonewald. 1997. "Establishment of an osteocyte-like cell line, MLO-Y4." *Journal of Bone and Mineral Research* 12 (12):2014-2023. doi: 10.1359/jbmr.1997.12.12.2014.

Kim, B. S., A. J. Putnam, T. J. Kulik, and D. J. Mooney. 1998. "Optimizing seeding and culture methods to engineer smooth muscle tissue on biodegradable polymer matrices." *Biotechnology and Bioengineering* 57 (1):46-54.

Kim, D. H., N. Lee, D. A. Shin, S. Yi, K. N. Kim, and Y. Ha. 2016. "Matched Comparison of Fusion Rates between Hydroxyapatite Demineralized Bone Matrix and Autograft in Lumbar Interbody Fusion." *Journal of Korean Neurosurgical Society* 59 (4):363-367. doi: 10.3340/jkns.2016.59.4.363.

Kischkel, F. C., S. Hellbardt, I. Behrmann, M. Germer, M. Pawlita, P. H. Krammer, and M. E. Peter. 1995. "CYTOTOXICITY-DEPENDENT APO-1 (FAS/CD95)-ASSOCIATED PROTEINS FORM A DEATH-INDUCING SIGNALING COMPLEX (DISC) WITH THE RECEPTOR." *Embo Journal* 14 (22):5579-5588. doi: 10.1002/j.1460-2075.1995.tb00245.x.

Kleinnulend, J., A. Vanderplas, C. M. Semeins, N. E. Ajubi, J. A. Frangos, P. J. Nijweide, and E. H. Burger. 1995. "SENSITIVITY OF OSTEOCYTES TO BIOMECHANICAL STRESS IN-VITRO." *Faseb Journal* 9 (5):441-445.

Kogianni, G., V. Mann, and B. S. Noble. 2008. "Apoptotic bodies convey activity capable of initiating osteoclastogenesis and localized bone destruction." *Journal of Bone and Mineral Research* 23 (6):915-927. doi: 10.1359/jbmr.080207.

Kuttenberger, J., E. Polska, and B. M. Schaefer. 2013. "A novel three-dimensional bone chip organ culture." *Clinical Oral Investigations* 17 (6):1547-1555. doi: 10.1007/s00784-012-0833-y.

Lee, J., C. L. Chavez, and J. Park. 2018. "Parameters affecting mechanical and thermal responses in bone drilling: A review." *Journal of Biomechanics* 71:4-21. doi: 10.1016/j.jbiomech.2018.02.025.

Liu, J., Z. H. Zhao, J. Li, L. Zou, C. Shuler, Y. W. Zou, X. J. Huang, M. L. Li, and J. Wang. 2009. "Hydrostatic Pressures Promote Initial Osteodifferentiation With ERK1/2 Not p38 MAPK Signaling Involved." *Journal of Cellular Biochemistry* 107 (2):224-232. doi: 10.1002/jcb.22118.

Livingston, A., T. Wang, C. Christou, M. H. Pelletier, and W. R. Walsh. 2015. "The effect of saline coolant on temperature levels during decortication with a Midas Rex: an in vitro model using sheep cervical vertebrae." *Frontiers in Surgery* 2. doi: 10.3389/fsurg.2015.00037.

Locksley, R. M., N. Killeen, and M. J. Lenardo. 2001. "The TNF and TNF receptor superfamilies: Integrating mammalian biology." *Cell* 104 (4):487-501. doi: 10.1016/s0092-8674(01)00237-9.

Majno, G., M. Lagattuta, and T. E. Thompson. 1960. "CELLULAR DEATH AND NECROSIS - CHEMICAL, PHYSICAL AND MORPHOLOGIC CHANGES IN RAT LIVER." *Virchows Archiv Fur Pathologische Anatomie Und Physiologie Und Fur Klinische Medizin* 333 (5):421-465. doi: 10.1007/bf00955327.

Malvisi, A., P. Vendruscolo, F. Morici, S. Martelli, and M. Marcacci. 2000. "Milling versus sawing: Comparison of temperature elevation and clinical performance during bone cutting." *Medical Image Computing and Computer-Assisted Intervention - Miccai 2000* 1935:1238-1244.

Mann, V., C. Huber, D. Kogiani, D. Jones, and B. Noble. 2006. The influence of mechanical stimulation on osteocyte apoptosis and bone viability in human trabecular bone. Journal of Musculoskeletal Neuronal Interaction.

Matsumoto, K., E. Kohmura, A. Kato, and T. Hayakawa. 1998. "Restoration of small bone defects at craniotomy using autologous bone dust and fibrin glue." *Surgical Neurology* 50 (4):344-346. doi: 10.1016/s0090-3019(98)00081-0.

Matthes M, Pillich DT, Rafaee EE, Schroeder HWS, Muller JU. 2018. "Heat Generation During Bony Decompression of Lumbar Spinal Stenosis Using a High-Speed Drill with or without Automated Irrigation and an Ultrasonic Bone-Cutting Knife: A Single Blinded Prospective Randomized Controlled Study." *World Neurosurg* 111:e72e-81. doi: 10.1016/j.wneu2017.11.172.

Matthes, M., D. T. Pillich, E. El Refaee, H. W. S. Schroeder, and J. U. Muller. 2018. "Heat Generation During Bony Decompression of Lumbar Spinal Stenosis Using a High-Speed Diamond Drill with or without Automated Irrigation and an Ultrasonic Bone-Cutting Knife: A Single-Blinded Prospective Randomized Controlled Study." *World Neurosurgery* 111:E72-E81. doi: 10.1016/j.wneu.2017.11.172.

Matthews, L. S., and C. Hirsch. 1972a. "TEMPERATURES MEASURED IN HUMAN CORTICAL BONE WHEN DRILLING." *Journal of Bone and Joint Surgery-American Volume* A 54 (5):1125-&.

Matthews, L. S., and C. Hirsch. 1972b. "TEMPERATURES MEASURED IN HUMAN CORTICAL BONE WHEN DRILLING." *Journal of Bone and Joint Surgery-American Volume* A 54 (2):297-&. doi: 10.2106/00004623-197254020-00008.

Matziolia, Doerte, Jens Tuischer, Georg Matziolis, Grit Kasper, Georg Duda, and Carsten Perka. 2011. Osteogenic predifferentiation of human bone marrow derived stem cells by short term mechanical stimulation. The Open Orthopaedic Journal.

McAllister, B. S., and K. Haghighat. 2007. "Bone augmentation techniques." *Journal of Periodontology* 78 (3):377-396. doi: 10.1902/jop.2007.060048.

McKibbin, B. 1978. "The biology of fracture healing in long bones." *J Bone Joint Surg Br* 60-B (2):150-62.

McNamara, L. M., R. J. Majeska, S. Weinbaum, V. Friedrich, and M. B. Schaffler. 2009. "Attachment of Osteocyte Cell Processes to the Bone Matrix." *Anatomical Record-Advances in Integrative Anatomy and Evolutionary Biology* 292 (3):355-363. doi: 10.1002/ar.20869.

McNamara, Laoise M. 2011. "Bone as a Material." In *Comprehensive Biomaterials*, 169 - 186. Elsevier Ltd.

Medical, DTR. "DTR Medical Website." https://dtrmedical.com/products/kerrison-rongeur/.

MenMuir, B., and L. C. Fielding. 2017. "Revision of Minimally Invasive Sacroiliac Joint Fixation: Technical Considerations and Case Studies Using Decortication and Threaded Implant Fixation." *International Journal of Spine Surgery* 11. doi: 10.14444/4008.

Miller, A. 1984. "COLLAGEN - THE ORGANIC MATRIX OF BONE." *Philosophical Transactions of the Royal Society B-Biological Sciences* 304 (1121):455-477. doi: 10.1098/rstb.1984.0040.

Miller, E. J., Vanderko.Jk, and L. Sokoloff. 1969. "COLLAGEN OF HUMAN ARTICULAR AND COSTAL CARTILAGE." *Arthritis and Rheumatism* 12 (1):21-&. doi: 10.1002/art.1780120105.

Miller, S. C., L. Saintgeorges, B. M. Bowman, and W. S. S. Jee. 1989. "BONE LINING CELLS - STRUCTURE AND FUNCTION." *Scanning Microscopy* 3 (3):953-961.

Moran, Michael J, Howard N Shapiro, Bruce R Munson, and David P DeWitt. 2003. *Introduction to Thermal Systems Engineering: Thermodynamics, Fluid Mechanics, and Heat Transfer*: John Wiley & Sons, Inc.

Mosley, J. R., and L. E. Lanyon. 1998. "Strain rate as a controlling influence on adaptive modeling in response to dynamic loading of the ulna in growing male rats." *Bone* 23 (4):313-318. doi: 10.1016/s8756-3282(98)00113-6.

Mulcahy, LE. 2012. Response of bone cells to micro injury. Trinity College Dublin.

Nakashima, T., M. Hayashi, T. Fukunaga, K. Kurata, M. Oh-Hora, J. Q. Feng, L. F. Bonewald, T. Kodama, A. Wutz, E. F. Wagner, J. M. Penninger, and H. Takayanagi. 2011. "Evidence for osteocyte regulation of bone homeostasis through RANKL expression." *Nature Medicine* 17 (10):1231-1234. doi: 10.1038/nm.2452.

Naqvi, Syeda Masooma, Juan Alberto Panadero-Perez, Vatsal Kumar, Anneke S.K. Verbruggen, and Laoise M. McNamara. 2020. A novel 3D osteoblast and osteocyte model revealing changes in mineralisation and pro-osteoclastogenic paracrine signalling during estrogen deficiency. *Frontiers in Bioengineering and Biotechnology*.

Noble, B. S. 2008. "The osteocyte lineage." *Archives of Biochemistry and Biophysics* 473 (2):106-111. doi: 10.1016/j.abb.2008.04.009.

Noble, BS. 2003c. "Bone microdamage and cell apoptosis." *European Cells and Materials* 6:46 - 56.

Noonan, K. J., J. W. Stevens, R. Tammi, M. Tammi, J. A. Hernandez, and R. J. Midura. 1996. "Spatial distribution of CD44 and hyaluronan in the proximal tibia of the growing rat." *Journal of Orthopaedic Research* 14 (4):573-581. doi: 10.1002/jor.1100140411.

Norgaard, R., M. Kassem, and S. I. S. Rattan. 2006. "Heat Shock-Induced Enhancement of Osteoblastic Differentiation of hTERT-Immortalized Mesenchymal Stem Cells." *Understanding and Modulating Aging* 1067:443-447. doi: 10.1196/annals.1354.063.

O'Sullivan, Laura M., Hollie Allison, Eoin E. Parle, Jessica Schiavi, and Laoise M. McNamara. 2020. Secondary alterations in bone mineralisation and trabecular thickening occur after long-term oestrogen deficiency in ovariectomised rat tibiae, which do not coincide with initial rapid bone loss. Osteoporosis International.

Ochsner, P. E., F. Baumgart, and G. Kohler. 1998. "Heat-induced segmental necrosis after reaming of one humeral and two tibial fractures with a narrow medullary canal." *Injury-International Journal of the Care of the Injured* 29:SB1-SB10.

Oconnor, J. A., L. E. Lanyon, and H. Macfie. 1982. "THE INFLUENCE OF STRAIN RATE ON ADAPTIVE BONE REMODELING." *Journal of Biomechanics* 15 (10):767-781. doi: 10.1016/0021-9290(82)90092-6.

Okazaki, R, D Inoue, M Shibata, M Saika, S Kido, H Ooka, H Tomiyama, Y Sakamoto, and T Matsumoto. 2002. "Estrogen promotes early osteoblast differentiation and inhibits adipocyte differentiation in mouse bone marrow stromal cell lines that express estrogen receptor (ER) alpha or beta." 143 (6):2349 - 2356.

Ortega, N., D. J. Behonick, and Z. Werb. 2004. "Matrix remodeling during endochondral ossification." *Trends in Cell Biology* 14 (2):86-93. doi: 10.1016/j.tcb.2003.12.003.

Pal, S, and S Saha. 1981. "Effect of cutting speed on temperature during drilling of bone." *Proceeding of the ACEMB* 23:289.

Parfitt, A. M. 1987. "BONE REMODELING AND BONE LOSS - UNDERSTANDING THE PATHOPHYSIOLOGY OF OSTEOPOROSIS." *Clinical Obstetrics and Gynecology* 30 (4):789-811. doi: 10.1097/00003081-198712000-00004.

Parfitt, A. M. 1994. "OSTEONAL AND HEMI-OSTEONAL REMODELING - THE SPATIAL AND TEMPORAL FRAMEWORK FOR SIGNAL TRAFFIC IN ADULT HUMAN BONE." *Journal of Cellular Biochemistry* 55 (3):273-286. doi: 10.1002/jcb.240550303.

Parle, E., S. Tio, A. Behre, J. J. Carey, C. G. Murphy, T. F. O'Brien, W. A. Curtin, S. R. Kearns, J. P. McCabe, C. M. Coleman, T. J. Vaughan, and L. M. McNamara. 2020. "Bone Mineral Is More Heterogeneously Distributed in the Femoral Heads of Osteoporotic and Diabetic Patients: A Pilot Study." *JBMR Plus* 4 (2):e10253. doi: 10.1002/jbm4.10253.

Patel, V. V., S. M. Estes, E. M. Naar, E. M. Lindley, and E. Burger. 2009. "Histologic evaluation of high speed burr shavings collected during spinal decompression surgery." *Orthopedics* 32 (1):23. doi: 10.3928/01477447-20090101-17.

Perez-Cruet M, Begun EM, Collins R, Fahim D. 2013. "Initial Experience with BoneBac Press: A novel autologous bone graft harvesting and collecting device." *Open Journal of Orthopedics* 3:243-247. doi: 10.4236/ojo.2013.35045.

Perez-Cruet, Mick, Evan M. Begun, Robert Collins, and Daniel Fahim. 2013. Initial experience with BoneBac Press™: A novel autologous bone graft harvesting and collecting device. *Open Journal of Orthopedics*.

Peter, M. E., and P. H. Krammer. 1998. "Mechanisms of CD95 (APO-1/Fas)-mediated apoptosis." *Current Opinion in Immunology* 10 (5):545-551. doi: 10.1016/s0952-7915(98)80222-7.

Prideaux, M., D. M. Findlay, and G. J. Atkins. 2016. "Osteocytes: The master cells in bone remodelling." *Current Opinion in Pharmacology* 28:24-30. doi: 10.1016/j.coph.2016.02.003.

Rauh, J., F. Milan, K. P. Gunther, and M. Stiehler. 2011. "Bioreactor Systems for Bone Tissue Engineering." *Tissue Engineering Part B-Reviews* 17 (4):263-280. doi: 10.1089/ten.teb.2010.0612.

Roach, H. I. 1994. "Why does bone matrix contain non-collagenous proteins? The possible roles of osteocalcin, osteonectin, osteopontin and bone sialoprotein in bone mineralisation and resorption." *Cell Biol Int* 18 (6):617-28. doi: 10.1006/cbir.1994.1088.

Roschger, P., E. P. Paschalis, P. Fratzl, and K. Klaushofer. 2008. "Bone mineralization density distribution in health and disease." *Bone* 42 (3):456-466. doi: 10.1016/j.bone.2007.10.021.

Roth AA, Tang PC, Ye MJ, Mohammad KS, Nelson RF. 2017. "Improved autologous cortical bone harvest and viability with 2Flute otologic burs." *Laryngoscope* 128 (1):E40-E46. doi: 10.1002/lary.26779.

Roth, Adam A., Pei-Ciao Tang, Michael J. Ye, Khalid S. Mohammad, and Rick F. Nelson. 2018. Improved Autologous Cortical Bone Harvest and Viability with 2Flute Otologic Burs. The Laryngoscope.

Rubio-Moscardo, F., D. Blesa, C. Mestre, R. Siebert, T. Balasas, A. Benito, A. Rosenwald, J. Climent, J. I. Martinez, M. Schilhabel, E. L. Karran, S. Gesk, M. Esteller, R. deLeeuw, L. M. Staudt, J. L. Fernandez-Luna, D. Pinkel, M. J. S. Dyer, and J. A. Martinez-Climent. 2005. "Characterization of 8p21.3 chromosomal deletions in B-cell lymphoma: TRAIL-R1 and TRAIL-R2 as candidate dosage-dependent tumor suppressor genes." *Blood* 106 (9):3214-3222. doi: 10.1182/blood-2005-05-2013.

Saelens, X., N. Festjens, L. Vande Walle, M. van Gurp, G. van Loo, and P. Vandenabeele. 2004. "Toxic proteins released from mitochondria in cell death." *Oncogene* 23 (16):2861-2874. doi: 10.1038/sj.onc.1207523.

Saha, S., S. Pal, and J. A. Albright. 1982. "SURGICAL DRILLING - DESIGN AND PERFORMANCE OF AN IMPROVED DRILL." *Journal of Biomechanical Engineering-Transactions of the Asme* 104 (3):245-252. doi: 10.1115/1.3138356.

Savill, J., and V. Fadok. 2000. "Corpse clearance defines the meaning of cell death." *Nature* 407 (6805):784-788. doi: 10.1038/35037722.

Schreurs, B. W., Vjjf Busch, M. L. Welten, N. Verdonschot, Tjjh Slooff, and J. W. M. Gardeniers. 2004. "Acetabular reconstruction with impaction bone-grafting and a cemented cup in patients younger than fifty years old." *Journal of Bone and Joint Surgery-American Volume* 86A (11):2385-2392. doi: 10.2106/00004623-200411000-00004.

Schwarz, R. P., T. J. Goodwin, and D. A. Wolf. 1992. "Cell culture for three-dimensional modeling in rotating-wall vessels: an application of simulated microgravity." *J Tissue Cult Methods* 14 (2):51-7. doi: 10.1007/BF01404744.

Sener, B. C., G. Dergin, B. Gursoy, E. Kelesoglu, and I. Slih. 2009. "Effects of irrigation temperature on heat control in vitro at different drilling depths." *Clinical Oral Implants Research* 20 (3):294-298. doi: 10.1111/j.1600-0501.2008.01643.x.

Shah, Kalpit N., Jennifer Racine, Lynne C. Jones, and Roy K. Aaron. 2015. "Pathophysiology and risk factors for osteonecrosis." *Current reviews in musculoskeletal medicine* 8 (3):201-9. doi: 10.1007/s12178-015-9277-8.

Sharawy, M., C. E. Misch, N. Weller, and S. Tehemar. 2002. "Heat generation during implant drilling: The significance of motor speed." *Journal of Oral and Maxillofacial Surgery* 60 (10):1160-1169. doi: 10.1053/joms.2002.34992.

Shin, H. C., and Y. S. Yoon. 2006. "Bone temperature estimation during orthopaedic round bur milling operations." *J Biomech* 39 (1):33-9. doi: 10.1016/j.jbiomech.2004.11.004.

Sittichockechaiwut, A., A. M. Scutt, A. J. Ryan, L. F. Bonewald, and G. C. Reilly. 2009. "Use of rapidly mineralising osteoblasts and short periods of mechanical loading to accelerate matrix maturation in 3D scaffolds." *Bone* 44 (5):822-829. doi: 10.1016/j.bone.2008.12.027.

Sittichokechaiwut, A., J. H. Edwards, A. M. Scutt, and G. C. Reilly. 2010. "SHORT BOUTS OF MECHANICAL LOADING ARE AS EFFECTIVE AS DEXAMETHASONE AT INDUCING MATRIX PRODUCTION BY HUMAN BONE MARROW MESENCHYMAL STEM CELLS." *European Cells & Materials* 20:45-57.

Sladkova, Martina, and Giuseppe Maria de Peppo. 2014. "Bioreactor Systems for Human Bone Tissue Engineering." *Processes* 2:494 - 525. doi: doi:10.3390/pr2020494.

Spengler, D. M., E. R. Morey, D. R. Carter, R. T. Turner, and D. J. Baylink. 1983. "EFFECTS OF SPACEFLIGHT ON STRUCTURAL AND MATERIAL STRENGTH OF GROWING BONE." *Proceedings of the Society for Experimental Biology and Medicine* 174 (2):224-228.

Stryker. "Orthopaedic products." https://www.stryker.com/us/en/portfolios/orthopaedics/spine--ortho-.html.

Subbiah, R., M. P. Hwang, S. Y. Van, S. H. Do, H. Park, K. Lee, S. H. Kim, K. Yun, and K. Park. 2015. "Osteogenic/Angiogenic Dual Growth Factor Delivery Microcapsules for Regeneration of Vascularized Bone Tissue." *Advanced Healthcare Materials* 4 (13):1982-1992. doi: 10.1002/adhm.201500341.

Suliman, A., A. Lam, R. Datta, and R. K. Srivastava. 2001. "Intracellular mechanisms of TRAIL: apoptosis through mitochondrial-dependent and -independent pathways." *Oncogene* 20 (17):2122-2133. doi: 10.1038/sj.onc.1204282.

Sumpio, B. E., J. T. Riley, and A. Dardik. 2002. "Cells in focus: endothelial cell." *International Journal of Biochemistry & Cell Biology* 34 (12):1508-1512. doi: 10.1016/s1357-2725(02)00075-4.

Thompson, W. R., S. Modla, B. J. Grindel, K. J. Czymmek, C. B. Kirn-Safran, L. Y. Wang, R. L. Duncan, and M. C. Farach-Carson. 2011. "Perlecan/Hspg2 Deficiency Alters the Pericellular Space of the Lacunocanalicular System Surrounding Osteocytic Processes in Cortical Bone." *Journal of Bone and Mineral Research* 26 (3):618-629. doi: 10.1002/jbmr.236.

Thurner, P. J., S. Lam, J. C. Weaver, D. E. Morse, and P. K. Hansma. 2009. "Localization of Phosphorylated Serine, Osteopontin, and Bone Sialoprotein on Bone Fracture Surfaces." *Journal of Adhesion* 85 (8):526-545. doi: 10.1080/00218460902996424.

Toews, A. R., J. V. Bailey, H. G. G. Townsend, and S. M. Barber. 1999. "Effect of feed rate and drill speed on temperatures in equine cortical bone." *American Journal of Veterinary Research* 60 (8):942-944.

Tsiridis, E., N. Upadhyay, and P. Giannoudis. 2007. "Molecular aspects of fracture healing: Which are the important molecules?" *Injury-International Journal of the Care of the Injured* 38:S11-S25. doi: 10.1016/j.injury.2007.02.006.

Udagawa, N., N. Takahashi, T. Akatsu, H. Tanaka, T. Sasaki, T. Nishihara, T. Koga, T. J. Martin, and T. Suda. 1990. "ORIGIN OF OSTEOCLASTS - MATURE MONOCYTES AND MACROPHAGES ARE CAPABLE OF DIFFERENTIATING INTO OSTEOCLASTS UNDER A SUITABLE MICROENVIRONMENT PREPARED BY BONE MARROW-DERIVED STROMAL CELLS." *Proceedings of the National Academy of Sciences of the United States of America* 87 (18):7260-7264. doi: 10.1073/pnas.87.18.7260.

Verbruggen, S. W., M. J. Mc Garrigle, M. G. Haugh, M. C. Voisin, and L. M. McNamara. 2015. "Altered Mechanical Environment of Bone Cells in an Animal Model of Short- and Long-Term Osteoporosis." *Biophysical Journal* 108 (7):1587-1598. doi: 10.1016/j.bpj.2015.02.031.

Vico, L., D. Chappard, C. Alexandre, S. Palle, P. Minaire, G. Riffat, B. Morukov, and S. Rakhmanov. 1987. "EFFECTS OF A 120 DAY PERIOD OF BED-REST ON BONE MASS AND BONE CELL ACTIVITIES IN MAN - ATTEMPTS AT COUNTERMEASURE." *Bone and Mineral* 2 (5):383-394.

Vunjak-Novakovic, G., B. Obradovic, I. Martin, P. M. Bursac, R. Langer, and L. E. Freed. 1998. "Dynamic cell seeding of polymer scaffolds for cartilage tissue engineering." *Biotechnology Progress* 14 (2):193-202. doi: 10.1021/bp970120j.

Wajant, H. 2002. "The Fas signaling pathway: More than a paradigm." *Science* 296 (5573):1635-1636. doi: 10.1126/science.1071553.

Walter, B. A., S. Illien-Junger, P. R. Nasser, A. C. Hecht, and J. C. Iatridis. 2014. "Development and validation of a bioreactor system for dynamic loading and mechanical characterization of whole human intervertebral discs in organ culture." *Journal of Biomechanics* 47 (9):2095-2101. doi: 10.1016/j.jbiomech.2014.03.015.

Walter, S., and J. Buchner. 2002. "Molecular chaperones - Cellular machines for protein folding." *Angewandte Chemie-International Edition* 41 (7):1098-1113. doi: 10.1002/1521-3773(20020402)41:7<1098::aid-anie1098>3.0.co;2-9.

Watanabe, H., T. Yanagisawa, and J. Sasaki. 1995. "CYTOSKELETAL ARCHITECTURE OF RAT CALVARIAL OSTEOCLASTS - MICROFILAMENTS, INTERMEDIATE FILAMENTS, AND NUCLEAR MATRIX AS DEMONSTRATED BY DETERGENT PERFUSION." *Anatomical Record* 243 (2):165-174. doi: 10.1002/ar.1092430203.

Woo, S. L., S. C. Kuei, D. Amiel, M. A. Gomez, W. C. Hayes, F. C. White, and W. H. Akeson. 1981. "The effect of prolonged physical training on the properties of long bone: a study of Wolff's Law." *J Bone Joint Surg Am* 63 (5):780-7.

Wylie, A, J Kerr, and A Currie. 1980. "Cell Death: the significance of apoptosis." *International Review Cytolology* 68:251 - 306.

Xiong, J. H., M. Onal, R. L. Jilka, R. S. Weinstein, S. C. Manolagas, and C. A. O'Brien. 2011. "Matrix-embedded cells control osteoclast formation." *Nature Medicine* 17 (10):1235-U262. doi: 10.1038/nm.2448.

Xiong, J. H., M. Piemontese, M. Onal, J. Campbell, J. J. Goellner, V. Dusevich, L. Bonewald, S. C. Manolagas, and C. A. O'Brien. 2015. "Osteocytes, not Osteoblasts or Lining Cells, are the Main Source of the RANKL Required for Osteoclast Formation in Remodeling Bone." *Plos One* 10 (9). doi: 10.1371/journal.pone.0138189.

Xu, L. L., C. Y. Wang, M. Jiang, H. Y. He, Y. X. Song, H. Y. Chen, J. N. Shen, and J. Y. Zhang. 2014. "Drilling Force and Temperature of Bone under Dry and Physiological Drilling Conditions." *Chinese Journal of Mechanical Engineering* 27 (6):1240-1248. doi: 10.3901/cjme.2014.0912.151.

Xue, Q. Y., H. S. Li, X. N. Zou, M. Bunger, N. Egund, M. Lind, F. B. Christensen, and C. Bunger. 2005. "The influence of alendronate treatment and bone graft volume on posterior lateral spine fusion in a porcine model." *Spine* 30 (10):1116-1121. doi: 10.1097/01.brs.0000162929.19985.d2.

Ye, S., K. B. Seo, B. H. Park, K. J. Song, J. R. Kim, K. Y. Jang, Y. J. Chae, and K. B. Lee. 2013. "Comparison of the osteogenic potential of bone dust and iliac bone chip." *Spine Journal* 13 (11):1659-1666. doi: 10.1016/j.spinee.2013.06.012.

Yilmaz, T., S. Dalbayrak, O. Yaman, M. Yilmaz, M. Ayten, Y. Turan, and K. Ozturk. 2015. "A Modified Technique for the Treatment of Isthmic Spondylolisthesis." *Turkish Neurosurgery* 25 (3):394-403. doi: 10.5137/1019-5149.jtn.10298-14.2.

You, L. D., S. C. Cowin, M. B. Schaffler, and S. Weinbaum. 2001. "A model for strain amplification in the actin cytoskeleton of osteocytes due to fluid drag on pericellular matrix." *Journal of Biomechanics* 34 (11):1375-1386. doi: 10.1016/s0021-9290(01)00107-5.

Zhang, X. P., E. M. Schwarz, D. A. Young, J. E. Puzas, R. N. Rosier, and R. J. O'Keefe. 2002. "Cyclooxygenase-2 regulates mesenchymal cell differentiation into the osteoblast lineage and is critically involved in bone repair." *Journal of Clinical Investigation* 109 (11):1405-1415. doi: 10.1172/jci200215681.

Ziegler, U., and P. Groscurth. 2004. "Morphological features of cell death." *News in Physiological Sciences* 19:124-128. doi: 10.1152/nips.01519.2004.